Analysis of the Hydro-Climatic Regime of the Snow Covered and Glacierised Upper Indus Basin Under Current and Future Climates

Nazeer, A.

Publication date
2022

Document Version
Final published version

Citation (APA)
Nazeer, A. (2022). *Analysis of the Hydro-Climatic Regime of the Snow Covered and Glacierised Upper Indus Basin Under Current and Future Climates*. [Dissertation (TU Delft), Delft University of Technology].

Analysis of the Hydro-Climatic Regime of the Snow Covered and Glacierised Upper Indus Basin Under Current and Future Climates

Aftab Nazeer

ANALYSIS OF THE HYDRO-CLIMATIC REGIME OF THE SNOW COVERED AND GLACIERISED UPPER INDUS BASIN UNDER CURRENT AND FUTURE CLIMATES

Aftab Nazeer

ANALYSIS OF THE HYDRO-CLIMATIC REGIME OF THE SNOW COVERED AND GLACIERISED UPPER INDUS BASIN UNDER CURRENT AND FUTURE CLIMATES

DISSERTATION

Submitted in fulfillment of the requirements of
the Board for Doctorates of Delft University of Technology
and
of the Academic Board of the IHE Delft
Institute for Water Education
for
the Degree of DOCTOR
to be defended in public on
Tuesday, 6 December, at 15.00 hours
in Delft, the Netherlands

by

Aftab NAZEER
Master of Science in Agricultural Engineering
University of Agriculture Faisalabad, Pakistan

born in Multan, Pakistan

This dissertation has been approved by the
promotor: Prof.dr. M.E. McClain
copromotor: Dr. S. Maskey

Composition of the doctoral committee:

Rector Magnificus TU Delft	Chairman
Rector IHE Delft	Vice-Chairman
Prof.dr. M.E. McClain	IHE Delft / TU Delft, promotor
Dr. S. Maskey	IHE Delft, copromotor
Independent members:	
Prof.dr.ir. R. Uijlenhoet	TU Delft
Prof.dr. M.J. Polo Gomez	University of Córdoba, Spain
Prof.dr. P. Willems	KU Leuven, Belgium
Prof.dr. R.B. Kayastha	Kathmandu University, Nepal
Prof.dr. D.P. Solomatine	IHE Delft / TU Delft, reserve member

Dr. T. Skaugen of the Norwegian Water Resources and Energy Directorate (NVE), Oslo, Norway has significantly contributed towards the supervision of this dissertation

This research was conducted under the auspices of the Graduate School for Socio-Economic and Natural Sciences of the Environment (SENSE)

Published by IHE Delft Institute for Water Education
www.un-ihe.org

ISBN 978-90-73445-47-5

To my mother, Shamim Fatima,

for her endless love and sacrifices, she has made for us!

ACKNOWLEDGEMENTS

Firstly, I am incredibly thankful to Almighty Allah for empowering me to finish my PhD study. I believe the Almighty has rewarded me much more than I deserve. Secondly, there are countless people to whom I owe my deepest gratitude for their unconditional support. Without them, this would have been impossible to achieve.

I express my sincere gratitude to my promoter, Professor Michael McClain, for allowing me to work as a PhD student. Working under your supervision has been an inspirational journey, which kept my motivation amazingly high until the end of my degree. Your guidance, motivational insights and encouragement have played a vital role in this successful endeavour. Many thanks for your continuous support in improving my work and finalising my research articles and dissertation. Above all, I appreciate for continuously being available and providing all possible support on a priority basis.

To my co-promoter, Associate Professor Shreedhar Maskey, I extend my sincerest thanks for your guidance, support, constructive feedback and in-depth knowledge. Your efforts enabled me to achieve this milestone; these efforts are highly acknowledged. Your critical evaluations and consistent inputs during this journey have allowed me to achieve the best possible outcomes. Thank you for your continuous support in finalising my research articles and dissertation. I am grateful to you for constantly pushing me out of my comfort zone and enabling me to learn more and more.

I am sincerely thankful to Research Professor Thomas Skaugen from the Norwegian Water Resources and Energy Directorate (NVE), Oslo (Norway), for his vital contributions during my PhD journey. From proposal development to dissertation write-up, the way you have inspired and guided me is truly amazing. Thanks for developing and sharing a substantial hydrological model (DDD) and organising exclusive training sessions at NVE. I am also thankful to your research student Anne Stavang for her support regarding the model setup.

The technical expertise and guidance of various other colleagues have helped me conclude my PhD in time. Thanks to Professor Bob Su (University of Twente) for evaluating my research proposal and sharing in-depth knowledge. Thanks to Associate Professor Ilyas Masih for the helpful discussions throughout my PhD journey. I am very grateful to Senior lecturer Raymond Venneker for translating my dissertation's summary into Dutch (Samenvatting). I am also thankful to Senior lecturers Hans van der Kwast and Sajid Pareeth for helping me with issues related to GIS. Special thanks to Zakir Hussain Dahri (Pakistan Agricultural Research Council) for sharing in-depth knowledge and continued support. I am also grateful to Asif Khan (UET Peshawar, Pakistan), Shabeh ul Hasson (University of Hamburg) and Adnan Ahmad Tahir (COMSATS University, Pakistan) for their input and helpful discussions. I am highly obliged to Shakeel Hayat

and Hameed Jamali (IMS-Peshawar, Pakistan) for always showing me the way forward and for their consistent support.

Special gratitude to all the members of the evaluation committee. It is an honour to have all of you assess my dissertation. Thanks to all the scientific experts who reviewed the publications included in this dissertation.

I thank the Higher Education Commission Pakistan, Bahauddin Zakariya University (BZU) Multan, Pakistan, and IHE-Delft Institute for Water Education, the Netherlands, for their financial support. I duly acknowledge Prof. Dr Zahid Mahmood Khan, my departmental head at BZU-Multan (Pakistan), for his support and encouragement. I thank the Water and Power Development Authority (WAPDA) and the Pakistan Meteorological Department (PMD) for sharing the hydro-climatic data.

Many aspects of my stay at IHE Delft were well-accomplished due to the support from Jolanda, Niamh, Cindy, Maria, Anique, Floor, Ellen, and Taco. Thanks, Ruth, for organising a weekly run with IHE colleagues; it enabled me to stay physically fit and to accomplish challenging tasks like a half-marathon. There are several others; apologies in advance if I am missing any. Thanks to Jeewa for supporting me and cheering on all my achievements like an (elder) sister. It helps me to accomplish this milestone more confidently and comfortably. Thanks to Ataul for supporting me whenever I need you and for the long walks full of discussions. Thanks to Constanza (Coti) for joining on refreshing coffee breaks and exciting talks. Thanks to Dikman, Taha, Musaed, Ahmed, Hadeel, Omar, Bota, Mohaned, Nasir, Sebrian, Haris, Hesham, Bruce, Janaka, Febi, Janvi, Lina, Saidee, Meseret, Sida, Milk, Adele, Kelly, Celia, Jairo, Miao, Beni, Sumiran, and Yuxi. Thanks to the Muslims Students Association (MSA-IHE Delft) and PhD Association Board (PAB) for wonderful activities and continuous support.

To my Pakistani colleagues, you have made my stay in the Netherlands more pleasant and memorable. I thank the Pakistan Student Association (PSA-Delft) for organising exciting activities, including BBQs, Eid gatherings, sports events and much more fun. I especially thank Tanveer and Mohsan for helping to strengthen my programming and statistics skills. I am highly obliged to Nauman, Qasim, Saad, Hussam, Ahmad, Samad, Aitzaz, Haris, Osama, Shozab, Mubariz, Haider, Usman, Hassan, Rehan, Waqas, Uzair, Izbha, Maha, Maria, Yasir, Abdul Rahim, Shakeel, Sohrab, Junaid(s), Faisal, Irfan(s), Izhar, Ali, Abdul Wahab and Shehryar for their fantastic company. Thanks to my wonderful friends in Pakistan; Saeed Khan, Imtiaz Lashari, Junaid Afridi, Imran, Abid, and Faizan (Germany), Ateeq (Belgium), Kashif (Germany) and Usman (Italy) for helping me to learn what is best for me and how to achieve it. Special gratitude to my scouting family for their support throughout my personal and professional development.

The ultimate love and gratitude go to my family. Yet, you remained faithful through all the reservations and sufferings and kept me in your prayers. Today with words of gratefulness for all of you, I can proudly say that the PhD Journey is over. Special

gratitude to my siblings, Amna, Shehzad, Asiya, Asma and Hammad, and my sisters-in-law, Sadia and Arzo, for their affection and care. Thanks to other family members, Rana Nazeer Ahmad Noon, Rana Bashir Ahmad Noon, Mamun Jugnu, Ghulam Farid, Javed, Waqas, Asif, Nomi and all of my cousins, nieces and nephews, for their support. Thank you all for your trust, cheering on my success, and providing me with reasons to keep striving.

Last but not least, I am indebted to my beloved wife, Rubab, for your constant support, dedication and unconditional love. I started my PhD as a single and boring man, but as soon as you came into my life, you filled it with wonderful colours. During this challenging journey, you have given me lovely reasons (my cute sons, Shafin and Zohran and an angel, Shehzal) to do my best. Thank you for trusting in me when I need it the most and staying next to me during all crucial phases of this journey. Thanks for cooking delicious foods and boosting my morale and energy to the highest. I love you all, and you are my reason to forge ahead.

SUMMARY

In the high elevation Hindukush Karakoram Himalaya (HKH) mountain region, the complex weather system and sparse measurements make the elevation-distributed precipitation among the most significant unknowns and limit the realistic and comprehensive assessment of precipitation. In addition, due to local orographic effects, precipitation can vary highly over short horizontal distances. Accurate quantification of precipitation, however, is critical for understanding hydro-climatic dynamics. Moreover, snow and glacier dynamics, and their contribution to river flow in the HKH region, are also mostly unknown, leading to serious concerns about current and future water availability. The recent acceleration in climate change (CC) heightens concerns about future water availability from high elevation mountain regions. The HKH region heavily depends on its upstream frozen water resources, and an accelerated melt may severely affect future water availability. In line with rapid population growth in the Indo-Gangetic plain, there will be increased water, food and energy demands in the future. Therefore, increasing knowledge of the hydro-climatic regime and glacier and snowmelt contributions to the river flow under current and future climate change scenarios is essential.

The Indus basin, with a downstream population of around 250 million, is among three highly populated river basins originating from the HKH mountains, followed by Ganges and Brahmaputra. This PhD research was designed to quantitatively and comprehensively assess precipitation and its distribution for the Gilgit and Hunza sub-basins of the Upper Indus Basin (UIB). In addition, the hydrological regime and snow and glacier dynamics were investigated, and the future hydro-climatic regime and water availability from the highly glaciated Hunza basin were analysed. For the present-day investigations, the elevation-distributed precipitation was derived from better performing global precipitation datasets which include the high resolution (0.1°x0.1°) and newly developed ERA5-Land, and a coarser resolution (0.55°x0.55°) JRA-55. These estimates were forced to a data parsimonious precipitation-runoff model, Distance Distribution Dynamics (DDD), with its energy balance and temperature index approaches for snow/glacier melt simulation. The model was calibrated from 1997–2005 and validated from 2006–2010. For future scenarios, the ERA5-Land corrected precipitation against the observed flow was employed to bias correct the precipitation from two global circulation models (GCM) using the newly released Coupled Model Intercomparison Project Phase 6 (CMIP6) climate projections. The DDD model was set up again using these bias corrected GCM projections for baseline (1991–2010), mid-century (2041–2060) and end-century (2081–2100) projections under Shared Socioeconomics Pathways (SSP) SSP1, SSP2 and SSP5 emission scenarios.

The mean of total annual precipitation data was estimated at 888 and 947 mm by ERA5-Land and 951 and 1322 mm by JRA-55 for Gilgit and Hunza sub-basins, respectively. Most of the precipitation (56–69 %) in the study area falls in the winter and spring seasons (Dec-May). The elevation-distributed precipitation estimates showed more precipitation at lower elevations. A linear elevation-dependent precipitation gradient is found unsuitable for these high elevation basins. The daily river flow is well simulated, with Kling Gupta Efficiency (KGE) ranging from 0.72–0.78 and 0.84–0.88 for Gilgit and Hunza, respectively. The simulated snow cover area (SCA) was validated using MODIS SCA and the results are quite promising. The river flow in Gilgit depends more on snowmelt (37–38 %), followed by glacier melt (31 %) and rainfall (26 %). While Hunza's flow depends more on glacier melt (45–48 %), followed by snowmelt (30–34 %) and rainfall (21–23 %).

The future projection showed increasing temperature for all scenarios, with a basin-scale increase between 1.1°C and 8.6°C depending on the scenarios and GCMs used. Relative to the baseline period, the ECE3 GCM shows 19–32 % increases in annual precipitation and ESM GCM shows 12–28 % increases for mid-century (2041–2060) and end-century (2081–2100). Moreover, changes in precipitation cycles, a reduction in precipitation as snow and an increase in precipitation as rainfall are also expected. Relative to the baseline period, the ECE3 GCM shows 53–265 % increases in glacier melt contribution to river flow and ESM shows 38–172 % increases for mid-century (2041–2060) and end-century (2081–2100). The elevation-distributed glacier melt simulations suggest increasing melt contribution from all elevations in the future with maximum melt from the higher elevations. Relative to the baseline period, the ECE3 GCM shows 31–126 % increases in Hunza's flow and ESM shows 23–99 % increases for mid-century (2041–2060) and end-century (2081–2100) due to glacier melt and increased total precipitation.

Based on the findings from a comparatively new modelling framework, an improved hydrological understanding of the study area is presented. The more realistic elevation-distributed precipitation estimates have significantly improved the flow simulations and the water balance. Most previous investigations were based on coarse approaches and/or were forced with unrealistic precipitation inputs. In the first modelling framework, energy balance based sub-routines are employed to simulate snow cover, glacier melt and actual evapotranspiration, and a temperature index based sub-routine for glacier melt was employed in a second modelling framework. The simulated elevation-distributed snow cover areas were validated using satellite data, independently, which confirmed the results of the modelling approach. Moreover, the research presented an improved assessment of the hydro-climatic regime and CC associated implications for the study area. The findings may assist policymakers and other stakeholders with respect to hydropower and reservoir development, sustained agriculture production, CC adaptation, and efficient management of the water resources. Future work is recommended to acquire more observational data at a reasonable scale, covering the higher elevation. Also, measuring individual glacier flows, using radar remote sensing or drone technology for

mass balance investigation and field-based calibration of a few parameters such as liquid content in snow, snow and glacier density and degree-day factors should be considered in future research. Finally, focused work on obtaining sufficient data and validating methods for future glacier recessions is recommended.

SAMENVATTING

In het hooggebergte van de Hindukush Karakoram Himalaya (HKH) regio zorgen het complexe weersysteem en de spaarzaamheid van metingen ervoor dat de hoogte distributie van neerslag grotendeels onbekend is hetgeen een diepgaande neerslaganalyse bemoeilijkt. Daarbij kan de neerslag sterk varieren over korte afstanden als gevolg van orografische effecten. Niettemin is een accurate neerslag kwantificering noodzakelijk om de hydro-klimatologische dynamiek te begrijpen. Bovendien zijn tevens de sneeuw en gletsjer dynamica en de contributie hiervan aan de rivierafvoeren in de HKH regio grotendeels onbekend, hetgeen leidt tot serieuze zorgen omtrent de huidige en toekomstige waterbeschikbaarheid. Versnelling in klimaatverandering versterken deze zorgen voor hoogebergten in het algemeen. De HKH regio is sterk afhankelijk van bovenstroomse bevroren watervooraden, en het verneld smelten hiervan kan ernstige gevolgen hebben voor de waterbeschikbaarheid in de toekomst. In samenhang met de snelle bevolkingsgroei in de Indo-Ganges vlakte zal de vraag naar water verder toenemen. Daarom is meer kennis van het hydro-klimatologische regime en de bijdragen van gletsjer- en sneeuw smeltwater aan de rivierafvoer essentieel voor huidige en toekomstige klimaatverandering scenarios.

Met een benedenstroomse bevolking van 250 miljoen is het Indus stroomgebied, tesamen met dat van de Ganges en de Brahmaputra, een van de drie dichtbevolkte zuid-Aziatische stroomgebieden afkomstig van het HKH gebergte. Dit promotieonderzoek was opgezet voor een diepgaande kwantitatieve studie van de neerslag en de distributie hiervan in de Gilgit en Hunza sub-stroomgebieden van de boven-Indus. Ook werden het hydrologische regime, de sneeuw en gletsjer dynamica, het toekomstige hydro-klimatologiche regime, en de waterbeschikbaarheid van het ruim met ijs bedekte Hunza stroomgebied onderzocht. Voor analyse van de huidige situatie, hoogte-gedistribueerde neerslag was afgeleid van globale datasets zoals de hoge-resolutie (0.1°×0.1°) ERA5-Land, en het lagere resolutie (0.55°×0.55°) JRA-55. Deze gegevens werden ingevoerd in een data-spaarzaam neerslag-afvoer model, Distance Distribution Dynamics (DDD) waarin energie balans en temperatuur index benaderingen worden gebruikt om sneeuw- en gletsjer smelt te simuleren. Dit model was gecalibreerd voor de periode 1997–2005 en gevalideerd voor de periode 2006–2010. Voor de toekomst-scenarios, de ERA5-Land gecorrigeerde neerslag tegen waargenomen afvoer was gebruikt voor correctie van de neerslag afwijking in twee globale circulatie modellen (GCM) onder de recente Coupled Model Intercomparison Project Phase 6 (CMIP6) klimaatprojecties. Het DDD model was opnieuw ingesteld voor deze afwijking-gecorrigeerde GCM projecties voor de basislijn (1991–2010), midden-eeuw (2041–2060) en eind-van-de-eeuw (2081–2100) projecties onder de Shared Socioeconomics Pathways SSP1, SSP2 en SSP5 emissie scenarios.

De gemiddelde jaarlijkse neerslag in de Gilgit en Hunza stroomgebieden is 888 respectievelijk 947 mm in de ERA5-Land data en 951 respectievelijk 1322 mm in de JRA-55 data. Het grootste deel van de neerslag (56–69 %) valt in de winter en lente (December–Mei). De hoogte-gedistribueerde neerslag schattingen laten meer neerslag zien op lagere hoogten. Voor deze hooggebergte stroomgebieden blijkt een lineaire neerslag – hoogte relatie ongeschikt te zijn. De dagelijkse rivierafvoeren worden goed gesimuleerd met Kling-Gupta efficientiewaarden van 0.72–0.78 voor de Gilgit en 0.84–0.88 voor de Hunza. De gesimuleerde sneeuwbedekking was gevalideerd met MODIS SCA en de resultaten van de validatie zijn veelbelovend. De Gilgit rivierafvoer hangt het sterkst af van sneeuwsmelt (37–38 %), gevolgd door gletsjersmelt (30–34 %) en regen (26 %). De Hunza afvoer is meer afhankelijk van gletsjersmelt (45–48 %), gevolgd door sneeuwsmelt (30–34 %) en regen (21–23 %).

Toekomstprojecties laten een stijgende temperatuur zien voor alle scenarios, met een toename van 1.1 °C tot 8.6 °C op stroomgebiedsschaal, afhankelijk van het toegepaste GCM en scenario. Ten opzichte van de basislijn laten het ECM3 GCM een toename van 19–32 % en het ESM GCM een toename van 12–28 % in de jaarlijkse neerslag zien voor het midden (2041 2060) het einde (2081–2100) van de eeuw. Ook worden veranderingen in neerslag cycli, een afname in sneeuwval en een toename in regenval verwacht. Ten opzichte van de basislijn laten het ECE3 GCM een toename van 53–265 % en het ESM GCM een toename van 38–172 % in de gletsjersmelt bijdrage aan rivierafvoeren zien voor het midden (2041–2060) en het einde (2081–2100) van de eeuw. Hoogte-verdeelde gletsjersmelt simulaties suggereren een toename van gletsjersmelt bijdragen op alle hoogtes met maximale smelt op grotere hoogtes. Ten opzichte van de basislijn laten het ECE3 GCM een toename van 31–126 % en het ESM GCM een toename 23–99 % zien de de Hunza rivierafvoer voor het midden (2041–2060) en het einde (2081–2100) van de eeuw als gevolg van toenames in gletsjersmelt en neerslag.

Gebaseerd op de bevindingen van een relatief nieuwe modelopzet wordt een verbeterd hydrologisch begrip van het studiegebied gepresenteerd. De meer realistische hoogte verdeling in neerslagschattingen leidden tot significante verbeteringen in de afvoer simulaties en de waterbalans. Eerdere onderzoeken waren grotendeels gebaseerd op ruwe benaderingen en/of uitgevoerd met onrealistische neerslag invoer. In de eerste modelopzet worden energiebalans sub-routines gebruikt voor simulatie van sneeuwbedekking, gletsjersmelt and actuele verdamping, terwijl een temperatuur index gebaseerde sub-routine voor gletsjersmelt gebruikt werd in een tweede modelopzet. De gesimuleerde hoogte verdeling van sneeuwbedekking en gletsjersmelt zijn onafhankelijk gevalideerd met satelliet data, hetgeen de resultaten van de modelbenadering bevestigd. Tevens presenteerd dit onderzoek een verbeterde analyse van het hydro-klimatologidsche regime en klimaatsverandering gerelateerde implicaties voor het studiegebied. De bevindigen kunnen beleidsmakers en andere belanghebbenden ondersteunen met betrekking tot waterkracht en stuwmeer ontwikkeling, duurzame landbouwproduktie, adaptatie aan klimaatverandering en efficient waterbeheer. Aanbevelingen voor

toekomstig onderzoekswerk behelzen het verzamelen van meer waarnemingen op redelijke schaal en grotere hoogte. Ook wordt aangeraden om individuele gletsjerstromen te meten met radar remote sensing of drone technologie ten behoeve van massabalans onderzoek, en veld calibratie van parameters zoals vloeibaar watergehalte van sneeuw, sneeuw en gletsjer dichtheid en graad-dag factoren in beschouwing te nemen voor toekomstige studies. Tenslotte wordt gefocust werk voor het verkrijgen van voldoende gegevens en validatie methodes voor toekomstige gletsjerrecessie aangeraden.

CONTENTS

1

INTRODUCTION

1.1 BACKGROUND

Precipitation (P) governs renewable and freshwater resources. Precipitation is important for agriculture, socio-economic development and hydropower production. It is vital to maintain the hydro-climatic balance and ecosystem (Langella et al., 2010; Ma et al., 2018). Moreover, precipitation is a key component in the hydrological cycle and one of the primary inputs in hydrologic models (Sorooshian et al., 2011). However, obtaining accurate precipitation data of sufficiently high spatio-temporal resolution is challenging (Fang et al., 2013). At present, there are four principal methods to estimate precipitation: (1) ground-based gauges, (2) ground-based radar, (3) satellite-based remote sensing and (4) atmospheric reanalysis models (Michaelides et al., 2009). The ground-based gauges have a problem of lower gauge density and cannot reflect the precipitation spatial variability and thus results in inaccurate assessments of areal precipitation (Andréassian et al., 2001). Ground-based radar has a higher spatio-temporal resolution, but the problem is they are limited in coverage and thus restricted to regional-scale estimates (Martens et al., 2013). Satellites are able to observe precipitation with large spatial coverage and are suitable for estimating rainfall in the tropics due to the heterogeneous precipitation patterns (Smith, 2006). However, satellite-based approaches are vulnerable to systematic biases, unresponsive to low intensity rainfall, and perform poorly over snow and ice covered surfaces (Mugnai et al., 2013). Reanalysis models are suitable for developing large scale weather systems but tend to fail over the extremes. Also, reanalysis models have low resolution and are deficient for sub-grid developments (Kidd et al., 2013). The accuracy of interpolated precipitation estimates, on the other hand, is highly dependent on degree of spatial consistency and gauge network, both of which vary highly (Chen et al., 2008).

Glaciers are one of the major reservoirs of fresh water. Changes in glaciers and ice peaks are among the fifty most critical climatic variables characterized by the Global Climate Observing System (GCOS). Glaciers are very sensitive to climate and hence act as a climate change indicator (Minora et al., 2016). Also, glaciers are located in the headwaters of many rivers worldwide, and they contribute significantly to downstream water supplies (Hasson, 2016). Glacier melt is also significant in raising the sea water level in the polar region (Marzeion et al., 2017). In recent decades, glaciers have experienced negative mass

balance and terminal recessions in most of the world's mountains (Oerlemans and Klok, 2004). Snow is also an important part of the climatic system and hydrological cycle and a major moisture source. Snow depth, density and melting dynamics srtrongly infleunce the flow regimes of most rivers of the temperate latitudes worldwide (Young, 1985). Also, snow significantly influences atmospheric processes because of its low thermal conductivity and high albedo (Hall and Riggs, 2007).

Calculating the glacier mass balance using field surveys and direct glaciological methods, is difficult, laborious, and time-consuming with site accessibility problems. It requires a lot of logistical and financial support (Hasson, 2016). Consequently, only a few glaciers are being continuously monitored in diverse climatic regions. The World Glacier Monitoring Service (WGMS) derived the direct field-based, uninterrupted glacier mass balance monitoring for only 40 glaciers for a time series longer than 40 years (Zemp et al., 2006). The WGMS includes 440 glaciers for continuous monitoring worldwide, which is a tiny number (about 0.25%) in comparison to the total of nearly 200,000 glaciers, recorded in the Randolph Glacier Inventory (RGI) database (Pfeffer et al., 2014). This small sample is inadequate for properly understanding the relationship between glacier mass balance changes and the regional and global climate. Moreover, it limits understanding of the influence of glaciers on biodiversity and freshwater resources. Satellite imagery with good temporal and spatial resolution coupled with the geographical information system (GIS) has been proved to be a powerful tool for mapping glaciers and snow covers in inaccessible terrains (Parajka et al., 2012; Tong et al., 2009). Remote sensing based snow and glacier monitoring, however, is subject to various limitations and biases, including cloud coverage, dense vegetation, surface heterogeneity, course resolution, and spectral similarities (Berthier et al., 2006).

Due to the emission of greenhouse gases and subsequent warming, the threat of climate change (CC) is continuously rising (Ciais et al., 2014). Evidence revealed that the impacts and risks associated with CC are most substantial for natural systems (IPCC 2021; (Masson-Delmotte, 2021)). Increasing population and population densities with associated infrastructure development and accelerated economic activities increase CC vulnerability (Quincey et al., 2007). With continued warming and associated changes in climate, significant changes in precipitation quantity and trends are projected for the 21st century. These changes may cause more frequent droughts and floods in the future. Moreover, CC may adversely impact hydrological processes, including timing and volume of flow, floods and droughts, evapotranspiration and soil moisture. This may further impact sedimentation, plant growth, nutrient flow, and other atmospheric and environmental processes (Zhang et al., 2014). Changes in such processes may affect agricultural productivity, water availability and supply, power generation, wildlife and ecosystems (Zhang et al., 2008).

Owing to these numerous existing issues and conditions, numerical models are commonly used to simulate the behaviour of the earth systems. A model is the basic illustration of the system (Moradkhani and Sorooshian, 2009). Models are primarily used for investigating processes and forecasting. Specific applications of earth system models include flood forecasting, erosion and sedimentation, water resource management, changes in land use, climate change impacts, and assessment of water quality and nutrient cycling (Devia et al., 2015). The model that provides accurate results by using the least parameters and with the least complexity is ranked as the best (Skaugen et al., 2018). Various hydrological models with diverse applications, ranging from small catchments to the global scale, have been developed (Skaugen et al., 2018). However, modelling is associated with significant uncertainties (Pellicciotti et al., 2012). These uncertainties can be attributed to model parameterization, model input and calibration data (Ismail et al., 2020; Ragettli et al., 2013). Different sources of uncertainty influence projected results differently, hence quantifying these uncertainties is essential (Dahri et al., 2021).

Hydrological models can be classified as lumped, semi-distributed and distributed models, on a spatial scale basis. The whole catchment is considered a single unit in lumped models. In semi-distributed models, the model structure is more process-based and the whole basin is subdivided into smaller subbasins. While in a distributed model, inputs, outputs and model's parameters are fully allowed to vary at a user-defined spatial scale (Moradkhani and Sorooshian, 2009). Based on the physics used, models can be classified as empirical, conceptual, and physically-based models. Empirical models are driven using observed data, only consider the existing information and do not involve the structures and processes of the hydrological system (Devia et al., 2015). In a conceptual model, semi-empirical mathematical equations are employed, and the parameters are evaluated by calibration against available observation data. A physically based model is a more detailed mathematical representation of the phenomenon. These models require the assessment of the various parameters related to the physical features of the basin (Abbott et al., 1986).

Several glacier- and snow-melt models have been designed for specific needs and diverse hydrologic conditions. These models are in general hydrological models but also simulate the snow/glacier and hydrological dynamics and associated CC implications (for example; SRM (Martinec (1975), DDD (Skaugen and Onof, 2014), SPHY (Terink et al., 2015), GDM (Kayastha and Kayastha, 2020). In this study, the Distance Distribution Dynamics (DDD) model is used which is a hydrological model specially designed for snow and glaciers dominated catchments and applied in Norway (Skaugen and Onof, 2014). More details about this model are discussed in section 2.3.5. There are two basic modelling approaches for melt estimation, the energy balance and the temperature index (Prasad and Roy, 2005). The snow/glacier models are data intensive and/or complex to handle. Only a few models can handle diverse hydrologic conditions (Tekeli et al., 2005).

Investigating snow and glacier dynamics in data-scarce basins and with changing climate requires models that: (1) are efficient in terms of running at varying spatial and temporal scales; (2) are parsimonious in terms of input data; and (3) have more physical and identifiable model parameters (Skaugen et al., 2018). Many snow model intercomparison projects have been launched in recent decades with different purposes. They came up with common conclusions, including: (1) there is no "best" snow model and; (2) the complexity of the model's structure does not mean improved performance (Essery et al., 2013). The choice of hydrological model is often based on the model structure, model performance, data availability, site-specific conditions, and study objectives (Kay and Davies, 2008).

1.2 STUDY AREA: THE UPPER INDUS BASIN (UIB)

The Upper Indus Basin (UIB) is a transboundary river basin in the Hindukush Karakorum Himalaya (HKH) mountainous region. The basin has an area of about 167,000 km^2 and extends from 74.5° E–76.5° E and from 35.2° N–37° N. The catchment area extending from Lake Manasarovar in Tibet to Tarbela reservoir in Pakistan is called the Upper Indus Basin (Figure 1.1). The UIB is a transboundary basin with about 58 % of the catchment area in Pakistan (Khan et al., 2014). The altitudinal variation of UIB ranges from 455 masl at Tarbela reservoir (the largest earth-filled dam worldwide) to 8611 meters above sea level (masl) at K-2, the second highest peak in the world. About 35 % of the basin's total area is located above 5000 masl (Bocchiola et al., 2011). About 60–80 % of vertical descent in UIB occurs in less than 10% of length, and the midsections are of a comparatively gentle gradient (Hewitt, 2011). River Indus (3,180 km long) originates from the western Tibet region and discharges into the Arabian Sea, south of Pakistan (Yu et al., 2013). The river flows northwest toward the Hindukush and Karakorum mountain range and then takes a sharp southward turn and enters into the hills and plains (Mukhopadhyay and Khan, 2014a). With an altitudinal variation of about 8000 m, UIB has a complex, arid to semi-arid, climate (Sharif et al., 2013). The basin's climate results from the complex interaction among monsoon circulation, westerly effects and the basin's topography. Precipitation in the basin has two main periods; the westerlies-influenced period from January to March/April and the monsoon period from July through August. The mean flow of UIB at Tarbela reservoir is 2415 m^3/sec based on the data from 1969–2010 obtained from Pakistan's Water and Power Development Authority (WAPDA). 70 % of the UIB's total flow generates from the melt, with 26 % from the glacier and 44 % from snowmelt (Mukhopadhyay and Khan, 2014a). The snowmelt regime generates its peak flow during early summer (May/June), while the glacial melt regime observes its peak flow during late summer (July/August). The basin hosts an extensive glacier system with more than 13,000 glaciers covering and area of 19,370 km^2, roughly 12 % of the

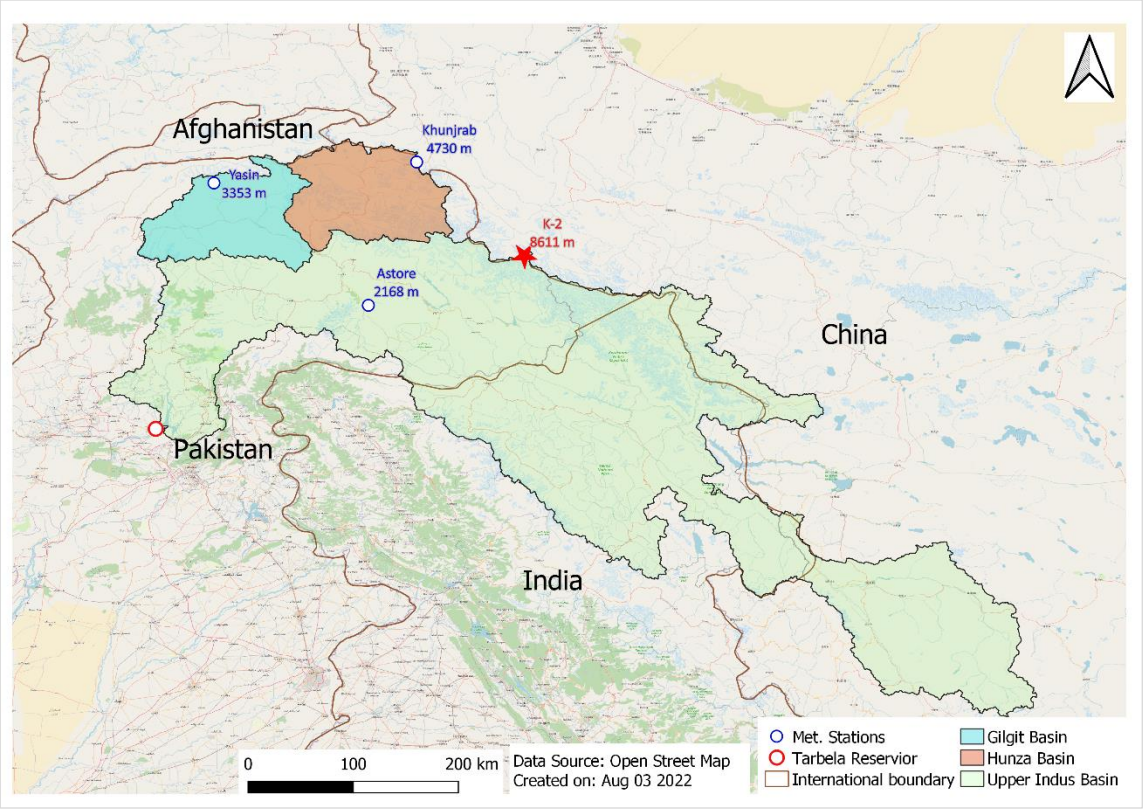

Figure 1.1. Upper Indus Basin (UIB) with Gilgit and Hunza sub-basins

basin's total area (Hasson, 2016). The Indus basin generates the second highest snow and glacier melt contribution after the Brahmaputra Basin among the basins in high mountains of Asia (Armstrong et al., 2019). In contrast, the other large river systems of high mountains of Asia are largely dependent on the summer monsoonal regime.

The UIB has five main sub-basins: Shyok, Shigar, Hunza, Gilgit, and Astore, from three mountain ranges: Hindukush, Karakorum and Himalaya. The Shyok, Shigar, and Hunza are sub-basins from the Karakorum mountain range. Gilgit is a sub-basin from the Hindukush, and Astore is a sub-basin from the Himalayas. Himalayan based Shingo and Zanskar sub-basins and two main stem sub-basins till Kharmong also contribute to UIB. This PhD research investigates hydro-climatic dynamics in two sub-basins of UIB; Hindukush based Gilgit and Karakorum based Hunza. The Gilgit is the least studied sub-basin of UIB and Hunza is one of the highly glaciated sub-basins.

1.3 HYDRO-CLIMATIC REGIME OF THE STUDY AREA

In the Himalayan range, the monsoon is the primary and largest source of precipitation. The lower elevation Himalayan streams on the southern face generate significant direct flow due to summer monsoon rainfall (Archer and Fowler, 2008). But moving toward the north-western direction, this influence decreases, and the mid-latitude westerlies become the primary source of precipitation (Lutz et al., 2016b). These westerlies provide the main nourishment for the glaciers of the Karakorum region (Bocchiola et al., 2011). The mean monthly temperatures in westerlies influenced areas to remain below the freezing point; consequently, there is very low direct flow due to rainfall between October and March. Summer flow is mainly generated from the glacier melt and seasonal snowmelt, with the glacier melt dominant in Karakorum tributaries, such as Hunza and Shyok, and the seasonal snowmelt dominant in Himalayan based sub-basins like Astore (Archer and Fowler, 2008).

The widest glaciers worldwide after the polar region are situated in the HKH region (Bolch et al., 2012). The melt water from the HKH and the neighbouring Tibetan Plateau (TP) is the origin of large river systems such as the Brahmaputra, Gangas, and Indus. The region hosts many peaks with an elevation exceeding 7000 masl (Sharif et al., 2013). Like the global trends of glacier mass depletion (Cogley, 2012), most of the glaciers in the HKH region are retreating.

These glaciers have been retreating since the end of the Little Ice Age, and recent observations in the 1990s showed an increase in such retreats (Bolch et al., 2012). The river flow in UIB is highly influenced by the state and fate of the Karakoram glaciers. Where more recent field-based studies showed that the Karakoram glaciers are either balanced in mass or have experienced an advancement (Mukhopadhyay and Khan, 2014b). The glacier mass balance in the Karakoram region was positive from 2003 to 2008 (Bolch et al., 2012) and there had been thickening and advancement in some glaciers of the Karakorum (Gardelle et al., 2012). Rankl et al. (2014) presented the surging behaviour of 134 glaciers since 2000 out of 1334 glaciers in the Karakoram. Hewitt (2007) in his field visits from 1997–2001, reported that 33 glaciers in the UIB region have thickened and advanced by 5–20 m. One of the recent mass balance measurements in the region comprised only eight glaciers in India and three in Nepal, with a time series of one year only (Dyurgerov and Meier, 2005). Against the region's total glacier cover of about 60,000 km^2, these 11 glaciers, however, only cover 121 km^2 (Berthier et al., 2007).

Consistent with the rapid global warming, the Himalayan mountain range has experienced substantial warming in recent decades. The Indus basin is recognized as a hotspot of CC due to significant transformations in the hydro-climatic regime (Lutz et al., 2016b; Wijngaard et al., 2018). Significant changes are expected for the basin's future hydro-

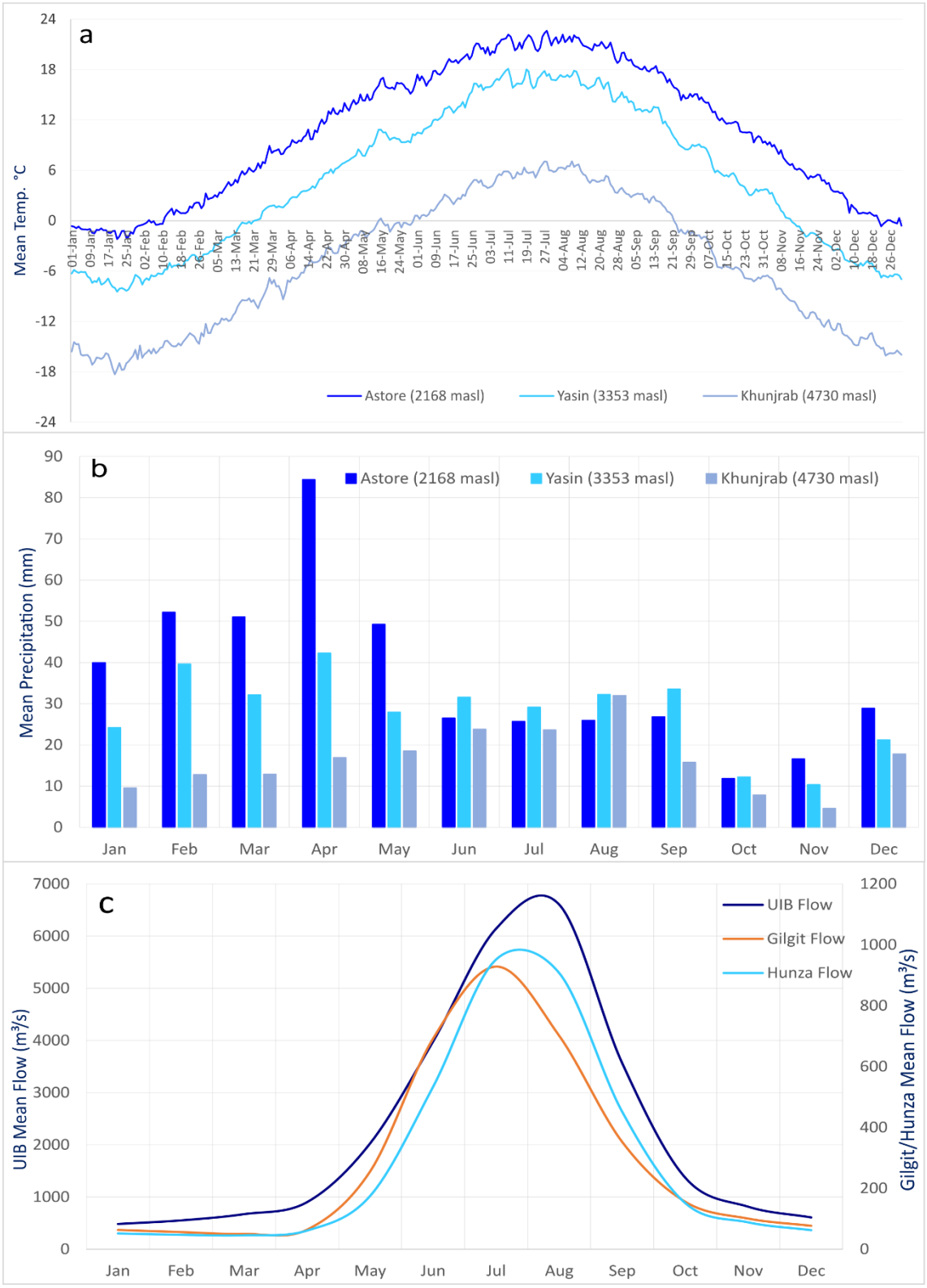

Figure 1.2. Observed hydro-climatic regime of the selected gauges from the case study; a) mean daily average temperature, b) mean monthly precipitation and c) mean daily observed flow

climatic regime (Dahri et al., 2021). Due to these projected changes in climate, implications for glacier mass balance and snow accumulation could be challenging and create new opportunities for water resource management (Latif et al., 2020).

Figure 1.2 indicates the observed hydro-climatic regime of the case study. Observed data from three meteorological gauges representing lower, middle and higher elevation ranges in UIB and three flow gauges: two sub-basins selected for this study and the main UIB are shown in this figure. The case study is comprised of all three high mountain ranges with the elevation varying from 455 to 8611 masl. The Astore (2168 masl) is a Himalayan sub-basin representing the low elevations, Yasin (3353 masl) is a Hindukush sub-basin representing the medium elevations and Khunjrab (4730 masl) is a Karakorum sub-basin representing the high elevations climates. The flow gauge data are shown for the whole UIB and two sub-basins selected for this research.

1.4 PROBLEM STATEMENT

The magnitude and distribution of precipitation in the HKH region are one of its largest unknowns (Immerzeel et al., 2013; Winiger et al., 2005). The relationship between high elevations of the HKH region and precipitation is also largely unknown because of the lack of reliable rainfall measurements (Bookhagen and Burbank, 2006). Accurate quantification of precipitation is critical for understanding hydro-climatic dynamics, especially in data-scarce and glaciated catchments (Dahri et al., 2016). Therefore, there is a need to develop and improve the quantification of precipitation and its spatial distribution at high elevations (Immerzeel et al., 2015; Lutz et al., 2014).

The quantification of the contributions of seasonal snow and glacier melt to the river flow is challenging but crucial for managing water resources (Schaner et al., 2012). The glaciers of the Himalayan mountains are retreating at similar rates to other regions worldwide; however, the Pamir and Karakoram glaciers have neutral mass balances with even advancing glaciers (Hewitt, 2007; Hewitt, 2011; Quincey et al., 2011). This phenomenon is named the Karakoram anomaly. However, this phenomenon is still hypothetical and requires further investigation and interpretation of snow/glacier dynamics at high elevations (Dahri et al., 2018). Consequently, a great debate has prevailed concerning these trends during the last decade (Lutz et al., 2016b). Insufficient in-situ data, projecting a small-scale study's results over the large scale or entire basin, errors in up-scaling and/or down-scaling of results, and neglecting land use changes and the impacts of debris cover can attribute these contrasting claims (Dahri et al., 2021). Such conflicting hydro-climatic regimes and existing information about snow and glacier contributions contribute to uncertainty in current and future water resources management.

Lack of understanding of snow cover evaluation also hinders the calibration and validation of hydrological models (Hasson et al., 2014). Snow-accumulation

measurements with snow pillows and snow pits are also rare and generally limited to short record periods (Immerzeel et al., 2012). Consequently, there could be significant uncertainties in precisely representing the Indus basin's hydro-climatic regime (Dahri et al., 2021; Lutz et al., 2014).

The recent acceleration in CC heightens concerns about future water availability from these high elevation catchments (Hasson, 2016). An accelerated melt due to this CC may eventually lead to water shortages for downstream plains with intensive agricultural activities (Immerzeel et al., 2010). Moreover, CC will change the frequency and magnitude of climatic variables such as precipitation and temperature (Hasson et al., 2019). Also, projected increases in population will intensify the pressures on already scarce water and energy resources. Also, more frequent extreme weather events in the future projections pose serious challenges for a region where severe flooding and other natural hazards are already prevailing. However, most of the present conclusions about the climate and hydrology of HKH are based on insufficient analyses with very limited data and need further investigation.

The Indus basin (basin area up to the Arabian sea), with a downstream population of around 250 million, is among three highly populated river basins in South Asia originating from HKH (Figure 1.1), followed by Ganges and Brahmaputra (Lutz et al., 2016b; Mukhopadhyay and Khan, 2014a). In line with remarkable population growth in the Indo-Gangetic plain, there would be an increased food demand in future. The Indus basin hosts the Indus Basin Irrigation System (IBIS), one of the world's largest and most intensive man-made irrigation networks (Karimi et al., 2013). Irrigation water for the IBIS originates from HKH and is regulated by two major reservoirs, i.e. Tarbela dam on River Indus and Mangla on River Jhelum. The rainfall on the IBIS is deficient in general (<200mm) (Ali et al., 2009); hence these upstream water sources are critical to sustaining this irrigation system. Thus, any change in the UIB's hydro-climatic regime will directly affect the inflow to IBIS and, consequently, the food supplies of millions of people living downstream (Tahir et al., 2011). Also, water logging with poor drainage, soil salinity, increasing supply and demand gap, environmental degradation, and political disagreements among stakeholders are other significant challenges in UIB (Qureshi, 2011). All of these challenges may be exacerbated by climate change. Therefore, modelling the hydro-climatic regime and glacier and snowmelt contribution to the river flow under current and future CC scenarios is essential.

1.5 RESEARCH QUESTIONS AND OBJECTIVES

The overarching aim of this PhD research study is to improve understanding of the hydro-climatic regime of the high altitude Upper Indus Basin under current and future scenarios. The research attempts to reduce underlying uncertainties in precipitation and temperature observations by utilising global precipitation and temperature datasets and improved water balance and flow simulations. To address and answer the scientific concerns discussed in previous sections, the following main research questions were explored in this study:

1. How successfully can a data parsimonious model reproduce the daily flow in the data-scarce region using global precipitation products?
2. What are the basin-scale and elevation-distributed glacier and seasonal snowmelt contributions to the river flow?
3. How differently do temperature index and energy balance based sub-routines simulate the glacier melt?
4. What is the future hydro-climatic regime due to projected changes in precipitation and temperature under climate change by the end of the 21st century?

The particular objectives for this study include:

1. Simulating the hydrological regime of the snow-fed and glaciarised Gilgit Basin in the Upper Indus using global precipitation products and a data parsimonious precipitation-runoff model (Research questions 1 and 2 addressed in Chapter 2)
2. Analysing the elevation-distributed hydrological regime of the highly glaciated and snow-fed Hunza Basin in the Hindukush Karakoram Himalaya (HKH) region (Research questions 1, 2 and 3 addressed in Chapter 3)
3. Changes in the hydro-climatic regime of the Hunza Basin in the Upper Indus under CMIP6 climate change projections (Research question 4 addressed in Chapter 4)

2

SIMULATING THE HYDROLOGICAL REGIME USING GLOBAL PRECIPITATION PRODUCTS AND A DATA PARSIMONIOUS PRECIPITATION-RUNOFF MODEL

This chapter is based on the following publication.

Nazeer, A., Maskey, S., Skaugen, T., McClain, M.E:. Simulating the hydrological regime of the snow fed and glaciarised Gilgit Basin in the Upper Indus using global precipitation products and a data parsimonious precipitation-runoff model: Science of the Total Environment: 149872. https://10.1016/j.scitotenv.2021.149872. 2021

ABSTRACT

In many high altitude river basins, the hydro-climatic regimes and the spatial and temporal distribution of precipitation are little known, complicating efforts to quantify current and future water availability. Scarce, or non-existent, gauged observations at high altitudes coupled with complex weather systems and orographic effects further prevent a realistic and comprehensive assessment of precipitation. Quantifying the contribution from seasonal snow and glacier melt to the river runoff for a high altitude, melt dependent region is especially difficult. Global scale precipitation products, in combination with precipitation-runoff modelling may provide insights to the hydro-climatic regimes for such data scarce regions. In this study, two global precipitation products; the high resolution (0.1°×0.1°), newly developed ERA5-Land, and a coarser resolution (0.55°×0.55°) JRA-55, are used to simulate snow/glacier melts and runoff for the Gilgit Basin, a sub-basin of the Indus. A hydrological precipitation-runoff model, the Distance Distribution Dynamics (DDD), requires minimum input data and was developed for snow dominated catchments. The mean of total annual precipitation from 1995–2010 data was estimated at 888 mm and 951 mm by ERA5-Land and JRA-55, respectively. The daily runoff simulation obtained a Kling Gupta efficiency (KGE) of 0.78 and 0.72 with ERA5-Land and JRA-55 based simulations, respectively. The simulated snow cover area (SCA) was validated using MODIS SCA and the results are quite promising on daily, monthly and annual scales. Our result showed an overall contribution to the river flow as about 26% from rainfall, 37-38% from snow melt, 31% from glacier melt and 5% from soil moisture. These melt simulations are in good agreement with the overall hydro-climatic regimes and seasonality of the area. The proxy energy balance approach in the DDD model, used to estimate snow melt and evapotranspiration, showed robust behaviour and potential for being employed in data poor basins.

Key Words: Distance distribution dynamics (DDD), energy balance, ERA5-Land, Gilgit basin, glacier melt, JRA-55, hydrological regime, snow simulations, Upper Indus basin, water balance

2.1 INTRODUCTION

Precipitation (P) is the major component in the hydrological cycle but its estimation is the most difficult (Herold et al., 2017). In the Hindukush Karakoram Himalaya (HKH) region, the spatial and temporal distribution of precipitation is largely unknown (Immerzeel et al., 2015). Precipitation can vary enormously over short horizontal distances because of orographic effects and the relation between altitude and precipitation (Bookhagen and Burbank, 2006). The Eastern and South Eastern parts of the HKH region receive summer precipitation due to the Indian monsoon, while the Western part receives most of its precipitation in the winter and spring seasons (mostly as snow) under the westerlies effect from the Caspian and Mediterranean seas (Minora et al., 2016). This east to west synoptic scale inconsistency in the precipitation system in the HKH region leads to variations in glacier accumulation (Minora et al., 2013). Moreover, there is a very low gauge density in the valley floors and virtually no gauges at high altitudes, making rainfall estimates uncertain. Therefore, there is a persistent need to develop and improve the quantification of precipitation at high-altitudes (Immerzeel et al., 2015; Lutz et al., 2014).

In high elevation mountainous watersheds, glacier and snow melt make a significant contribution to flow, which makes them important to the hydrological cycle and downstream water supply, particularly during dry periods (Barnett et al., 2005; Hasson et al., 2014). The largest glaciers of the world after the polar regions (i.e. Arctic circle and Antarctica) are situated in the HKH region (Mukhopadhyay and Khan, 2014a). Water from the HKH region and the neighbouring Tibetan Plateau (TP) are the origin of large river systems such as the Brahmaputra, Ganges, and Indus. Thus, any changes in the glaciers in these mountain ranges may have serious consequences for the future availability of water for almost 800 million people residing in these large river basins (Mukhopadhyay and Khan, 2014b).

Quantifying the contributions from seasonal snow and glacier melt to river runoff are challenging but essential for the management and planning of water resources (Schaner et al., 2012). Snow-accumulation measurements with snow pillows and snow pits are also rare and generally limited to short records in the HKH region (Immerzeel et al., 2012). In 1995, the Water and Power Development Authority (WAPDA) of Pakistan installed snow pillows at various sites on the Pakistan side of the HKH region in a joint venture with a Canadian team (SIHP: Snow and Ice Hydrology, 1997). However, many of the installed pillows faced transmission system issues and unexpected “jumps” associated with ruptures and ice bridging effects. The remotely sensed data coupled with a geographical information system (GIS) has proved a powerful tool for mapping glaciers and snow covers in inaccessible and rugged terrains (Tong et al., 2009). However, these snow and glacier monitoring techniques by remote sensing data are subject to various limitations and biases, including cloud coverage, dense vegetation, surface heterogeneity, low

resolution and spectral similarities (Berthier et al., 2006). Consequently, the current understanding of snow and glacier cover status and their contribution to the river runoff is poor and based on insufficient analysis with very limited data. So increased measurement of ongoing accumulation and melt rates for snow and glaciers is needed to estimate future regional water resources availability (Barnett et al., 2005).

Recent studies by Cannon et al. (2015) in the HKH region indicate a strong and enhanced frequency of winter westerlies (1979-2010) and consequently increased winter precipitation. Kapnick et al. (2014) concluded that the Karakoram snow fall is not reduced due to climatic warming as the seasonal snowfall cycle is subjected to the westerlies instead of monsoon winter precipitation. Michaelides et al. (2009) noted that there are four principal methods to estimate precipitation: (1) ground-based gauges, (2) ground-based radar, (3) satellite based remote sensing 4) atmospheric reanalysis products. The ground based gauges have a problem of gauge density and cannot reflect the true rainfall variability and thus resulting in inaccurate assessments of areal rainfall (Andréassian et al., 2001). The ground based radars have higher spatio-temporal resolution but have limited coverage and are thus restricted to regional scale estimates (Martens et al., 2013). Satellites can observe large areas with high spatio-temporal resolution compared to radar (Smith, 2006) but satellite based estimates are vulnerable to systematic biases, unable to detect low intensity rainfall, and perform poorly over surfaces covered with snow and ice (Mugnai et al., 2013). Reanalysis products are suitable for describing large-scale weather systems, but tend to fail on the variability because of their low spatio-temporal resolution (Kidd et al., 2013). These products can, however, potentially provide precipitation estimates in data scarce regions, assist to fill gaps in data, and ultimately support a better understanding of the hydrology (Shafeeque et al., 2019).

Hydrological models vary in process representation, applications and spatial scale ranging from small catchments to global scale (Skaugen et al., 2018). For snowmelt estimation, there are two basic modelling approaches, i.e. the energy balance and the temperature index (Prasad and Roy, 2005). Several snowmelt estimating models have been designed for specific needs and various hydrologic conditions. Some of these models are very intensive regarding input data and/or complicated to set up and operate**.** Only a few models can handle difficult hydrologic conditions (Tekeli et al., 2005), like in the HKH region with its very high altitude, complex topography and weather system. Investigating snow and glacier conditions in data poor basins and with a changing climate requires models that: (1) are efficient in terms of running at varying spatial and temporal scales; (2) are parsimonious in terms of input data; and (3) have physical and identifiable model parameters (Skaugen et al., 2018). Many snow model inter comparison projects have been launched in the last decades for different aims with common conclusions

including: (1) there is no 'best' snow model and; (2) complexity in model structure does not necessarily mean improved performance (Essery et al., 2013).

The economy of the Indus region largely depends upon irrigated agriculture, and irrigation systems in the region are highly depend on melt water (Akhtar et al., 2008). There is an increasing food demand in line with a remarkable growth of population in the Indo-Gangetic plain. Almost 70% of the total flow in the River Indus is generated by seasonal snow and glacier melt from the UIB (Mukhopadhyay and Khan, 2015; SIHP: Snow and Ice Hydrology, 1997). The Indus Basin Irrigation System (IBIS) is the largest irrigation system world-wide, irrigating 17 million hectares (M ha) of a total 24 M ha of the cultivable area in Pakistan (Akhtar et al., 2008; Khan et al., 2014).

The primary analysis of observed hydro-meteorological data of Gilgit River (one of the main tributaries of Indus) shows an annual average runoff of about 743 mm for the 1995–2010 period. But the basin-averaged annual precipitation derived by the arithmetic mean of the data from four installed stations in the Gilgit Basin shows 277 mm for the same period. During the hydrological model's calibration and validation frameworks, this underestimated precipitation is often compensated through sub-optimal adjustment of the model's parameters (for example evapotranspiration, soil properties, melt factors, etc.) (Lutz et al., 2014). These calibrated parameters can hence induce uncertainties and biases for flow dynamics. Few modelling based investigations (Adnan et al., 2017; Latif et al., 2020; Tahir et al., 2016) were carried out for the Gilgit basin and all of these used a temperature index approach. In snow fed and glaciated basins, the temperature-index based hydrological models often inadequately represent the prevailing energy balance and may not accurately simulate hydrologic processes (Dahri et al., 2021). To derive and understand the hydrological processes, especially for glaciated and snow covered basins with little or no observations, we see a need for more realistic and spatially distributed precipitation estimates. Hence our analysis is novel in four ways; i) in our model, the snowmelt and evapotranspiration are simulated using the energy balance approach, not using calibrated temperature index models, ii) the parameter parsimony of our model makes it more realistic where, unlike other modelling approaches, the flow dynamics are derived partly from catchment characteristics using GIS, iii) we also took advantage of more recent global precipitation datasets, for example, ERA5-Land and the satellite datasets, for example, Randolph glacier inventory (RGI) version 6.0 and LandSat-8 and iv) we have assessed the performance of our model using the Kling Gupta efficiency (KGE) that describes correlation, errors in variability and bias and addresses several apparent shortcomings in Nash–Sutcliffe Efficiency (NSE). In addition, we have also attempted to quantify the different flow components and the water balance for the Gilgit basin. The overarching objective of this study is to improve the current understanding of hydrological regime of the snow fed and glaciated Gilgit basin using precipitation-runoff

modelling and global precipitation products. To derive and understand the hydrological processes for a glaciated and snow covered basin with little or no observations, we see a need for more realistic and spatially distributed precipitation estimates using more recent global data sets. In addition, we believe that by applying a comparatively newly developed modelling approach (semi-distributed, parameter-parsimonious and developed for different parts of the world but similarly snow/glacier dominated basins), this study complements the previous modelling studies to enhance our understanding of the basin's hydrological regime. The outcomes of this study include improved precipitation estimates, enhanced understanding of the flow regime, snow covered area (SCA), snow water equivalent (SWE) and glacier melt (GM). The study also includes the SCA validation against the satellite data and assesses the consistency of the snow water equivalent and glacier melt with the hydro-climatic regime of the region.

2.2 STUDY AREA

The Gilgit Basin, one of the sub-basins of the UIB in the Hindu Kush mountainous region, was selected for this study. The basin lies between the longitudes of 35°46'05" to 36°1'16" N and latitudes of 72°25'02" to 74°19'25" E with an area of 12726 km^2 as derived from the Shuttle Radar Topography Mission (SRTM) 30 m digital elevation model (DEM). The elevation of the basin varies from 1454-7151 meters above sea level (masl), with a mean elevation of 4054 masl. The Randolph Glacier Inventory (RGI 6.0) (Muhammad et al., 2019), showed that the basin has a glacier cover of about 8.1 % (1030 km^2) with more than 75% above an elevation of 4500 masl (Figure 2.1). The seasonal snow cover varies from 95 % in winter to 5 % in summer (Adnan et al., 2017; Hasson et al., 2014). The elevation gradient in the Gilgit basin is very steep and about 70% of the area lies between 3500-4900 masl (Table 2.1). Gilgit River starts from Shandoor Lake at an elevation of about 3738 masl. The seasons of this region are generally divided into four; winter season (Dec, Jan, Feb); spring season (March, April, May); monsoon season (June, July, August, September) and post monsoon season (October, November). The river network in this basin consists of a few main tributaries like the Yasin, Phandar, and Ishkoman. The river flows in a North West to South East direction, passes through Gilgit City, and joins River Hunza at Alam Bridge and finally joins the river Indus. Gilgit River has an annual mean runoff measured at the Gilgit Bridge gauging station from 50 years of record (1961-2010) of 288.6 m^3/s. However, hydrological modelling based quantitative evaluation of the contributions of melt water from seasonal and perennial snows and glaciers are rarely available.

As the climatic variables are strongly influenced by altitude, the altitudinal variation of about 6000 m gives Gilgit Basin a complex climate (Sharif et al., 2013). The valley floors of the basin are arid with annual rainfall ranging from 100 to 200 mm, but at a higher

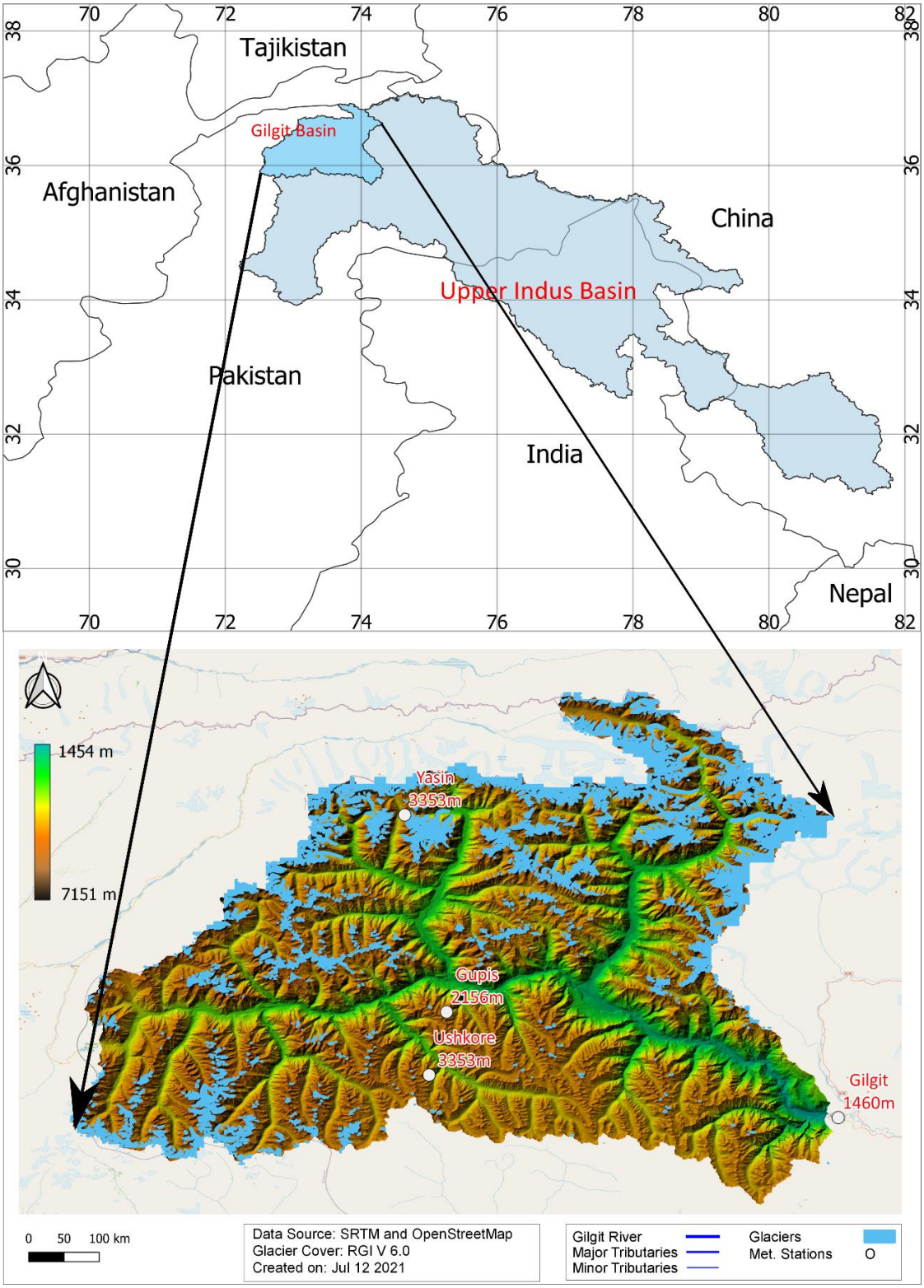

Figure 2.1. Location of study area with Digital Elevation Model (DEM), glacier cover, river network and meteorological stations

elevation, precipitation increases (Cramer and Leemans, 1993). The climate of the basin is a result of the complex interaction among monsoon circulation, westerlies effects and the local topography. The monsoon is the primary and largest source of precipitation in the Himalayan range, but this influence decreases moving in a north-western direction, and mid-latitude westerlies become the primary source of precipitation (Lutz et al., 2016b). The Hindukush range receives precipitation from both of these sources and gives the basin two main periods of maximum precipitation; the winter/spring period from December to April (i.e. the westerlies influenced period) and the summer period July through September (i.e. the monsoon influenced period) (Bocchiola et al., 2011). The mean monthly temperatures in areas above 3000 masl, influenced by the westerlies, remain below the freezing point between October and March. There is hence no direct flow during this period (Archer and Fowler, 2004). For this low flow period, runoff is mainly due to the precipitation from lower altitudes and groundwater discharge (Hasson, 2016). For summer, the runoff from higher elevations is primarily due to seasonal snow and glacier melt. The Gilgit Basin hosts four metrological stations (Gilgit, Gupis, Yasin and Ushkore) at elevation ranges from 1460 to 3353 masl. The Gilgit and Gupis stations are at low altitude and have long records available from 1951 to the present. While the high altitude Ushkore and Yasin stations records are available from 1995 to present.

Table 2.1. Hypsometry of the Gilgit basin (divided into 10 elevation bands of equal area) and glacier cover

Area	Area quantiles	Elevation range (m)	Mean elev. (m)	Glacier cover (%)
a1	10	1454-2916	2185	0
a2	20	2917-3441	3178	1
a3	30	3442-3772	3606	2
a4	40	3773-4019	3895	3
a5	50	4020-4213	4116	3
a6	60	4214-4369	4219	4
a7	70	4370-4515	4442	6
a8	80	4516-4677	4596	11
a9	90	4678-4899	4788	19
a10	100	4900-7151	6025	32

2.3 DATASETS & METHODOLOGY

2.3.1 Meteorological data

The meteorological data for Gilgit Basin were obtained for four stations in the basin from the Pakistan Metrological Department (PMD) and Water and Power Development Authority (WAPDA), federal level departments of Pakistan. Two of these stations; Gilgit (1460 masl) and Gupis (2156 masl) were installed by PMD and the remaining two; Yasin (3353 masl) and Ushkore (3353 masl) by WAPDA (Table A.1, Annexes). These data are freely available for research purposes. PMD records meteorological data are at relatively low altitudes from 1952 to present. WAPDA records hydro-meteorological data, with stations at comparatively high altitudes, but for a relatively short period. These stations have monthly maximum precipitation in the month of April and minimum in November, while the seasonal data have maximum precipitation in winter/spring season and minimum in the autumn/early winter. From the 1995–2010 records, the Gilgit station has the minimum precipitation and Ushkore station the maximum. The mean annual precipitation, recorded from to 1952-2008, is 135 mm and 185 mm for Gilgit and Gupis stations, respectively (Tahir et al., 2016), while the mean annual precipitation recorded from to 2002-2010 data is 367 mm for both Yasin and Ushkore stations (Figure A1, Annexes). All these records, however, contain missing data varying from a single day to a full year.

The annual average temperature at Gilgit, Gupis and Ushkore climatic stations was 15.99°C, 12.8°C and 6.02°C, respectively, for the 1995–2010 period. Monthly mean figures show that maximum temperature was recorded in July and minimum in January for all stations (Figure A.2, Annexes). There is clear daily variability in temperature that ultimately affects all hydrological processes related to temperature.

2.3.2 Runoff data

The Gilgit River has a gauging station installed at Gilgit Bridge at an elevation of 1454 masl. Daily runoff data are recorded and maintained by WAPDA with a period of record running from 1966 to the present. According to hydrological regimes defined by Krasovskaia et al. (1994), the observed runoff shows two major flow regimes. One is the low flow regime or the base flow from October to March. The main source of this flow is liquid precipitation and groundwater discharge. The second is the high flow regime from April to September. This high flow regime is further divided into two regimes: one is snowmelt dominated from April to mid/late June and the second is glacial melt dominated from late June to the end of September (Hasson, 2016; Mukhopadhyay and Khan, 2014a). Similar to other high elevation basins in the HKH region, melt contribution is significant in the Gilgit Basin. Runoff data from 1995 to 2010 were used in this study.

2.3.3 Precipitation from global datasets

Many global products have been developed and are freely available with varying data sources, temporal coverage, temporal resolution, spatial coverage and spatial resolution. The following two products are selected for this study.

i. ERA5-Land

The European reanalysis 5 (ERA5) Land is a newly developed data set available for the period from 1981 to the present with 2-3 months delays. ERA5-Land data have 0.1° degree spatial resolution and hourly temporal resolution and were acquired freely from https://cds.climate.copernicus.eu/. The temporal and spatial resolutions of ERA5-Land are high and make it very useful for all kinds of land surface applications such as flood or drought forecasting. The model used in the production of ERA5-Land is the tiled European Centre for Medium-Range Weather Forecasts (ECMWF) Scheme for Surface Exchanges over Land incorporating land surface hydrology (H-TESSEL). The data are produced under a single simulation without coupling to the atmospheric module of the ECMWF's Integrated Forecasting System (IFS) or to the ocean wave model of the IFS. It runs without data assimilation, making it computationally affordable for relatively quick updates (Muñoz Sabater, 2019). ERA5-Land is selected for this study because it is the latest published data from ECMWF and has a fine spatial resolution.

ii. JRA-55

The Japanese reanalysis (JRA-55) data set is the non-gauge corrected, third-generation reanalysis spanning from 1958 to the present with several days delay. The data have 0.56° spatial resolution and 3-hourly temporal resolution and were acquired freely from http://jra.kishou.go.jp/JRA-55/. Compared to the previous generation reanalysis data sets of the Japanese Meteorological Agency (JMA), JRA-25, JRA-55 uses a further advanced data assimilation scheme, several new observational data sources, increased model resolution and a new bias correction technique for satellite data (Kobayashi et al., 2015). JRA-55 is selected for this study due to its documented performance in literature and from an initial analysis where it showed reasonable precipitation estimates for our case study.

2.3.4 Satellite based data

The satellite based data used in this research include the Shuttle Radar Topography Mission (SRTM) 30 m DEM, the Randolph Glacier Inventory (RGI 6.0), and land cover data from LandSat-8 and Moderate Resolution Imaging Spectroradiometer (MODIS) satellite data. SRTM data are generated by the U.S. National Aeronautics and Space

Administration (NASA) and are accessed freely from their official website. These data were used for catchment delineation, area elevation information, river network and to derive model parameters for the precipitation-runoff model. The RGI is an initiative by Global Land Ice Measurements from Space (GLIMS) to monitor the world's glaciers using optical satellites. The RGI data are accessed from the GLIMS database and are used to derive glacier cover in elevation zones in the Gilgit Basin (Figure 2.1). LandSat-8 data are the most recent data by the Landsat Data Continuity Mission (LDCM) with 30 m spatial and 16 days temporal resolution. The MODIS snow and ice data were accessed from published data (Hussan et al., 2020) for the Gilgit basin and used for validating the SCA simulations by the precipitation-runoff model.

2.3.5 Runoff modelling

i. Distance Distribution Dynamics (DDD) hydrological model

The Distance Distribution Dynamics (DDD) model is a conceptual, semi-distributed, catchment based precipitation-runoff model scripted in R and Julia programming that can simulate runoff at daily or even smaller time steps (Skaugen and Onof, 2014). The model was developed by the Norwegian Water Resources and Energy Directorate (NVE) and is used at the Norwegian flood forecasting service. The main aim of developing this model was to keep the number of parameters requiring calibration at a minimum while maintaining the precision and required detail of the simulations (Skaugen et al., 2018). Moreover, a majority of model parameters are derived from observed data and not calibrated against runoff (Skaugen and Weltzien, 2016). The model requires temperature and precipitation input values for all zones. The model simulates runoff for a given catchment, accumulation, melt and distribution of snow, glacier melt, actual evapotranspiration (ET) and saturated and unsaturated soil water (Skaugen and Weltzien, 2016). Snowmelt and evapotranspiration are calculated using an energy-balance (EB) approach. The EB approach consists of proxy models and is driven entirely by precipitation and temperature data. The EB based parameters are calculated using geographical location, Julian day information (for short wave), and algorithms used in Skaugen and Saloranta (2015) and Walter et al. (2005) for energy-balance modelling. The following is the main EB equation used in the DDD model;

$$M = (S_w + L_a - L_t + H + LE + G + R - CC) \times \left(\frac{1}{\lambda_F \times \rho_w}\right) \qquad (2.1)$$

Where; M: change in the snow water equivalent in mm,
S_w: net short wave radiation in KJm^{-2}, L_a: atmospheric long wave radiation in KJm^{-2},
L_t: terrestrial long wave radiation in KJm^{-2}, H: sensible heat exchange in KJm^{-2},
LE: energy flux in KJm^{-2} (the latent heat of vaporization), G: ground heat conduction in KJm^{-2},

R: heat added due to precipitation in KJm^{-2}, CC: change in snowpack heat in KJm^{-2}, λ_F: 335 $KJKg^{-1}$ (latent heat of fusion) and, ρ_w: 1000 kgm^{-3} (density of water)

In the subsurface module, the capacity of the subsurface water reservoir is shared between a saturated groundwater zone and an unsaturated soil water zone (Skaugen and Mengistu, 2016). The subsurface variables are updated after evaluating if the current soil moisture together with the precipitation input (rain and snowmelt) represents an excess of water over the field capacity, which is fixed at 30% (Skaugen and Onof, 2014). If so, the excess water is added to the saturated zone.

ii. Setting up the DDD model

GIS analysis was performed using the SRTM 30 m DEM, RGI and LandSat-8 data. The catchment was divided into 10 elevation zones of equal areas as this is the requirement of the model. The LandSat-8 for land cover and SRTM 30 m DEM are used to derive the distances from the points in the catchment to the nearest river for bogs and soil parts of the catchment. These datasets are also used to derive the fractions of land use classes in the catchment (for example, soils and bogs) and the river network. The fraction of glacier area present in all sub areas is derived from RGI 6.0. The basin area is delineated and divided into 10 sub area/zones of equal size and mean elevation is derived for all zones (Figure A.3, Annexes). The runoff dynamics (for example, distances for river network) are derived entirely from catchment characteristics using GIS and recession analysis of runoff (Skaugen and Mengistu, 2016). The degree day factor for glacier melt is calibrated from the range 3.5–7.5 mm/°C/day (Skaugen and Onof, 2014) (Table A.3). The spatial distribution of snow is parameterized using spatial variability in observed precipitation (Skaugen and Weltzien, 2016), in which the shape parameter of gamma distributed unit snow (a_0) and decorrelation length (D) are derived from the relationship between the spatial mean and spatial variance of positive precipitation (excluding zeros). The temperature is calculated for each elevation zone applying temperature lapse rate on Ushkore station (3353 masl) data. To derive the lapse rate, first, the lapse rate existing among all stations located at different elevations was derived using equation 2.2. Then simple arithmetic mean was calculated to get one weighted value for the daily interval of n.

$$TLR = (T_i - T_j)/(Z_i - Z_j) \qquad (2.2)$$

TLR is the temperature lapse rate, T_i and T_j are the temperature values measured at stations *i* and *j*, respectively and Z_i and Z_j are elevations ofstations *i* and *j*, respectively.

The precipitation data were derived for the whole catchment from ERA5-Land and JRA-55 and were further derived for all 10 elevation zones. The precipitation data sets are

analysed using command line suite based Climate Data Operators (CDO). The study area is covered with more than 130 grid cells of ERA5-Land and 12 grid cells of JRA-55 data. To facilitate the data extraction for each elevation zone and to capture the northeast part of the study area well, a higher resolution grid size is needed. Both data sets were resampled from their actual resolution to a common resolution of 1 km^2 applying the nearest neighbour algorithm. The DDD model also needs to calibrate some parameters. Table A.2 (Annexes) shows these parameters with the calibration ranges and values used for the current simulations for both datasets. Table A.3 (Annexes) shows parameters calculated using GIS analysis, recession analysis and fixed values.

iii. Performance evaluation

For accuracy assessment, the skill scores of Kling Gupta efficiency (KGE) and bias (%) were used. The KGE (Eq. 2.3) is the goodness-of-fit measure developed by Gupta et al. (2009). KGE describes correlation and errors in variability and bias and addresses several apparent shortcomings in Nash–Sutcliffe Efficiency (NSE) (Knoben et al., 2019). It is increasingly used for model calibration and evaluation with values ranging from minus infinity to 1.

$$KGE = 1 - \sqrt{(r-1)^2 + \left(\frac{\sigma_{sim}}{\sigma_{obs}} - 1\right)^2 + \left(\frac{\mu_{sim}}{\mu_{obs}} - 1\right)^2} \qquad (2.3)$$

Where; r is the linear correlation between observations and simulations, σ_{sim} and σ_{obs} are the standard deviations of simulations and observations, respectively, and μ_{sim} and μ_{obs} are the means of simulations and observation, respectively.

2.4 RESULTS

2.4.1 Climatology of temperature

The mean elevation of the highest elevation zone is 6025 masl, whereas the highest temperature gauge is at 3353 masl. In order to derive the mean temperature for all zones, a temperature lapse rate was applied, considering the Ushkore station (3353 masl) data as a reference. The variation in temperature derived for all zones is high due to the high variation in gauged data. The weighted lapse rate values for all days of the 1995–2010 period were obtained using Equation 2.2. Daily lapse rate (DLR) varied highly from a maximum of -11.48 °C km^{-1} to -3.83 °C km^{-1}. Lapse rates were also calculated for the whole catchment for the whole period (a fixed lapse rate) as well as on a monthly and seasonal basis. The fixed lapse rate (FLR) for the whole time series is estimated as -5.74 °C km^{-1}. For monthly lapse rate (MLR), twelve mean values were derived for all months

showing a maximum lapse rate of -7.04 °C km^{-1} for the month of March and minimum values of -4.81 °C km^{-1} for the month of September. The seasonal lapse rate (SLR) was determined as -6.09 °C km^{-1}, -6.65 °C km^{-1}, -5.03 °C km^{-1} and -5.28 °C km^{-1} for winter, spring, monsoon and post-monsoon seasons, respectively. After comparing these options, SLR was used to derive the temperature of all zones for this study because it induces the least variations in derived temperature for all elevation zones.

2.4.2 Climatology of precipitation

The precipitation for the Gilgit basin is derived from the coarse resolution (0.55°x0.55°) re-analysis data set JRA-55 and the high resolution (0.1°x0.1°) data set ERA5-Land. The daily estimates are quite reasonable for both data sets, except that the JRA-55 data have more wet days compared to the ERA5-Land data. The maximum daily basin mean precipitation in ERA5-Land is 59 mm (on 27 August 1997) and in JRA-55 is 37 mm (on 25 April 2003). Both global datasets have more rainy days in the study area compared to the gauged data. The monthly and annual mean (Figure 2.2) precipitation estimates from global data sets showed improvement in both quantification and temporal variability when compared to runoff than gauged precipitation. The variability in mean monthly precipitation is higher for JRA-55, with a maximum of 141 mm for March and a minimum of 39 mm in July compared with ERA5-Land, which showed a maximum of 108 mm in March and a minimum of 48 mm in November.

The ERA5-Land data indicate the study area receives 25% of its precipitation during winter, 32% during spring, 32% during monsoon and 11% during post monsoon season. The JRA-55 data indicate this proportion to be 32% during winter, 36% during spring, 19% during monsoon and 13% during post monsoon season. As the study area is dominated by westerlies precipitation, both products are in line in capturing the spring precipitation. The basin also receives significant monsoon summer precipitation that generates river flow. The comparison of gridded precipitation with station's data shows JRA-55 performs poorly in observing the monsoon precipitation. However, the ERA5-Land data behave very well in regards to the monsoon precipitation, which might be due to its high spatial resolution. The gauged data showed that the basin has minimum precipitation in the post monsoon season (Oct-Nov), and both datasets capture this. The seasonal trends of maximum precipitation in spring and minimum in post monsoon showed by both data sets are also evident from station data especially for the spring period. The ERA5-Land data showed annual mean precipitation of 888 mm and JRA-55 951 mm, from 1995–2010 data. The ERA5-Land data had maximum rainfall in 1999 followed by 2010 and JRA-55 in 2010 followed by 2003. While the minimum rainfall recorded by both ERA5-Land and JRA-55 was in the years 2000 and 2001. Overall, both data sets are reasonably good for capturing the maximum and minimum precipitation.

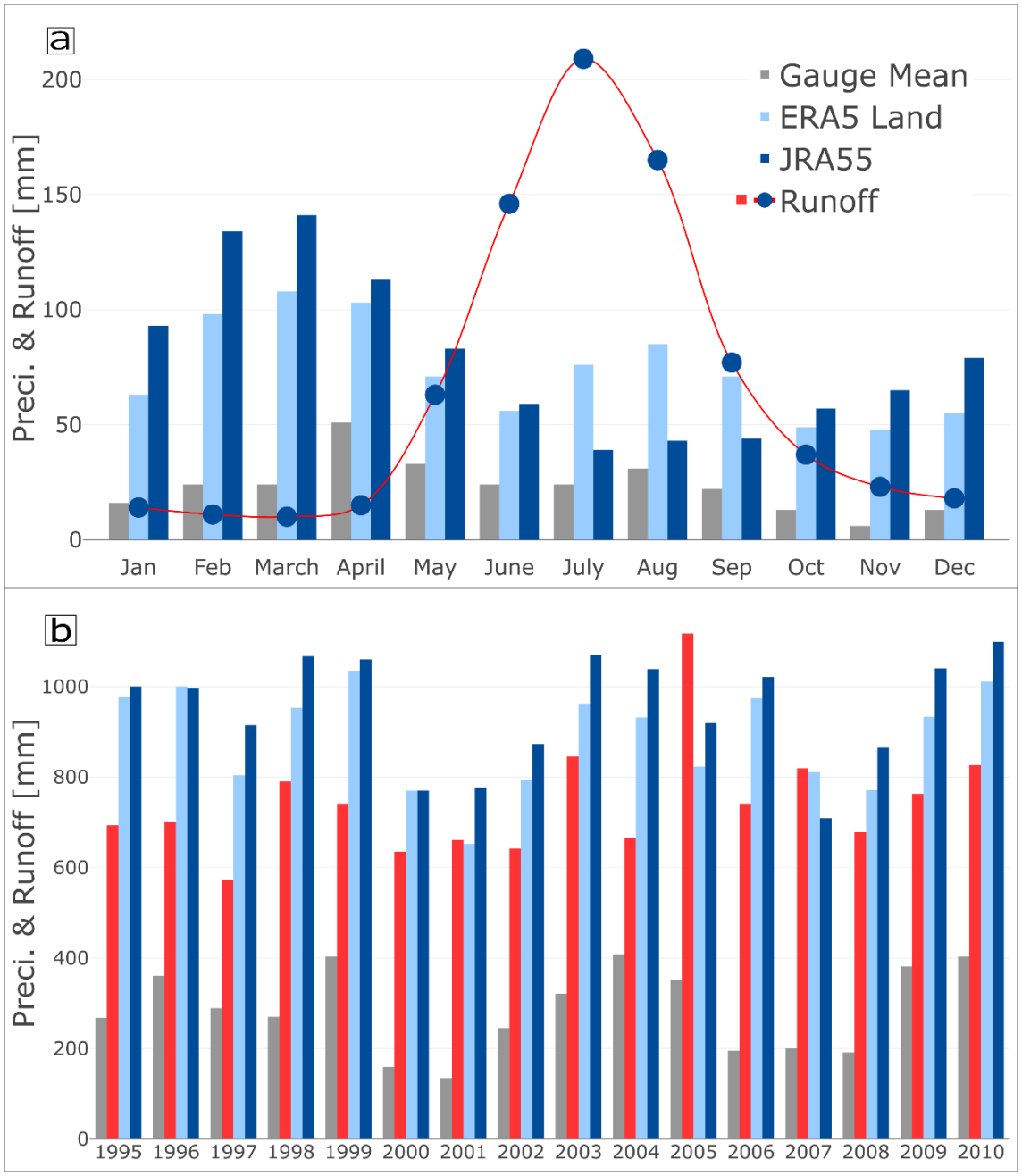

Figure 2.2. Mean a) monthly and b) annual precipitation from European reanalysis 5 (ERA5-Land), Japanese reanalysis (JRA-55), basin-averaged station data and runoff from 1995–2010

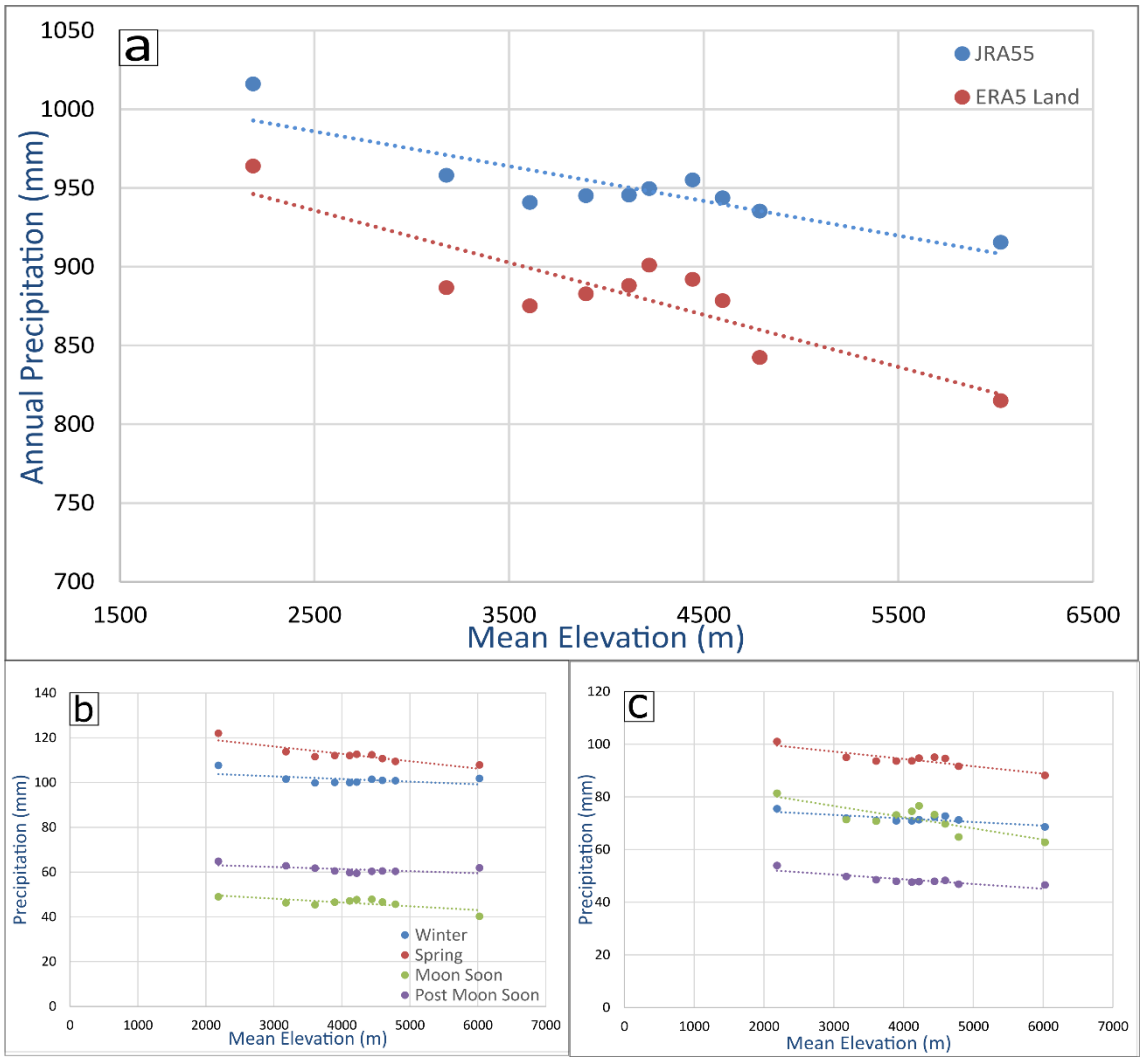

Figure 2.3. Altitudinal variation of a) annual and seasonal b) Japanese reanalysis (JRA-55) and c) European reanalysis 5 (ERA5-Land) based precipitation for 10 elevation zones of the Gilgit basin

The altitudinal analysis of the precipitation estimates from the global data sets revealed unusual characteristics in the study area. The lowest elevation zone showed the maximum annual precipitation while the highest elevation zone received the least annual precipitation for both data sets (Figure 2.3 a). This zonal based analysis shows a negative precipitation gradient in the three lowest zones of the basin (1454 to 3772 masl), a slight positive gradient from the fourth to seventh zones (3773 to 4515 masl) and a negative gradient for the remaining three highest zones (4516 to 7151 masl). The seasonal precipitation also shows a slight negative gradient for both JRA-55 based (Figure 2.3 b) and ERA5-Land based estimates (Figure 2.3 c).

2.4.3 Runoff simulations

The precipitation-runoff model is set up for the Gilgit basin to improve our understanding of the hydrological regime, and in particular, the snow and glacier melts. The model is driven by global precipitation data (JRA-55 & ER5-Land) and gauged based temperature data as main inputs. The SRTM DEM based topography and river network, LandSat-8 based land cover data, and RGI V6.0 based glacier cover data were also used to estimate model parameters and determine catchment characteristics. The over- and/or under-estimation of precipitation by the global products are corrected by applying rain and snow correction factors (Pkorr and Skorr) in the model. The satellite derived snow cover data were used to validate the simulated snow cover area. The model was calibrated on daily flow from 1995-2004 and validated on 2006–2010 data (Figure 2.4). To evaluate the performance of the model in the calibration and validation periods, the efficiency criteria of KGE was used. The model performs satisfactorily in calibration and validation mode using both precipitation products as input to the model. The simulated runoff by the DDD model using ERA5-Land and JRA-55 as precipitation input (respectively) matches reasonably well with the observed flow. Simulations showed promising results for the study area with slightly better performance using ERA5-Land data. The simulations based on ERA5-Land achieved a maximum KGE of 0.76 and 0.78, whereas the JRA-55 based simulation achieved 0.70 and 0.72 for calibration and validation, respectively. The DDD model also simulates the actual evapotranspiration based on the Priestley-Taylor equation, which is quite similar but simplified compared to the Penman-Monteith equation. The annual mean actual evapotranspiration is 203 mm for ERA5-Land based and 221 mm for JRA-55 based simulations. The simulated flows have two peaks, one in early summer, possibly due to the snowmelt contributions and the second in late summer due to the glacier melt. As snow or glacial melt curves are normally gradually changing so the late summer flow peak may be a combination of monsoon and glacier melt, where monsoon causes short term variations in peaks. The simulated flow recession is in good agreement with the observed recession for the whole period. The high peaks of observed flow were not simulated well by the model; however, ERA5-Land data performed slightly better in this regard.

2.4.4 Snow cover area simulations and validation

To simulate the snow in each elevation zone, the model uses a temperature threshold to decide whether the precipitation is snow or rain. Figure 2.5(a) shows how the snow starts melting in March, has a minimum in August and starts accumulating in September. The simulations showed JRA-55 has a slightly higher SCA and more intense snow events due to overestimation of precipitation compared with ERA5-Land. These simulations are

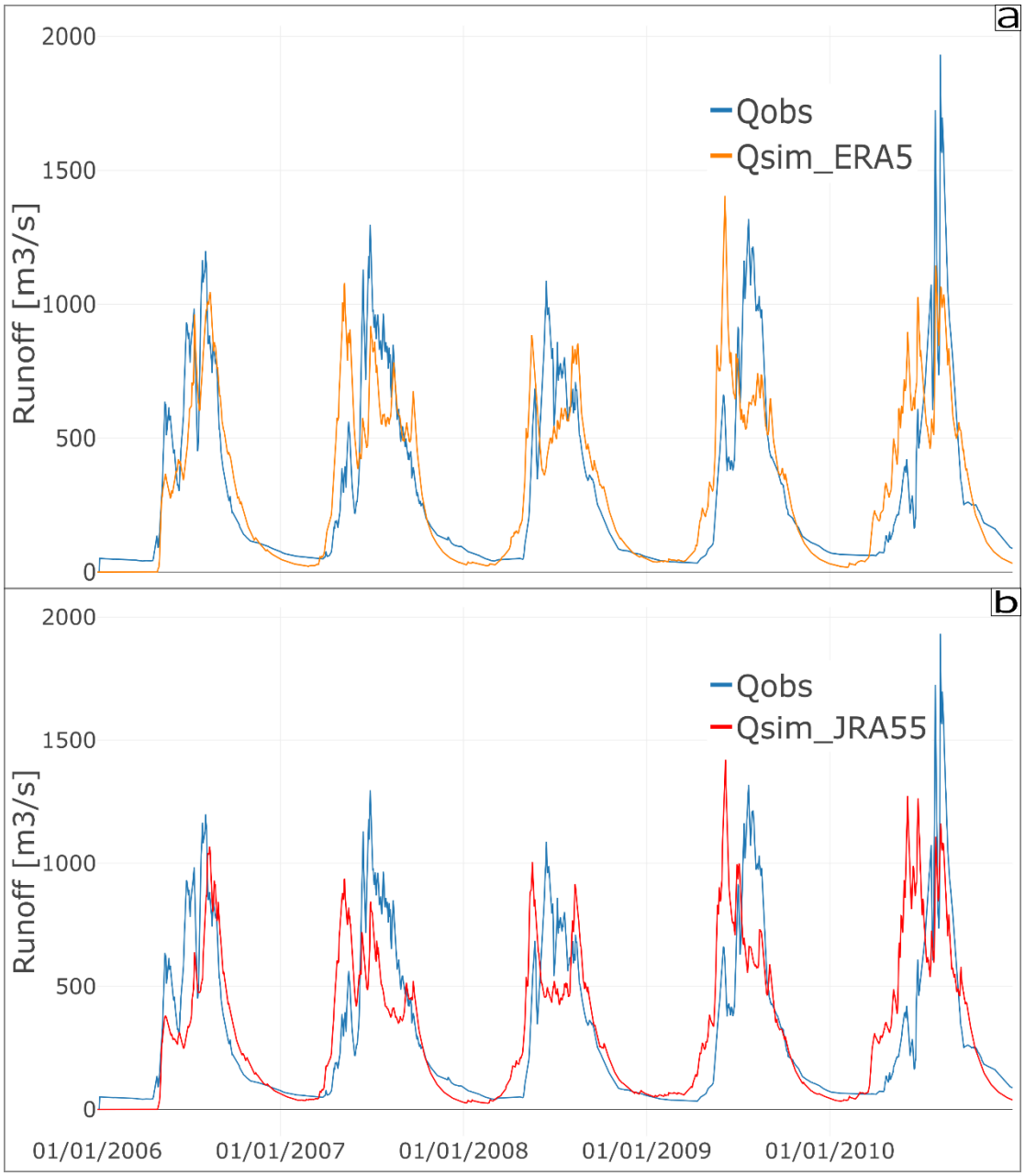

Figure 2.4. Observed runoff vs simulated runoff by model for validation period (2006–2010) using a) European reanalysis 5 (ERA5-Land) and b) Japanese reanalysis (JRA-55) as input

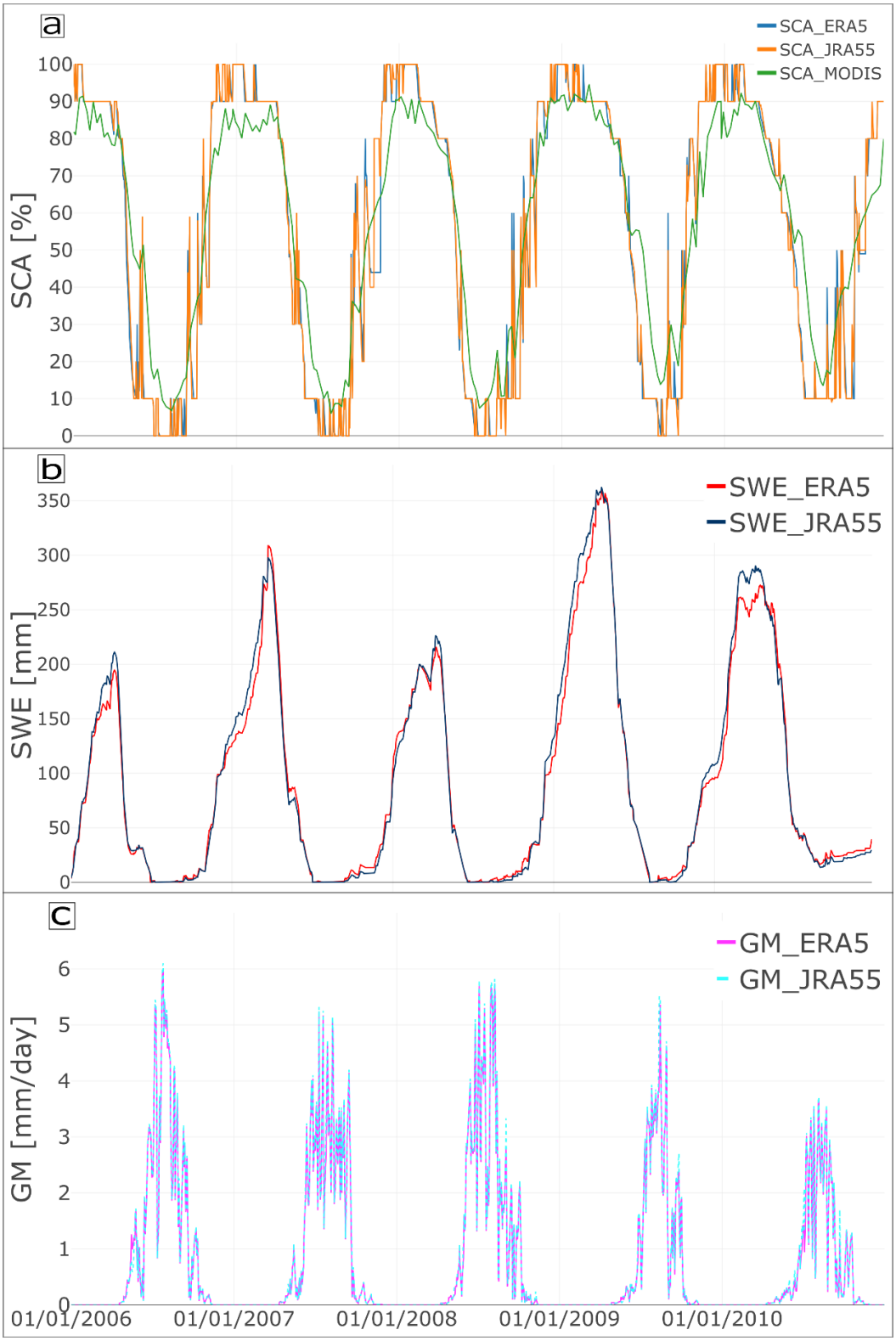

Figure 2.5. Annual mean snow cover area (SCA), snow water equivalent (SWE) and glacier melt (GM) by model and SCA by MODIS

validated with MODIS satellite derived daily SCA from published data (Hussan et al., 2020) for the Gilgit basin from 2006–2010 (Figure 2.5 a). The ablation and accumulation timing of simulated SCA also seems in good agreement with satellite derived SCA. The sudden rise or drop of temperature in the winter or summer season, respectively, generates very short and abrupt snowmelt or snow accumulations. That ultimately causes sudden changes in snow cover evident from both; MODIS SCA and model based SCA. The monthly mean estimates for SCA from DDD and MODIS are in good agreement except that DDD derived SCA has a slightly higher SCA than the MODIS during winter months. The DDD simulated the maximum monthly mean snow cover for January as 97% for both data sets while the MODIS has its maximum in February as 87%. The minimum monthly mean snow cover by both products is 5% as simulated by the DDD model compared to 13% by MODIS data. However, the model simulated SCA for the early summer months (May-July) is slightly lower than the MODIS SCA. The annual mean snow cover (Table 2.2) simulated by the DDD model is 55.3% by ERA5-Land, 55.6% by JRA-55 and 57.5% by MODIS data. The higher values by the MODIS data may be because MODIS considers glacier cover also as snow.

2.4.5 SWE simulations

Figure 2.5(b) shows the time series of SWE simulated by the DDD model using JRA-55 and ERA5-Land as input to the model. The SWE increases in October and peaks in February. With the rise in temperature in March, snowmelt starts contributing significantly to the river runoff and becomes less significant with the start of glacier melt but continues melting until the winter starts in October. Similar to SCA, the SWE based on JRA-55 data is slightly higher than ERA5-Land based estimates. The SWE varies highly due to variability in temperature. The model simulated the maximum monthly mean SWE in February as 336 mm using ERA5-Land and 360 mm using JRA-55. Maximum SWE is simulated for 2009 as 382 mm by ERA5-Land and 376 mm using JRA-55, while minimum SWE is for 2007, 272 mm and 241 mm by ERA5-Land and JRA-55, respectively. The annual mean (Table 2.2) simulated SWE is 316 mm and 312 mm by ERA5-Land and JRA-55, respectively.

2.4.6 Glacier melt simulations

The glacier melt from the study area is calculated using a degree day approach, built as a subroutine in the DDD model. The study area has 8.1 % glacier coverage (RGI 6.0) between elevations of 3000 m to 7151 m, with more than 75% of glacier cover at an elevation of more than 4500 m. The day to day glacier melt varies greatly mainly because of variation in temperature. The simulated glacier melt based on both data sets indicates melt matches well with the flow regime (Figure 2.5 c). The glaciers begin melting in early

summer (end of April) at low altitude (Table 2.1). This melt became significant at the start of May and had a daily mean peak on 10 August of about 5 mm by both JRA-55 and ERA5-Land based simulations. The contribution of glacier melt begins to decline after August and becomes zero by the end of October. The analysis of monthly melt indicates that glacier melt contributes significantly to the river runoff from May to October with a peak in August. Simulations based on both data sets are well matched, except the JRA-55 simulation showed comparatively slightly higher melt for May-June and ERA5-Land showed higher melt for July-September. The annual mean (Table 2.2) melt is 299 mm by ERA5-Land and 307 mm by JRA-55 for the 2006–2010 period. Maximum melt is simulated for 2006 at 361 mm and 366 mm while the minimum is for 2010 at 209 mm and 218 mm by ERA5-Land and JRA-55 based simulations, respectively.

Table 2.2. Annual mean snow cover area (SCA), snow water equivalent (SWE) and glacier melt (GM) by model and SCA by MODIS

Year/	**SCA (%)**			**SWE (mm)**		**GM (mm)**	
Results	ERA5	JRA-55	MODIS	ERA5	JRA-55	ERA5	JRA-55
2006	51.1	51.3	55	347	364	361	366
2007	52.3	53.4	53.1	272	241	328	334
2008	54.5	54.6	56.5	296	319	355	362
2009	62.6	62.3	63.7	382	376	245	253
2010	56.1	56.2	59	285	258	209	218
Mean	55.3	55.6	57.5	316	312	299	307

2.5 DISCUSSION

The temperature is a key input in hydrological modelling and one of the primary sources for analysing energy available for the melt process in high altitude river basins like Gilgit. However, due to an insufficient number of stations installed at higher altitudes and their non-uniform distribution, a temperature lapse rate is being used to derive temperature for higher elevations. Fixed values of lapse rate ranging from -5 to -8 °C km^{-1} have been applied in UIB (Adnan et al., 2017; Tahir et al., 2011) and Qinghai Lake basin of north-eastern TP (Zhang et al., 2014). In this study, available temperature data from stations at different elevations are used to derive monthly lapse rates owing to the notable seasonal variation of temperature lapse rates. We found that the method used to derive the temperature lapse rate (e.g. using annual, seasonal or monthly mean temperatures) makes a significant impact in a melt dominated catchment like the Gilgit. The TLR in the area is at its minimum in the post monsoon season and increases in September and reaches its highest in March. This minimum lapse rate observed for the post monsoon season may be associated with the strong heat exchange process during warm and moist atmospheric conditions (Kattel et al., 2013). Because of the monsoonal effect, moist adiabatic air motion is also frequent. This causes the release of latent heat due to water vapour condensation that increases the near-surface temperature at the higher elevations (Kattel et al., 2015). The winter/early spring records show the highest lapse rate values, potentially due to the weak heat exchange process during cool and dry atmospheric conditions (Barry and Chorley, 2009; Kattel et al., 2013). Moreover, with the increased albedo effect of fresh snow cover during this season, cooling is strengthened at higher elevations.

The precipitation estimates appear more realistic and improved compared to gauged values from 1995–2010. The temporal precipitation distribution in the study area indicates that the basin receives significant precipitation in the form of snowfall during the winter and spring seasons. This is similar to the findings of Tahir et al. (2016), who suggested that the runoff of the Gilgit Basin depends much more on snow and glacier melt than on rainfall. The distribution of precipitation in the study area indicates a very complex weather system due to local orographic effects and the multiple moisture sources, including the winter westerlies and the Indian summer monsoon. Another possible reason may be that the study area is located just above the junction of three high mountain ranges the Hindukush, Himalaya and Karakorum. All these mountain ranges have different and diverse weather systems that ultimately generate very complex and mixed precipitation patterns in the Gilgit basin. In addition, the basin is facing West Karakorum on its eastern part, so the influence of the Karakorum based westerlies winter precipitation is evident from gauged data as well. There is one gauging station very close to the study area on the eastern side (Naltar; 2810 masl) in Karakorum Range. Those

station data show annual average precipitation of about 700 mm and most of it falls in the winter/spring season in the form of snowfall. Winiger et al. (2005) have reported from 1991-96 data maximum annual snow depths of around 1200 and 1800 mm at Dame (3670 masl) and Diran (4050 masl) stations, respectively, in Bagrot Valley (Karakoram range), 20 km northeast of the Gilgit. They also reported that, along the Gilgit-Khunjrab transect within the Hunza basin, precipitation ranges between 600 and 1200 mm within the altitudes of 3500-4500 masl, of which 90% falls as snow.

The global data used in the current study showed a slightly negative precipitation gradient in the study area. One possible reason for maximum precipitation in low elevation areas could be its wide elevation range (1454-2916 m) and the presence of valleys bottoms in this range. Similar features of decreasing precipitation with increasing elevation were observed by Pang et al. (2014) in the central Himalayas, where they concluded that precipitation above an elevation of 2400 masl decreases significantly with increasing elevation. Hasson (2016) suggested that the reason Gilgit has low snow coverage at the higher elevation is that accumulated snow does not persist at high elevations due to the steep slopes. Dahri et al. (2016) concluded from their altitudinal analysis of precipitation distribution in the HKH region that the typical orographic precipitation trend increases up to a certain height of maximum precipitation and thereafter decreases. This negative precipitation gradient is also evident from the station data. For instance, the Gupis station data showed the monthly mean precipitation in April as 62 mm while the higher altitude Yasin station data (3353 masl) showed this precipitation to be 45 mm for the same period. Similar features are evident between Gupis station (2198 masl) with a mean precipitation of 22.5 mm and Ushkore Station (3353 masl) with a mean precipitation of 21.5 mm for September. However, the number of stations is not sufficient and the scarcity of gauging stations discourages the development of a relationship between altitude and observed precipitation. Immerzeel et al. (2013), in their study in the Nepalese Himalayas, concluded that it is difficult to establish a uniform precipitation gradient due to the influence of several scale-dependent mechanisms. Dahri et al. (2016) also concluded that the complex altitudinal variation of precipitation in combination with highly diversified orography and multiple weather systems discourages the formulation of any single relation. Hence, the assumptions of linear increase in precipitation with elevation is not validated by this study.

The evaluation of calibration and validation results shows that the DDD model performs reasonably well for a poorly gauged basin. The model simulates flow and snowmelt based on a newly developed energy balance approach and glacier melt using a degree day approach with global precipitation as input. The model showed a realistic quantitative estimate of melt contributions to the river flow. The main components of the river runoff in the study area include base flow, rainfall, snowmelt and glacial melt. The base flow is

the low flow regime from October/November to March of next year. Base flow comes mainly from ground water, lakes in the study area and snowmelt at lower elevations during winter, where temperature rises above the melt threshold. The timings of peak flows in the observed and simulated hydrographs are different. This may be associated with the reason that these timings of peaks are largely determined by the input precipitation (rainfall/snowfall) and temperature than the parameters of the model. The model calibration aims to achieve the best model performance for the long-term daily discharge. Some improvements in the peak flows (magnitude and timing) may be gained if the calibration is targeted for peak flows only (e.g. if the purpose of the model is for flood forecasting), but even that would not be a lot effective for a long-term simulation. The global precipitation datasets have advantages, particularly at the higher elevation areas where observation data are non-existent. Variability and extremes are the major limitations of global data sets because of their low resolution and deficits in formulating the sub-grid developments (Kidd et al., 2013). So the sharp peaks generated by monsoon rainfalls may not be accurately simulated using global precipitation data sets. Another possible reason may be related to the spatial pattern of snow, which is also impacted by the limited availability of precipitation and temperature data. There are several other reasons associated with why very high skill scores are not achieved, including lack of gauged input data (precipitation and temperature in general), very sparse/no observations for cross validation of glacier melt and snow cover, very complex topography and local scale uncertainties.

Modelling a realistic status of snow, its spatial extent, variability, and contribution to river flow is important for understanding the hydrological regime of the study area. As mentioned previously, the observed temperature in the study area varies highly from a minimum of -14 °C to a maximum of +16 °C and eventually influences all the temperature dependent processes such as SWE, SCA and glacial melt. The initial snowmelt starts at low elevations and extends to areas at higher elevations; the temperature increases later in the summer. The snow accumulation starts in September and even earlier at higher altitudes and peaks in January/February when almost the entire study area (more than 90%) is covered with snow. Similar estimates of SCA were presented by (Hasson et al., 2014), who found the least SCA as 3±1% during the summer season and a maximum of 90±4% during the spring season for the Gilgit basin. Tahir et al. (2016) presented these estimates as varying between 12-85 % for the Gilgit basin based on 2000-2013 MODIS data. The RGI 6.0 data indicated that the study area has about 8.1 % permanent glacier cover. This glacier is covered by snow in winter, but in the summer months, MODIS data may classify 8.1 % of the area as snow when it really is glacier. The DDD model keeps track of SCA and glaciers and this may be the reason why DDD has less SCA than in summer compared to MODIS.

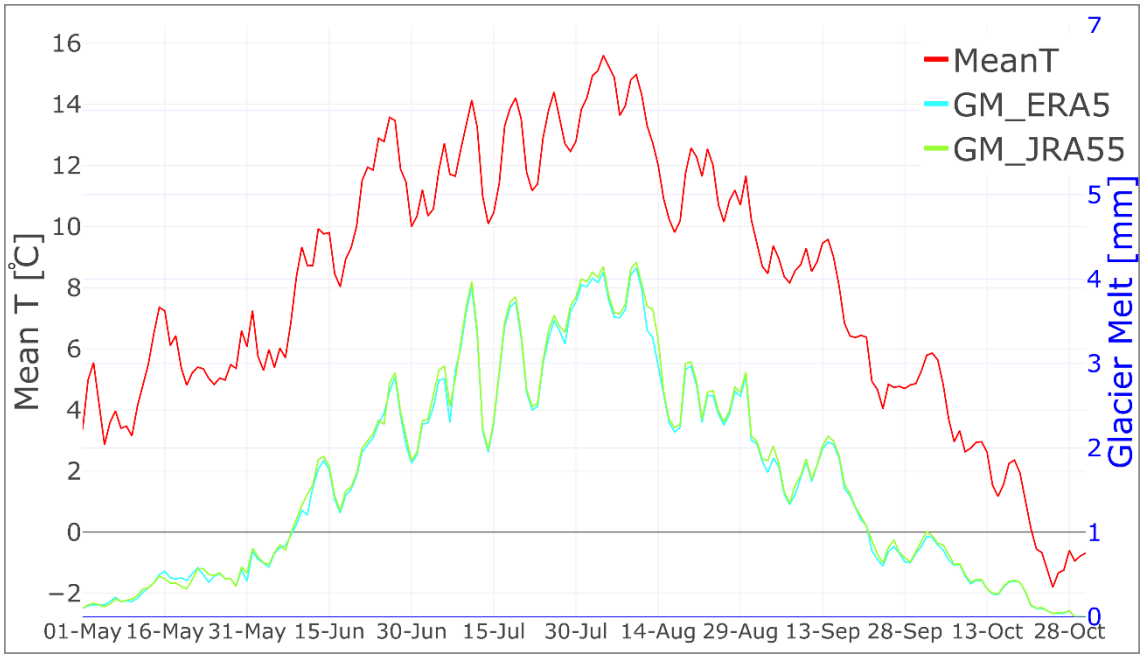

Figure 2.6. Mean daily simulated glacier melt (GM) for melt season (1 May-31 Oct) vs mean daily temperature

The SWE estimates for the basin from 2006–2010 also seem quite reasonable. The DDD model shows SWE estimates for the first time in the region. The snow pillows installed in the region by WAPDA faced transmission and rupture issues and made the SWE records limited to a very few stations. SWE measured at Deosai station (4149 masl) was between 400 and 700 mm from 2008 to 2013 (Hasson, 2016). These observations are higher than our simulated results, but these measurements are from the highly snowmelt dominated Astore Basin located in the Himalayan Mountains and the station is located at a high elevation while the DDD gives a catchment value.

The simulation of glacier melt is carried out using a degree day approach. The glaciers are located in different elevation zones in the study area (derived from Randolph Glacier Inventory V 6.0) and their spatial coverage is used as input to the model. The model simulates the glacier melt on a daily basis from the study area. The melt simulations are in good agreement with the high flow regime of the river. Similar to snowmelt, the glacier melt also varies greatly with the variation in temperature. Figure 2.6 shows variation in mean temperature of the basin versus variations in the glacier melt and possibly this is the main reason behind this variation in glacier melt. The glacier melt timing is in good agreement with the runoff and snowmelt timing of the study area. The snow starts melting in spring while glacier melt peaks in summer, but simulations showed there is an overlap of these melts (Figure 2.7). One reason for this overlap is that the increase in temperature

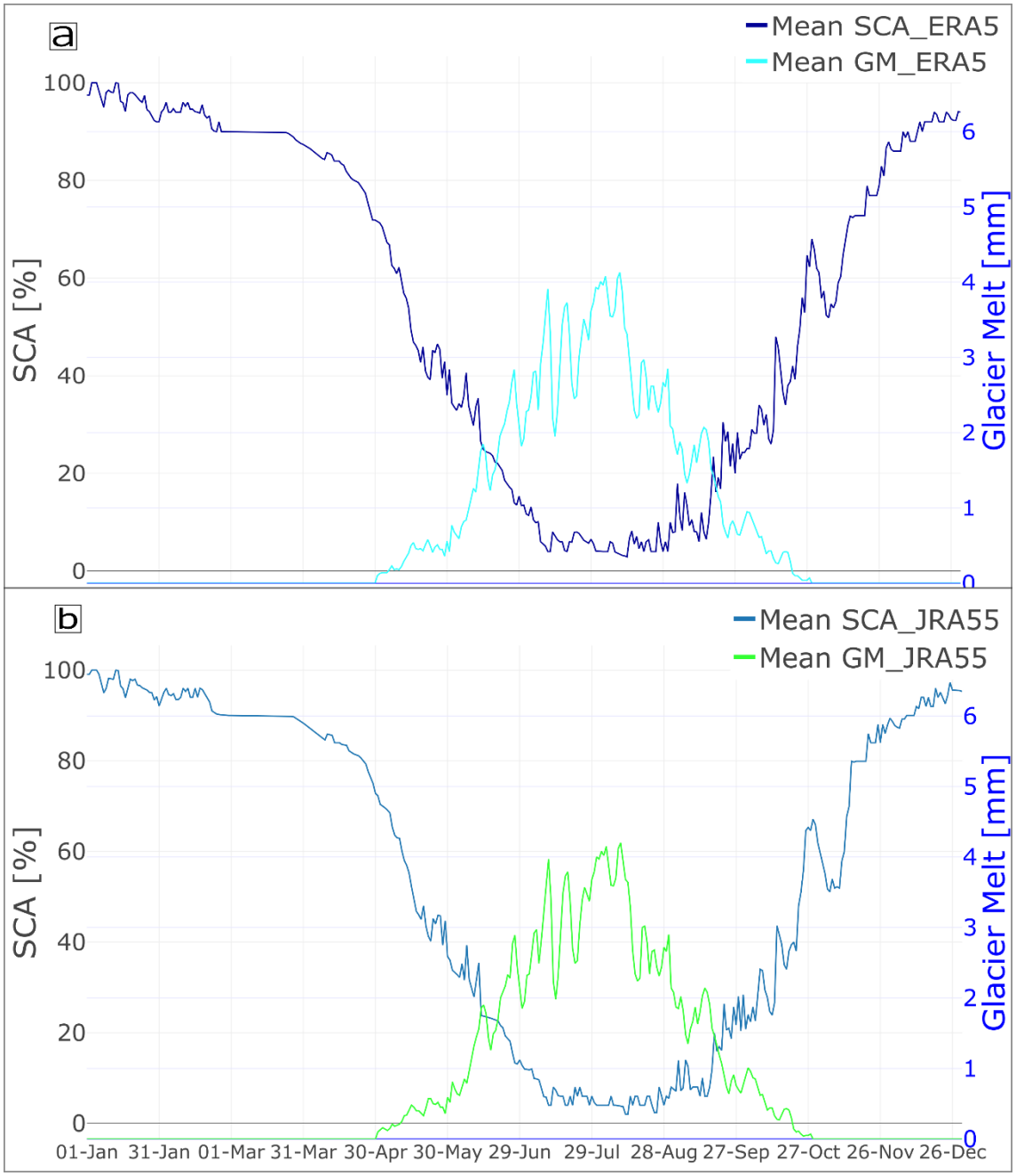

Figure 2.7. Mean daily snow cover area (SCA) vs glacier melt (GM) from simulations based on a) European reanalysis 5 (ERA5-Land) and b) Japanese reanalysis (JRA-55)

in early summer at low altitude can cause the glacier melts at the same time snow is still melting at higher altitudes. Another possibility for this overlapping melt from snow and glacier is that in the glacier melt season, precipitation might fall as snow at a higher

altitude and then melt and contribute to the river runoff. A reverse characteristic is evident at the start of the accumulation season when the snow starts to accumulate due to the decline in temperature in late summer at higher altitudes and at the same time, glaciers from comparatively lower altitudes are still melting. There might always be a mixed melt occurring in some part of the basin. Lutz et al. (2016b) suggested a similar flow composition and mixed melt regimes for the Hunza basin in the west Karakorum. Our findings suggest that separating these snow and glacier melt regimes based on the Julian day or the month as done by Mukhopadhyay and Khan (2015) does not apply in our study catchment.

2.6 WATER BALANCE

Water balance (WB) in a glaciated catchment can be represented as;

$$P + GM = Q + ET \pm \Delta S \qquad (2.4)$$

Where, P is precipitation, GM is the contribution from glacier melt, Q is runoff, ET is the actual evapotranspiration and ΔS is the contribution from storage and soil moisture

Water balance for the Gilgit basin based on our simulations along with the mean percentages of inflow and outflow components is shown in Table 2.3. The inflow components include precipitation as rain, precipitation as snow, glaciers melt, and contribution from snow and subsurface storage and from soil moisture (ΔS). The outflow components include simulated flow and actual evapotranspiration. For the first year, ΔS is minus which means water is added to the soil and this is associated with the presence of snow from the previous year. Our results showed that precipitation as snow contributes more than precipitation as rain in the Gilgit basin. Our simulations showed a mean annual contribution from rainfall of about 26%, snowmelt of about 37-38%, glacier melt of about 31% and storage and soil moisture of about 5% to the river runoff. Mukhopadhyay and Khan (2015) analysed these contributions from the monthly flow of the Gilgit river for two flow (defined as flow due to precipitation as rain plus remnant melt) of about 32.5%, snowmelt of about 38%, and glacier melt of about 29.4%. For the 1980–2010 period, they estimated base flow of about 32.1%, snowmelt of about 41.2%, and glacier melt of about 26.7%. In another paper, Mukhopadhyay and Khan (2014a), from their monthly flow analysis from 1962–2010, estimated mean contributions from the snowmelt of 38-43% and the glacier melt of 23-25%. However, their findings are based on flow regimes periods from 1966-1979 and 1980-2010. For the 1966-1979 period they estimated base analysis and hydrograph separation using historical monthly flow data. Our estimates are based on daily scale modelling results where snow cover is simulated using an energy

balance approach and glacier melt is simulated based on a degree day approach. Our simulation also showed an annual actual mean evapotranspiration of 202–221 mm (21-22% of total outflow). Bhutiyani (1999) estimated annual mean evaporation rates of 222 mm for the Siachen glacier (eastern Karakoram) from 1986 to 1991. Reggiani and Rientjes (2015) estimated this as 200±100 mm for the UIB from 1961 to 2009. Hence, our estimates of mean annual actual evapotranspiration also match well with the previous findings.

Table 2.3. Water balance of the Gilgit basin using European reanalysis 5 (ERA5-Land) and Japanese reanalysis (JRA-55) precipitations as input to the model

Precip. Input	**WB**	**WB/Year**	**2006**	**2007**	**2008**	**2009**	**2010**	**Mean (mm)**	**Mean (%)**
ERA5-L	Inflow	Rain	283	255	195	180	370	256	26.3
		Snow	399	313	344	472	338	373	38.4
		GM	361	328	355	245	209	299	30.8
		ΔS	-177	152	46	82	115	44	4.5
	Outflow	Qsim	656	836	713	798	849	770	79.2
		ET	210	211	226	181	183	202	20.8
JRA-55	Inflow	Rain	235	199	189	213	478	263	26.5
		Snow	434	277	374	460	315	372	37.4
		GM	366	334	362	253	218	307	30.9
		ΔS	-202	184	34	101	146	53	5.3
	Outflow	Qsim	597	753	712	831	970	773	77.8
		ET	235	241	247	195	186	221	22.2

2.7 LIMITATIONS OF THE STUDY

The study has a number of limitations associated with model structure and input data. Precipitation estimates are based on global precipitation products, which have certain limitations associated with spatial resolution, uncertainty, and limited ability to capture extremes. The proxy equations used in the energy balance approach for snowmelt and evapotranspiration have shown reasonable results, although the approach is coarse, i.e. neglecting spatial variability in topography, landscape types, temporal and spatial variability in wind speed and air pressure. The temperature data for all elevation zones in the basin were derived using lapse rates that are based on assumptions such as linear temperature increase with increasing elevation. The calibrated model parameters were not validated against any observed data from the study area. The model can potentially be improved by applying parameters determined by field observation and by applying a finer scale land use cover.

2.8 CONCLUSIONS

Snow and glacier melt contributions to river runoff in the Gilgit basin were simulated using Distance Distribution Dynamics (DDD) model. The DDD model, requires daily precipitation and temperature input data. The precipitation input was derived from Global data sets (JRA-55 and ERA5-Land) and temperature input from station data using estimated lapse rates. The following conclusions can be drawn from this study:

- The precipitation estimates using global data sets for the Gilgit basin showed quite promising results. The coarse grid size of the precipitation product does not necessarily translate into lower accuracy as the JRA-55 with 0.55° resolution performed comparably to ERA5-Land with 0.1° resolution. Most of the precipitation (68% by JRA-55 and 57% by ERA5-Land) in the study area falls as snow in the winter/spring season. A linear variation of precipitation with elevation cannot be applied for such high-altitude mountainous river basins with a complex topography and multiple weather system. The runoff from the study area depends more on snowmelt (37-38%) and glacier melt (about 31%) than on rainfall (26%). Realistic simulation of a variable for which the model is not calibrated against, such as SCA, gives confidence in the model structure and the realism of other simulated variables.
- The overlap in timing of melt from snow and glaciers (Figure 2.7) indicates simultaneous melting for some time periods. The glaciers are located in different elevation zones in the study area, with a higher fraction in higher altitude zones. The increasing temperature in early summer can melt simultaneously the glaciers

at lower altitudes and snow at higher altitudes. Another reason for this overlapping melt is that during the glacier melt season, precipitation may fall as snow at higher altitudes melts and begins contributing to river runoff. In addition, snow does not melt completely; instead, it keeps accumulating and melting throughout the year. The assumptions used in previous investigations that snow is melting first completely before the glacial melt starts are not supported by our results.

- The geographic information system, in combination with remotely sensed data, offers a great potential to understand and derive the runoff dynamics of the system. We found the DDD model reliable for data poor basins, especially with a dominant snow or glacier melt component. Our modelling results provide a basis for future studies to simulate snow and glacier melt in surrounding basins with higher glacier cover. This can eventually facilitate more effective and sustainable downstream water resources management. However, more research in surrounding sub-basins would help to strengthen and further substantiate current findings. The optimization of the model's parameters like liquid content in snow and threshold temperature for snow/rain by in situ measurements from the region might further improve the results.

3

SIMULATING THE ELEVATION-DISTRIBUTED HYDROLOGICAL REGIME USING A REVISED PRECIPITATION-RUNOFF MODEL AND IMPROVED DATA SETS

This chapter is based on the following publication.

Nazeer, A., Maskey, S., Skaugen, T. & McClain, M. E. Analysing the elevation-distributed hydro-climatic regime of the snow- and glacier-dominated Hunza Basin in the Upper Indus (submitted).

ABSTRACT

In the high altitude Hindukush Karakoram Himalaya (HKH) mountains, the complex weather system, inaccessible terrain and sparse measurements make the elevation-distributed precipitation and temperature among the most significant unknowns. The hydro-climatic regimes and elevation-distributed snow and glacier dynamics in the HKH region are also little known, leading to serious concerns about the current and future water availability and management. The Hunza Basin in the HKH region is a scarcely monitored, and snow- and glacier-dominated part of the Upper Indus Basin (UIB). The current study investigates the elevation-distributed hydrological regime in the Hunza Basin. The Distance Distribution Dynamics (DDD) model, with its degree day and an energy balance approach, is forced with precipitation derived from two global datasets (ERA5-Land and JRA-55). The mean annual precipitation for 1997–2010 is estimated as 947 and 1322 mm by ERA5-Land and JRA-55, respectively. The elevation-distributed precipitation estimates showed that the basin receives more precipitation at lower elevations. The daily river flow is well simulated, with KGE ranging between 0.84–0.88 and NSE between 0.80–0.82. The flow regime in the basin is dominated by glacier melt (45–48%), followed by snowmelt (30–34%) and rainfall (21–23%). The simulated snow cover area (SCA) is in good agreement with the MODIS satellite-derived SCA. The elevation-distributed glacier melt simulation suggested that the glacial melt is highest in the lower elevations, with a maximum in zone a2 (14–21 % of total melt). The findings improve understanding by providing helpful information about the elevation-distributed meltwater contributions, water balance and hydro-climatic regimes. The simulation showed that the DDD model reproduces the hydrological processes satisfactorily for such a data-scarce basin.

Key Words: Distance Distribution Dynamics (DDD), energy balance, ERA5-Land, Hindukush Karakoram Himalaya, Hunza basin, JRA-55

3.1 INTRODUCTION

Precipitation is one of the key drivers of the hydrological cycle, but is also among the significant unknowns at high elevations (Immerzeel, Pellicciotti et al. 2012, Ragettli and Pellicciotti 2012). Similar to other mountain basins globally, precipitation is also the main uncertainty in the Hindukush-Karakoram-Himalaya (HKH) region, yet critical for understanding high altitude hydrology (Immerzeel, Pellicciotti et al. 2012). The relationship between precipitation and elevation in the region is poorly defined due to the area's remoteness, inaccessible terrain and sparse measurements (Bookhagen and Burbank 2006, Immerzeel, Wanders et al. 2015).

In high elevation mountain basins, snow and glaciers significantly contribute to the river flow (Barnett, Adam et al. 2005). Snow is an integral part of the climatic system, significantly influencing atmospheric processes because of its low thermal conductivity and high albedo (Hall and Riggs 2007). The snow and glaciers in the HKH region sustain the freshwater availability in the Himalayan and adjacent plains. Seasonal snow and glaciers from the HKH region provide freshwater in the downstream areas from April-Oct (Hasson, Lucarini et al. 2014). Meltwater from the HKH region is critical for the irrigation, hydropower production, and drinking water needs of millions of people in South Asia. This meltwater is also associated with high water levels in lakes and reservoirs and a subsequent increased risk of downstream flooding (Qureshi, Yi et al. 2017).

Measurements of snow accumulation using snow pillows and snow pits in the region are rarely available and limited to short periods (Immerzeel, Pellicciotti et al. 2012). Due to the lack of precipitation data in the Indus Basin, the snow cover area (SCA), snow water equivalent (SWE), and glacier mass balance are not fully known (Bolch 2017). The current understanding of snow and glacier melt contribution to river runoff is based on insufficient analysis and very limited data (Nazeer, Maskey et al. 2021).

Many approaches have been developed within conceptual and distributed hydrologic modelling frameworks to better represent the snow and glacier processes (Shrestha, Koike et al. 2015). There are two basic approaches to simulate snow and glacier melt: degree day and energy balance. The degree day approach only uses temperature for melt simulations. The energy balance model considers the overall energy budget of the system for estimating snow and glacier melt. Energy balance based snow and glacier melt and flow modelling are better suited to accurately describe the hydrologic processes (Shrestha, Koike et al. 2015).

Many recent attempts have been made to simulate the hydrological regime of the Hunza Basin/Upper Indus Basin/ Hindukush-Karakoram-Himalaya region using a variety of input data and modelling approaches. Tahir, Chevallier et al. (2011) applied the snowmelt

runoff model (SRM) coupled with MODIS snow cover data to simulate the Hunza's daily flow under climate change scenarios. They concluded that new reservoirs would require to meet future water needs (e.g. for irrigation, hydropower generation, and drinking water supply) and flood control. Mukhopadhyay and Khan (2014) estimated flow for the Upper Indus Basin (UIB) and concluded there would be long-term reductions in river flows under climate change. Mukhopadhyay and Khan (2015) concluded that glacier melt contribution is higher than snowmelt in the rivers of the Karakoram. Hasson, Lucarini et al. (2014) suggested a decreasing annual snow trend for the westerlies-influenced sub-basins and an increasing trend for the monsoon-influenced sub-basins of the Indus. Shrestha, Koike et al. (2015) applied a distributed biosphere hydrological modelling framework and found that the snow strongly controls the Hunza's flow regime.

The agro-based economy in Pakistan depends on water supplied from the River Indus and its tributaries for irrigation (Raza, Ali et al. 2012). The water for the Indus Basin Irrigation System (IBIS), the largest irrigation system in the world, originates from the HKH region and is regulated by two major reservoirs, i.e. Tarbela on River Indus and Mangla on River Jhelum. The rainfall in the plains of the IBIS is, in general small (<200 mm/year) (Ali et al., 2009), so the upstream snow and glaciers are critical to sustain this irrigation system.

With only three installed precipitation gauges with relatively long records, the Hunza Basin is a scarcely monitored sub-basin of the Indus (Lutz, Immerzeel et al. 2016). Different studies (Tahir, Chevallier et al. 2011, Immerzeel, Pellicciotti et al. 2012, Ragettli and Pellicciotti 2012, Lutz, Immerzeel et al. 2014, Shrestha, Koike et al. 2015, Shrestha and Nepal 2019) used different data (e.g. gauges data with precipitation lapse rates, APHRODITE, virtual weather stations (VWSs), ERA-Interim) to estimate precipitation at high altitudes. From the three observed precipitation data in the Hunza basin from 2000–2004, the mean annual precipitation was 660 mm at Naltar (2810 masl), 292 mm at Ziarat (3669 masl) and 165 mm at Khunjrab gauge (4730 masl) (Shrestha, Koike et al. 2015). Since the mean annual flow is 730 mm for the same period (750 mm for 1997-2010) in the Hunza River, it may suggest that these three stations are insufficient to estimate precipitation of the entire basin and/or there is a significant contribution to the runoff from glacier storage. Also, there appears to be a negative precipitation gradient in the Hunza Basin, with maximum precipitation at lower elevations (Naltar station) and the minimum at higher elevations (Khunjrab station). So, deriving precipitation for higher elevations using simple lapse rates may introduce uncertainty in assessing the important hydrological process. Moreover, the degree day based hydrological models may not accurately simulate snow covered and glaciated basins (Dahri, Ludwig et al. 2021). Also, some studies used a distributed modelling approach; the elevation-distributed snow and glacier melt are rarely analysed.

The novelty and contribution of the current study is the simulation of detailed elevation-distributed hydro-climatic dynamics for the data-scarce Hunza Basin. In addition, we apply a comparatively new modelling approach which was tested in catchments in Norway (Skaugen and Onof 2014). The modelling framework also includes an energy balance (EB) approach for glacier melt simulation in addition to a degree day (DD) approach. The former is more physically based and has no parameters to be calibrated, whereas the latter uses a calibrated effective parameter, the degree-day factor. Moreover, the different components of flow and the water balance for the Hunza Basin are quantified. The elevation-distributed precipitation derived from global datasets is also validated. The overarching objective of this study is to analyse the elevation-distributed SCA, snow and glacier melt (GM), SWE, flow simulations and water balance of the Hunza Basin. This will increase understanding of the flow regime and hydrological processes of such high altitude snow- and glacier-dominated basins.

3.2 MATERIALS AND METHODS

3.2.1 Study area

The Hunza Basin (13,713 km^2) extends from 74.04–75.77°E and 36.05–37.08°N and is located in the Karakoram mountains of the HKH region (Figure 3.1). The Hunza Basin is one of the main sub-basins of the UIB and contributes about 12 % of the total flow of the River Indus upstream of the Tarbela reservoir (Shrestha, Koike et al. 2015). About 80 % of the total flow into this reservoir originates from the snow covered and glaciated parts, which is less than 20 % of the total basin area of the Indus (Archer and Fowler 2004). The Hunza Basin is a high altitude (1425–7889 masl) basin with a mean elevation of 4600 m (Table 3.1). The basin has a dense river network with the Hunza River as the main tributary (232 km long) and Shimshal, Verjerab, Hispar, Hoper, Naltar Rakaposhi, Khunjrab and a few others as minor tributaries (Garee, Chen et al. 2017). The 1966–2010 flow data recorded at the Danyore gauge by the Water and Power Development Authority (WAPDA) of Pakistan shows an average flow of 304 m^3/sec (~710 mm). The Hunza River has minimum flow during the snow accumulation seasons (Nov to early April). Flow increases with temperature and reaches a maximum in July/August (Shrestha, Koike et al. 2015). The climate in the Hunza Basin is arid to semiarid and divided into four seasons; winter (Dec-Feb), spring (March-May), monsoon (June-Sep), and post-monsoon season (Oct-Nov) (Nazeer, Maskey et al. 2021). The HKH region has two primary sources of precipitation; summer monsoon and winter westerlies. The Hunza Basin receives precipitation from both sources, although the winter westerlies contribute about two-thirds of the total precipitation (Bookhagen and Burbank 2010). At the seasonal snow maximum in winter, almost 85 % of the total area is covered with snow (Shrestha, Koike

et al. 2015). The glacier coverage is about 30 % of the total area and is found between 2300 and 7889 masl [RGI v6.0, (Arendt, Bliss et al. 2017)]. The basin hosts extensive glacier systems, including Hispar (339 km^2), Batura (238 km^2), Virjerab (112 km^2), Khurdopin (111 km^2) and a few others.

3.2.2 Input data

i. Hydro-metrological data

The Hunza Basin has three meteorological stations (Naltar 2810 masl, Ziarat 3669 masl, Khunjrab 4730 masl) installed and managed by WAPDA, covering elevations from 2810 to 4730 masl. The meteorological stations record daily temperature and total precipitation. The mean temperature and precipitation data from 1997–2010 are used in the current study. The Naltar and Ziarat stations record monthly maximum precipitation in April and minimum in November. The Khunjrab station records monthly maximum precipitation in August and minimum in October. The Naltar station records maximum annual precipitation of 701 mm, and the Khunjrab station recorded a minimum of 190 mm (average values from the 1997–2010 data).

The annual average temperature is 6.6 °C, 3.0 °C and -5.01 °C at Naltar, Ziarat and Khunjrab stations. The monthly mean temperature is maximum in July and minimum in January at all stations. The flow gauge of the Hunza Basin is installed at Danyore Bridge (1456 masl) just upstream of its confluence with the Gilgit River. The Hunza River has a low flow period from October to March and a high flow period from April to September. The high flow period is further divided into snowmelt dominated (April to June) and glacier melt dominated (late June to September) periods (Hasson 2016).

ii. Global precipitation and temperature data

1. ERA5-Land

The European reanalysis 5 Land (ERA5) is a newly developed precipitation dataset with data from 1981 to the present. The dataset has an hourly temporal resolution, 0.1° spatial resolution and global spatial coverage. The ERA5 data are produced under a single simulation and without coupling between the land and the atmosphere module of the Integrated Forecasting System (IFS). The datasets are produced without data assimilation, making it computationally affordable to produce updates (Muñoz Sabater, 2019) quickly. ERA5 data were used due to their good performance assessed through hydrological modelling by Nazeer, Maskey et al. (2021) and their high resolution to derive elevation-

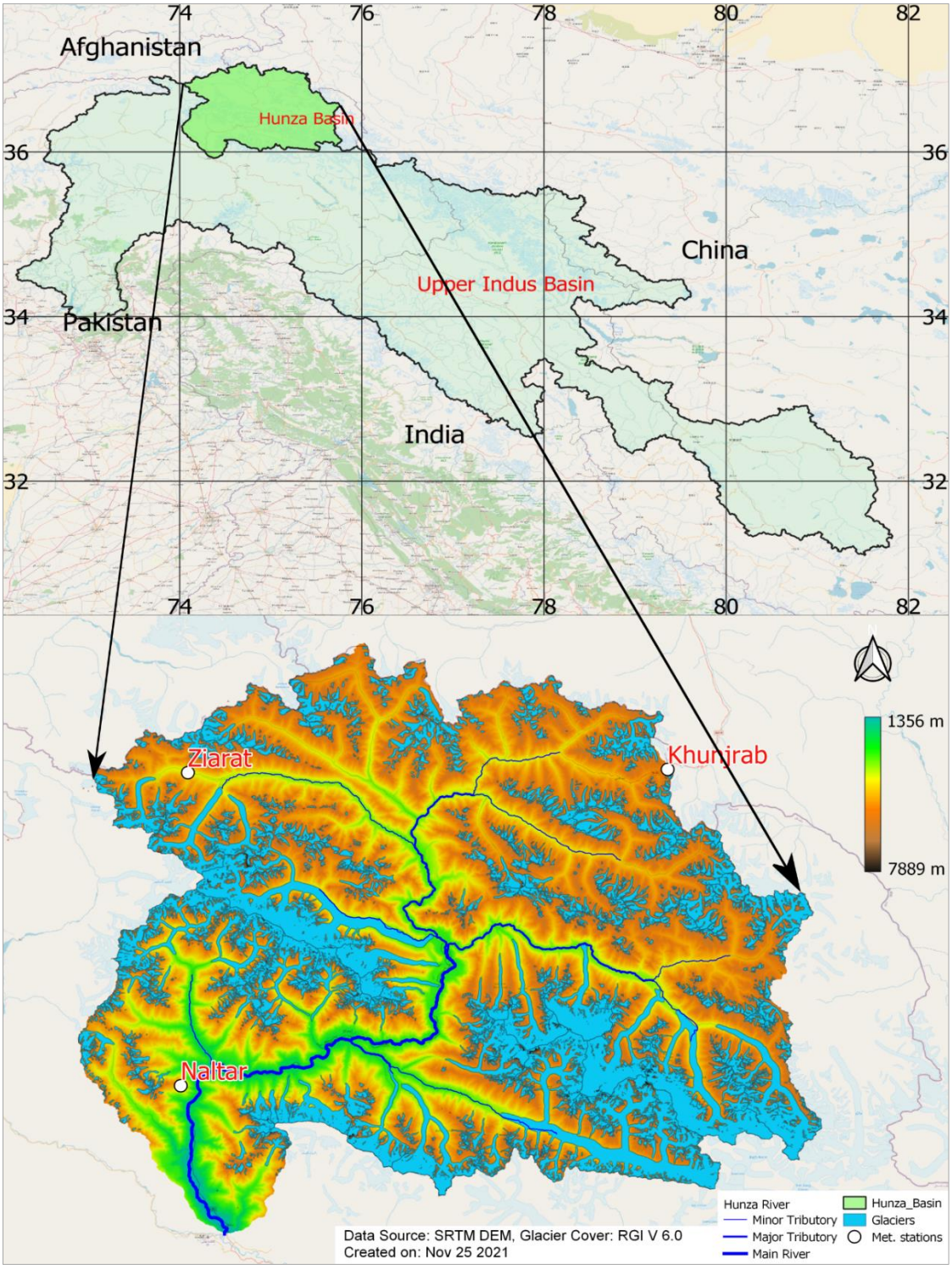

Figure 3.1. Location of the study area, glacier cover, river network and meteorological stations

Table 3.1: Hypsometry of the Hunza basin (divided into ten elevation bands of equal area) and glacier cover (Source: SRTM 30m DEM & RGI 6.0)

Area/ zone	Area quantiles (%)	Elevation range (masl)	Mean elev. (masl)	Glacier cover (%) of total
a1	10	1425–3217	2321	1.6
a2	20	3218–3755	3486	4.8
a3	30	3756–4123	3939	5.4
a4	40	4124–4403	4263	6.1
a5	50	4404–4640	4522	6.7
a6	60	4641–4849	4745	8.0
a7	70	4850–5053	4951	10.2
a8	80	5054–5264	5159	13.4
a9	90	5265–5549	5407	17.3
a10	100	5550–7889	6719	26.5

distributed precipitation for the Hunza Basin from 1997–2010. The dataset is freely available at https://cds.climate.copernicus.eu/ and was accessed in January 2021.

2. JRA55

The Japanese reanalysis (JRA-55) is the third-generation reanalysis dataset with data from 1958 to the present. The data have a 3-hourly temporal resolution, 0.56o spatial resolution, and global spatial coverage. The JRA-55 data, compared with previous datasets of the Japanese Meteorological Agency (JMA), are based on a further advanced data integration system, new observed data sources, enhanced model resolution and a new technique for satellite data bias correction (Kobayashi, Ota et al. 2015). JRA-55 data were used for the same reasons as ERA5. The dataset is freely available at http://jra.kishou.go.jp/JRA-55/ and was accessed in January 2021.

3. APHRODITE

The Asian Precipitation-highly Resolved Observational Data Integration towards Evaluation of Water Resources (APHRODITE) is the temperature and precipitation dataset developed from a gauged network in Asia and available from 1951 to the present. The dataset has a daily temporal resolution, 0.25° spatial resolution, and spatial coverage

of 60–150°E, -15–55°N. The datasets are mainly based on gauged data but include an improved algorithm where the local topography between the gauges and interpolated points is considered (Yatagai, Kamiguchi et al. 2012). APHRODITE data are used to derive the temperature lapse rate for the higher elevation where no gauge/reference data are available in the Hunza Basin. The dataset is freely available at http://www.chikyu.ac.jp/precip/ and was accessed in January 2021.

4. CHIRTS

The Climate Hazards Group InfraRed Temperature with Station data (CHIRTS) is a high-resolution temperature (maximum and minimum) dataset based on remotely sensed temperatures and a dense network of about 15,000 gauges (Berkeley Earth database). The dataset has a daily temporal resolution, a spatial resolution of 0.05° and global spatial coverage. The CHIRTS monitor temperature extremes by combining the monthly CHIRTSmax and the ERA5 data (Funk, Peterson et al. 2019). CHIRTS data were also used to derive the temperature lapse rate for the higher elevations where no gauge/reference data are available in the Hunza Basin. The dataset is freely available at https://www.chc.ucsb.edu/data/chirtsdaily and was accessed in January 2021.

iii. Satellite data

The Shuttle Radar Topography Mission (SRTM) DEM, the Randolph Glacier Inventory (RGI V6), the Landsat-8 and Moderate Resolution Imaging Spectroradiometer (MODIS) satellite datasets are used for the current study. The SRTM DEM data were developed by the United States National Aeronautics and Space Administration (NASA) with 30 m spatial resolution. The current study used the DEM data for catchment delineation, hypsometry, river network, and hydrological model parameters. The Global Land Ice Measurement from Space (GLIMS) develops the RGI dataset to monitor the glacier cover globally, with 30 m spatial resolution. The RGI data are used to derive the elevation-distributed glacier cover in the Hunza Basin (Figure 3.1). Landsat-8 data are developed by the Landsat Data Continuity Mission (LDCM) with 30 m spatial and 16 days temporal resolution. The Landsat-8 data are used to derive the land cover and the distances from the bogs and soil to the nearest stream of the Hunza Basin (Skaugen and Weltzien 2016). The MODIS snow data were accessed from Muhammad, Tian et al. (2019) for the Hunza Basin. These elevation-distributed snow data were used to validate the SCA simulations by the DDD model. The DEM, RGI (V6), and Landsat-8 data are freely available and were acquired from their respective websites.

3.2.3 Modelling framework

i. Model description and setup

The Distance Distribution Dynamics (DDD) model was developed by Skaugen and Onof (2014) of the Norwegian Water Resources and Energy Directorate (NVE). The model is a semi-distributed rainfall¬-runoff model written in the programming language Julia (Bezanson et al., 2012). The model simulates river flow, the elevation-distributed SCA, SWE, GM, actual evapotranspiration (ET) and subsurface water storage (Skaugen and Weltzien 2016). The model is data and parameter parsimonious and only needs precipitation and temperature as input. The model has several parameters, but most are derived from digitised maps and are hence not calibrated against runoff. The model has two approaches for calculating evapotranspiration, snow and glacier melt. One with energy balance based sub-routines for snowmelt and evapotranspiration and a degree day based sub-routine for glacier melt. The second with energy balance based sub-routines for all three variables. Combined with temperature, the energy balance elements are calculated using information about geographical location, Julian day, and algorithms used in Skaugen and Saloranta (2015) and Walter, Brooks et al. (2005). The model requires the basin to be divided into ten elevation zones of equal areas (a1–a10). The runoff dynamics in the Hunza Basin are described using unit hydrographs, which are determined from the GIS derived distance statistics and calibrated subsurface flow velocity (Skaugen and Mengistu 2016). The shape parameter of gamma distribution of snow (a0) and decorrelation length (D) are derived from spatial variability in the precipitation following Skaugen and Weltzien (2016). Table A.2 (Annexes) shows the model's calibration parameters with the calibration range and values used for the current simulations. Table A.3 (Annexes) shows the model's parameters derived using GIS and some parameters with fixed values. Further details on the model's description and setup can be found in Skaugen and Onof (2014) and Nazeer et al. (2021).

ii. Precipitation and temperature inputs

The DDD model requires elevation-distributed temperature and precipitation inputs. Elevation-distributed precipitation is derived from 1997 to 2010 from ERA5 and JRA-55 using climate data operators (CDO), a Linux based command line suite. About 170 ERA5 and 10 grids of JRA-55 data cover the whole Hunza Basin. To extract the precipitation data for each zone precisely and to better derive the data for the basin's edges, both datasets were resampled to a higher resolution (1 km^2), applying the nearest neighbour resampling algorithm (Nazeer et al, Maskey et al. 2021).

The gauged data and the temperature lapse rate for each zone are required to derive the elevation-distributed temperature. The gauged data was used as a reference and was assigned to the appropriate elevation zone. Naltar's data was used for a1, Ziarat's data for a2 and a3 and Khunjrab's data for all remaining zones (a4–10). The average lapse rate (Eq. 3.1) using three stations installed at elevations 2810, 3669 and 4730 masl was calculated as -6.0 ºC /km and applied for elevation zones a1–a6 with mean elevations from 2321-4745 masl. Because there are no observed temperature data for elevation zones a7-a10, the lapse rates for these elevation zones are used as a calibration parameter in the model. The range of the lapse rates for calibration is taken from -1 to -3 ºC /km, which is based on the analysis of the global datasets CHIRTS and APHRODITE. The calibrated lapse rate was -2.26 ºC /km for a7–a10.

$$TLR = (T_i - T_j)/(Z_i - Z_j) \qquad (3.1)$$

Where; TLR is the temperature lapse rate,

T_i and T_j are temperatures at gauges, Z_i and Z_j are elevations of gauges, respectively.

iii. Calibration and validation

The DDD model was set up for the Hunza Basin from 1997–2010. The period from 1997–2005 was used for calibration, and 2006–2010 for validation. The model was applied separately with the two methods for glacial melt: the energy balance (EB) and degree day (DD). In both cases, the model was forced with ERA5 and JRA-55 precipitation inputs separately, with the same temperature input data in all simulations. The modelling results hence include four simulations: ERA5-EB, ERA5-DD, JRA-EB and JRA-DD. By applying rain and snow correction factors, the model corrects the biases in the precipitation estimates seen as over- or under-estimated runoff. All model simulations and calibration, and validation were performed on a daily time step. The model uses the first three months as a warm-up period, which is necessary to obtain reasonable initial soil moisture states. The Kling-Gupta efficiency (KGE) (Gupta, Kling et al. (2009) and Nash-Sutcliffe Efficiency (NSE) (Nash and Sutcliffe 1970) were used to evaluate the model performance. Both; KGE (Eq. 3.21) and NSE (Eq. 3.3) can take values from minus infinity to one. KGE addresses some shortcomings of the NSE (Knoben, Freer et al. 2019) and is increasingly being used for model evaluation.

$$KGE = 1 - \sqrt{(r-1)^2 + \left(\frac{\sigma_{sim}}{\sigma_{obs}} - 1\right)^2 + \left(\frac{\mu_{sim}}{\mu_{obs}} - 1\right)^2} \qquad (3.2)$$

$$NSE = 1 - \frac{\sum_{i=1}^{n}(Qobs_i - Qsim_i)^2}{\sum_{i=1}^{n}(Qobs_i - \overline{Qobs})^2} \qquad (3.3)$$

Where; r is the linear correlation between simulated and observed data,

σ_{sim} and σ_{obs} are the standard deviations in simulations and observations,

μ_{sim} and μ_{obs} are the means in simulations and observation,

Qobsi is the observed flow and Qsimi is the simulated flow, for day i,

$\overline{Qobs}$: mean observed flow over the number of days, n.

3.3 RESULTS

3.3.1 Temperature distribution

Figure A.4 (a-c) (Annexes) shows the comparisons between gridded and gauged data for 1997–2010. The mean daily temperature derived for the current study, together with APHRODITE, CHIRTS, and gauged mean temperature, are shown in Figure A.4 (d) (Annexes). The gridded temperature estimates match well in seasonality with the gauged data, but there are also significant differences. The temperature difference decreases with elevation increase. For instance, the maximum difference between the station and APHRODITE data at the lowest station decreases at the median elevation station and becomes almost zero at the highest station.

3.3.2 Climatology of precipitation

The maximum daily precipitation of 48 mm was recorded on 27 April 1997, followed by 31 mm on 25 April 2003 by ERA5. For JRA-55, maximum precipitation of 44 mm was recorded on 25 April 2003, followed by 27 mm on 27 April 1997. For mean monthly estimates (Figure 3.2a) by ERA5, April received maximum precipitation of 83 mm, and October received a minimum of 35 mm. For JRA-55, February received a maximum of 152 mm and September a minimum of 45 mm. These monthly estimates match reasonably well with the station data, where the Naltar recorded maximum precipitation in April, followed by February and a minimum in October, followed by November. ERA5 seasonal estimates showed that the Hunza Basin receives 27, 29, 33, and 14 % precipitation during the winter, spring, monsoon and post-monsoon seasons. The JRA-55 showed 34, 35, 19, and 13 % precipitation during these seasons. The seasonal estimates by ERA5 data are in good agreement with the estimates by the Naltar station. The JRA-55 performed poorly for monsoon estimates. Also, JRA-55 overestimated the precipitation with more wet days than ERA5 and gauged data. The annual estimates (Figure 3.2b) from 1997–2010 showed maximum precipitation of 947 mm and 1322 mm in 1999 by ERA5 and JRA-55 datasets, respectively. ERA5 recorded a minimum of 594 mm in 2001, and JRA-55 recorded 822

mm in 2007. The mean annual precipitation showed 760 mm and 1103 mm by ERA5 and JRA-55 datasets, respectively.

i. Spatial distribution of precipitation

The spatial distribution of mean annual and seasonal precipitation for the Hunza basin from 1997–2010 are presented in Figures 3.3 & 3.4. The spatial analysis indicates that the basin receives more precipitation in the southern parts and less in the northern parts (Figure 3.4). The Naltar gauge is located in the basin's south and recorded the maximum precipitation (annual mean of 718 mm) compared to the other stations. Similarly, the Khunjrab station is located on the northern edge of the basin, and it records the least precipitation (annual mean of 206 mm). The spatial seasonal and annual precipitation estimates by global datasets are in good agreement with the gauged data.

ii. Altitudinal variation of precipitation

The altitudinal analysis of the derived precipitation indicated that the lower elevations received the maximum annual precipitation and the higher received the minimum in the Hunza basin (Figure A.5 (a), Annexes). This analysis further shows a negative precipitation gradient from a1 to a8 (2321 to 5159 masl), a slight negative gradient from a8 to a9 (5160 to 5407 masl), and then a strong positive from a9 to a10 (5408 to 6719 masl). These trends are consistent in both datasets. The seasonal analysis shows a slight negative gradient for JRA-55 (Figure A.5 (b), Annexes) precipitation and a strong negative gradient for ERA5-Land (Figure A.5 (c), Annexes) precipitation. However, monsoonal precipitation by JRA-55 indicates a slight positive gradient in the Hunza basin. The gauged data show a similar negative precipitation gradient in the Hunza basin. For instance, the lower elevation gauge (Naltar, 2810 masl) recorded its maximum annual precipitation of 832 mm in the year 2000 with an average of 701 mm from 1998–2010. The median elevation gauge (Ziarat, 3669 masl) recorded its maximum of 578 mm in 2004 with an average of 242 mm from 1998–2010. The highest gauge (Khunjrab, 4730 masl) recorded its maximum of 335 mm for 2010, with an average of 190 mm from 2003 to 2010. Similar trends are evident for minimum precipitation records at all gauges of the Hunza basin.

3.3.3 Runoff simulations

Flow simulations (Figure 3.5) were slightly better using ERA5-DD and achieved a KGE of 0.88 and NSE of 0.82. Simulations showed that the flow in winter is low and relatively constant at 30–35 m3/sec. The flow starts increasing in mid of April when the increase in

temperature initiates the snowmelt from low-elevation areas. With further warming, snow at higher elevations and glaciers from lower elevations start contributing. With the maximum temperature in July and August, glacier melt from higher elevations starts contributing, and the flow peaks around August (1100 m3/sec). The flow drops sharply in mid of August to less than 500 m3/sec (mean data) in mid of September. Such a sharp rise and fall in flow is also evident in the observed flow. The low flows last from

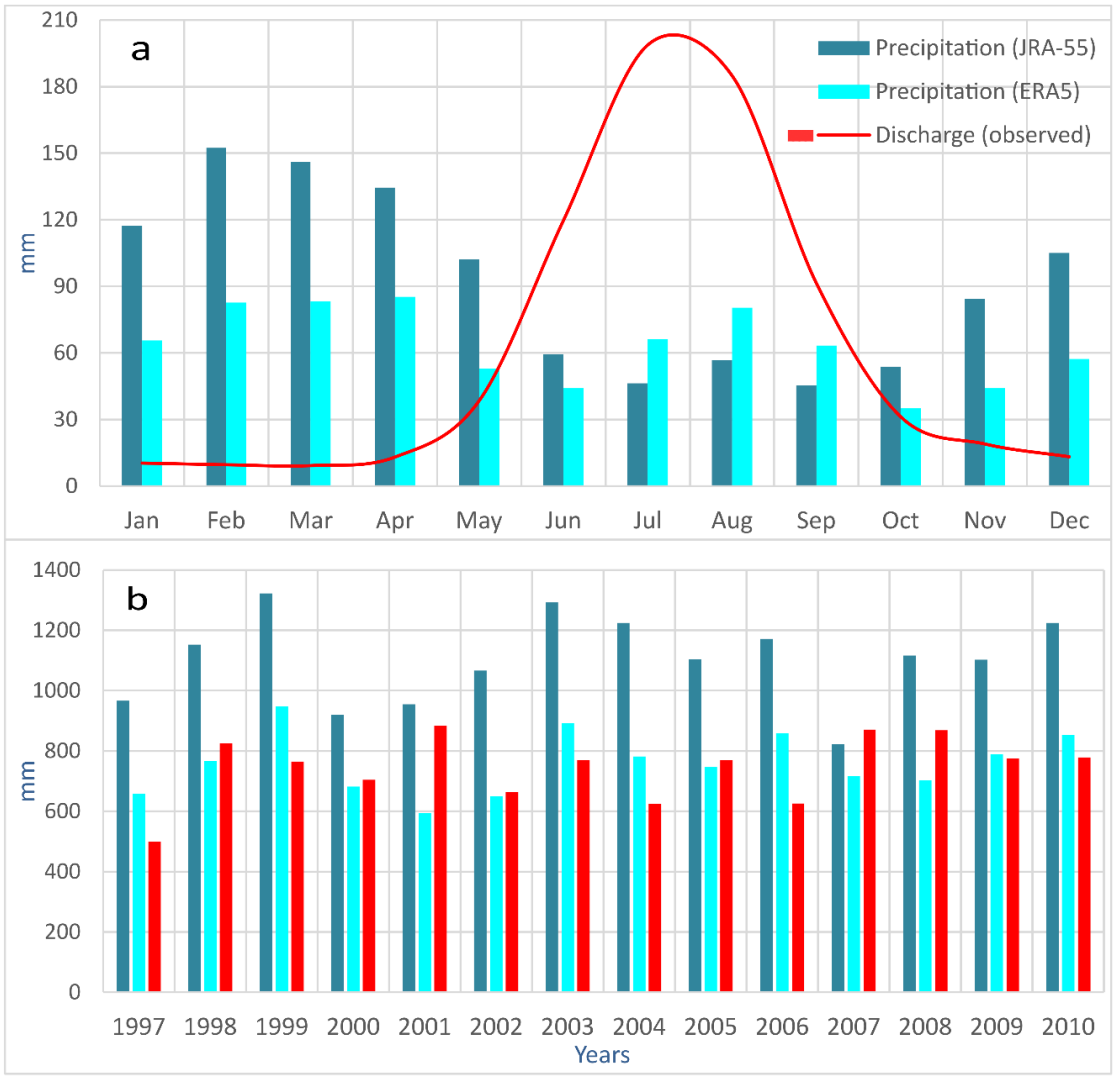

Figure 3.2. Mean a) monthly and b) annual precipitation from ERA5, JRA-55 data vs runoff (observed) from 1997–2010

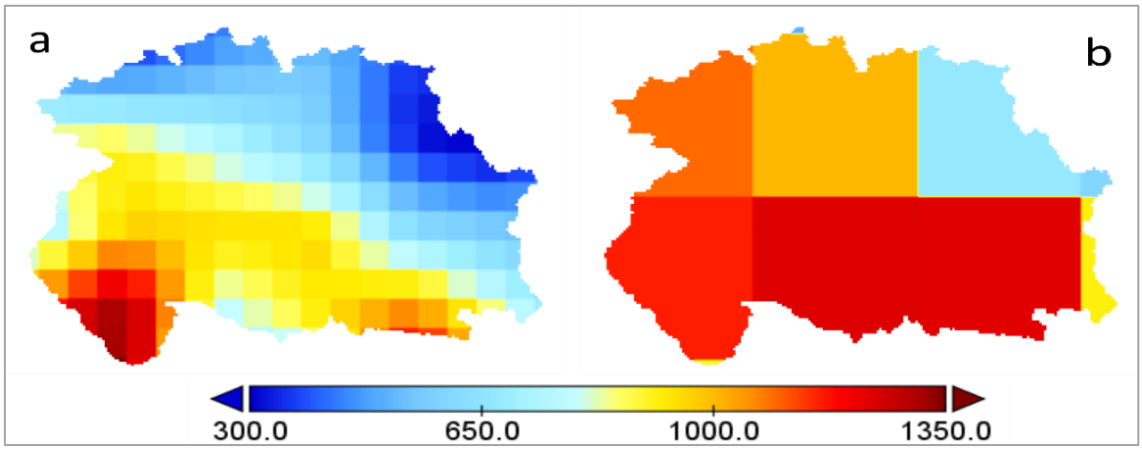

Figure 3.3. Mean annual spatial precipitation (mm) from a) ERA5-Land b) JRA-55 from 1995–2010

December until March and are sustained by snowmelt from low elevations and the base flow component. The high flows last from April until November due to snow and glacier melt and peak in July/August. The 1997–2010 observed data show only 6.3 % of total flow flows in the low flow period (Dec-March) and about 93.7 % in the high flow period (April-Nov). These characteristic flow periods are reproduced in the simulations with slightly underestimated low flow (4–5 % of total flow) and slightly overestimated high flow (about 95 %). The observed and simulated flow recessions are in good agreement for the whole period. The observed and simulated flow has several short-term peaks (mainly due to air temperature variations). The high peaks of observed flow were not simulated well by the model, but ERA5-DD is slightly better. The DDD model also simulates the actual evapotranspiration (ET) using an energy balance sub-routine based on the Priestley-Taylor equation, which is similar but simplified compared to the Penman-Monteith equation. Based on all four simulations, the minimum annual ET was from 196–199 mm for 2009, and the maximum was from 233 to 248 mm for 2007—the annual mean ET from 2006¬–2010 ranges from 213–227 mm.

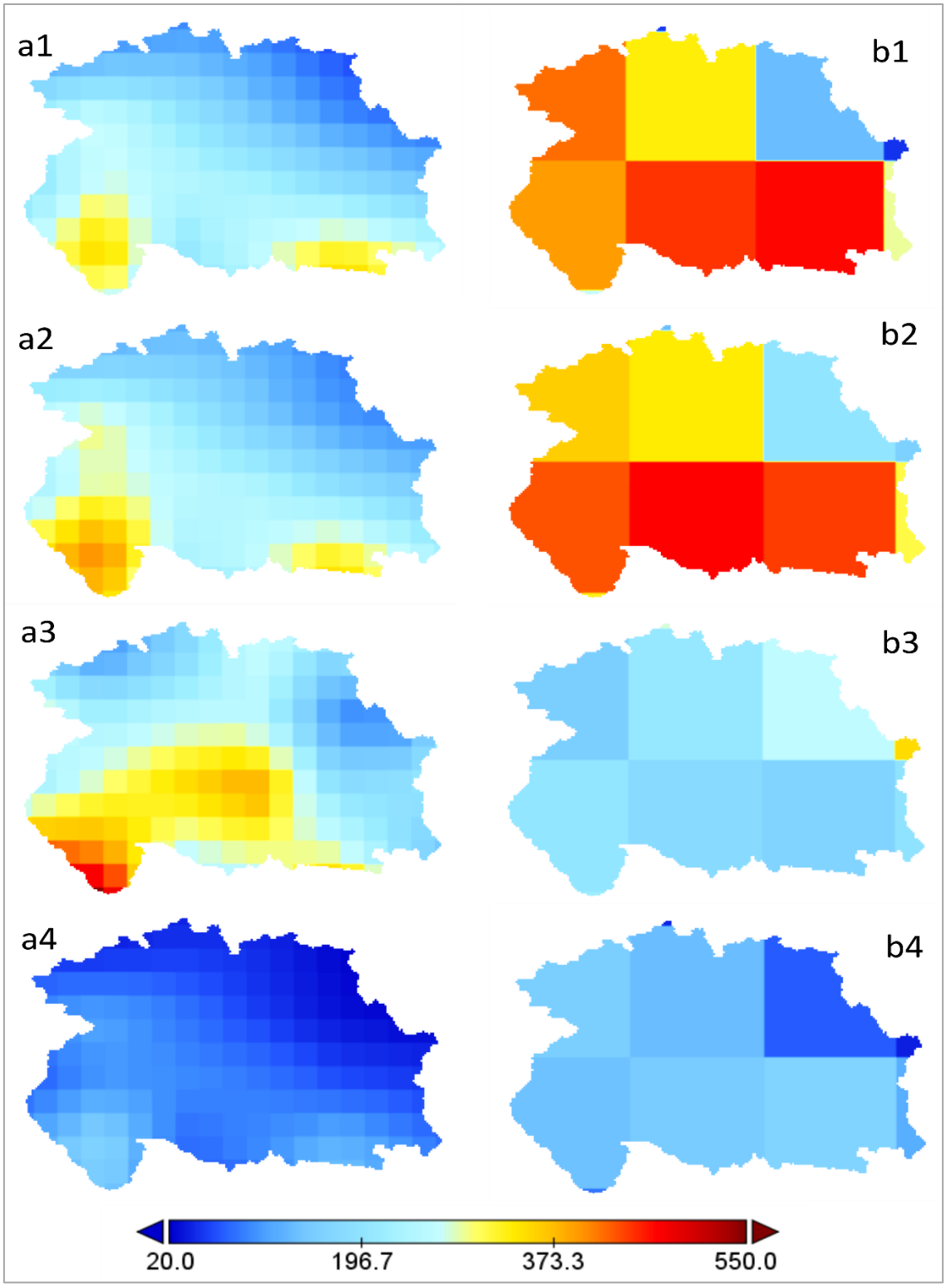

Figure 3.4. Mean seasonal spatial precipitation (mm) for 1) Winter, 2) Spring, 3) Monsoon, and 4) Post-monsoon seasons from a) ERA5-Land b) JRA-55

3.3.4 SCA and SWE simulations

Basin scale and elevation-distributed estimates of SCA and SWE from 2006–2010 for the Hunza basin based on all four simulations are shown in Tables 3.2 & 3.3. The SCA and SWE start increasing in September and peak in February. With the temperature rise in March, snow starts melting, and it keeps contributing to the flow until August. The JRA-55 based simulations showed a slightly higher SCA and SWE using glacier melt approaches than ERA5-Land. The simulated SCA is compared with the MODIS SCA derived from Muhammad et al. (2019) for 2006–2010. On the basin scale, the model simulates ERA5-Land and JRA-55 maximum SCA for January (99 %) followed by February (95 %) and a minimum in August (10 %) followed by July (20 %). The MODIS data have a maximum in February (85 %) followed by January (82 %) and a minimum in July (34 %) followed by August (38 %). The model has a basin scale mean annual maximum SCA of 70 % in 2009 in all four simulations, and MODIS has a maximum of 66.5 %, also in 2009. The minimum SCA by the model is 61 % for 2006, while MODIS had 57 % in 2007. The SCA simulations are consistently slightly higher than the MODIS data. For SWE, February showed a maximum of 270–320 mm, and August showed a minimum of 10–15 mm for all four simulations. On an annual scale (Table 3.2), maximum SWE was simulated in 2009 and a minimum in 2007. The JRA-55 simulation with energy balance approach showed an annual maximum SWE (278 mm), and the ERA5-Land with temperature index approach showed it minimum (252 mm).

The elevation-distributed estimates (Figure 3.6) of SCA are also consistent and in good agreement with MODIS data. The lowest elevation was snow covered for the winter months only, while the highest elevation was for almost the whole year. The snow accumulation starts in September, with the higher elevation zones snow covered first. In December, almost all elevation zones are snow covered. On an annual average, the lowest zone (a1) has 15 % area covered with snow by all simulations, compared to 11 % in the MODIS data. The highest elevation (a10) was 100 % covered with snow by the DDD model compared to 90 % by the MODIS data. SCA increases linearly from a1–a10 on a monthly and annual scale, consistent with the MODIS data. Compared to the MODIS data, the simulated SCA is slightly overestimated from zone a1–a5 and in a10. The elevation-distributed simulation of SWE follows the same melt and accumulation patterns as SCA. These simulations showed the minimum annual average SWE of 3–6 mm in the lowest elevation and a maximum SWE of 35–45 mm in zone 10. High SWE at higher elevations is associated with low temperature. At higher elevations with lower temperatures, more precipitation falls as snow. The precipitation amounts can still be less at higher elevations, but since it falls as snow, there is more SWE. Similar to SCA, the

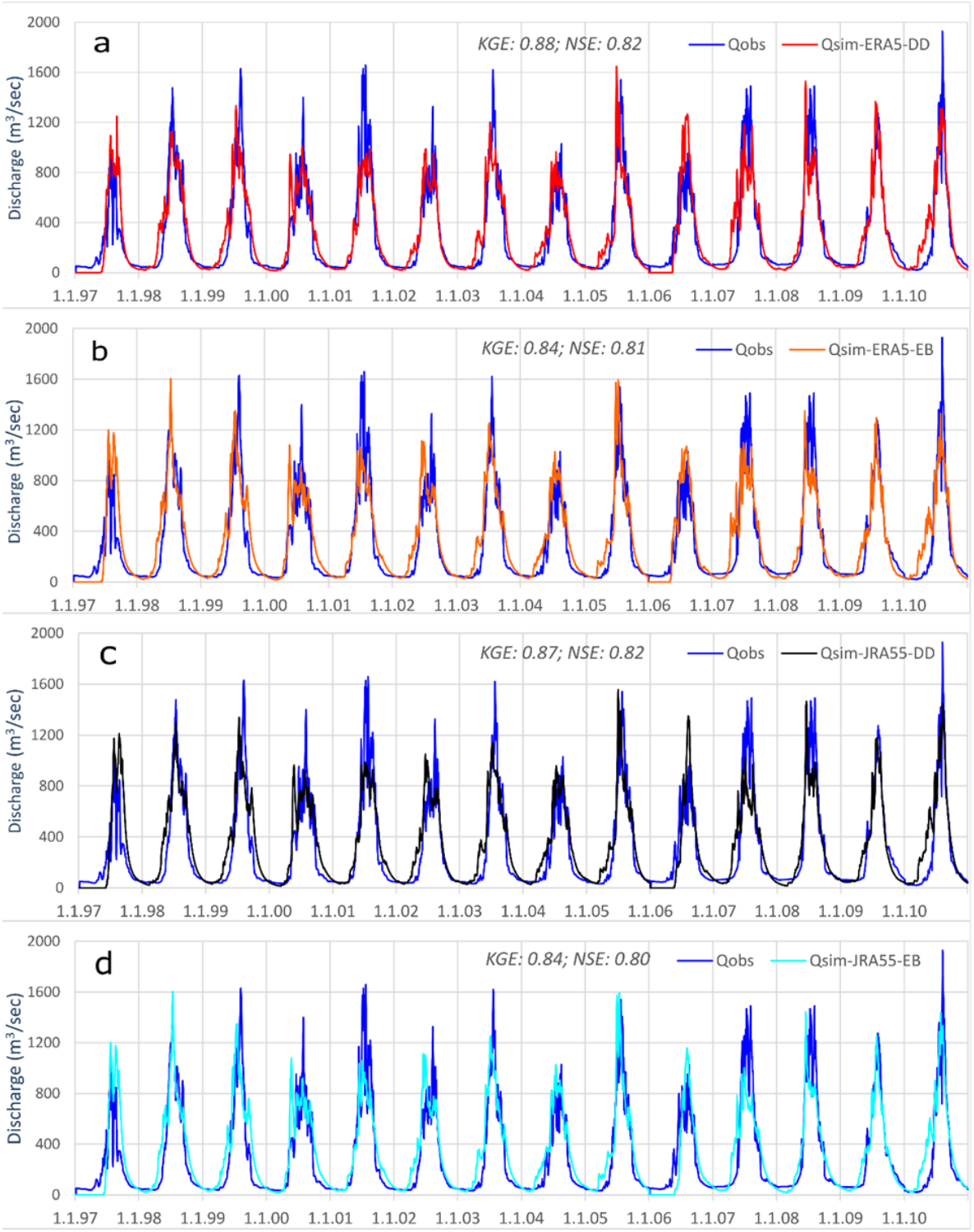

Figure 3.5. Observed flow vs simulated (m^3/sec) using a) DD based ERA5-Land b) EB based ERA5-Land c) DD based JRA-55 d) EB based JRA-55 simulations for calibration (1997–2005) and validation (2006–2010)

Table 3.2. Basin scale annual mean snow cover area (SCA), snow water equivalent (SWE), and glacier melt (GM) simulated by model and MODIS SCA

	Simulation/ year	**2006**	**2007**	**2008**	**2009**	**2010**	**Mean/ Total**
SCA (%)	ERA-DD	61	62	64	71	65	64
	ERA-EB	61	63	64	72	66	65
	JRA-DD	61	62	64	71	65	64
	JRA-EB	60	62	64	69	66	64
	MODIS	62	57	59	66	57	61
SWE (mm)	ERA-DD	286	214	244	306	210	252
	ERA-EB	304	228	258	325	223	268
	JRA-DD	296	202	259	285	220	253
	JRA-EB	325	220	280	318	248	278
GM (mm)	ERA-DD	568	504	497	371	429	474
	ERA-EB	545	497	486	335	395	452
	JRA-DD	575	513	506	379	430	481
	JRA-EB	548	509	469	350	383	452

Table 3.3. Elevation-distributed annual average zonal snow cover area (SCA), snow water equivalent (SWE), and glacier melt (GM) simulated by model and MODIS SCA

	Simulation/ zone	**a1**	**a2**	**a3**	**a4**	**a5**	**a6**	**a7**	**a8**	**a9**	**a10**	**Mean/ Total**
SCA (%)	ERA-DD	1.5	3.7	4.9	6.2	6.9	7.6	7.8	7.9	8.2	9.9	**64**
	ERA-EB	1.6	3.8	4.9	6.3	6.9	7.6	7.8	8.0	8.3	9.9	**65**
	JRA-DD	1.5	3.7	4.9	6.2	6.9	7.6	7.8	7.9	8.2	9.9	**64**
	JRA-EB	1.7	3.6	4.4	5.8	6.5	7.4	8.0	8.2	8.4	9.9	**64**
	MODIS	1.1	2.9	4.2	5.2	6.2	6.9	7.8	8.4	8.5	8.8	**61**
SWE (mm)	ERA-DD	3	15	21	27	28	29	28	28	29	43	**252**
	ERA-EB	4	17	23	28	30	31	30	30	31	45	**268**
	JRA-DD	5	18	24	27	28	29	29	29	29	35	**253**
	JRA-EB	6	18	25	29	31	31	31	31	32	46	**278**
GM (mm)	ERA-DD	56	99	82	48	39	32	35	39	40	4	**474**
	ERA-EB	27	61	58	47	44	40	46	57	64	8	**452**
	JRA-DD	57	100	83	47	39	32	36	39	41	6	**481**
	JRA-EB	29	63	61	48	43	42	46	54	60	7	**452**

mean annual SWE rises from lower to higher elevations. SWE is simulated slightly more in the energy balance approach than in the degree day approach.

3.3.5 Glacier melt simulations

The glacier melt simulations are in good agreement with the overall seasonality and observed flow regime. According to the simulations, the glaciers contribute to the flow almost throughout the year except for the winter season (Dec–Feb). The glaciers start melting in spring, at the end of March, very insignificantly from lower elevations. When temperature increases, glaciers at higher elevations start contributing. The melt peaks in August and then declines sharply, and the contribution becomes negligible by the end of November. Based on all four simulations, the basin scale monthly average glacier melt is maximum for August with 137 to 148 mm. Maximum annual glacier melt to be 575 mm and 568 mm for 2006 by JRA-DD and ERA5-DD simulations. While the minimum is to be 350 mm and 335 mm for 2009 by JRA-EB and ERA5-EB simulations. The annual mean basin scale glacier melt (Table 3.2) is estimated as 474 and 452 mm, using ERA5-DD and ERA5-EB approaches. While it is estimated as 481 and 452 mm using JRA-DD and JRA-EB approaches.

The elevation-distributed glacier melts are presented in Figure 3.7. Glaciers are melting and significantly contributing to the flow from all elevations of the Hunza basin. The lowest zone (a1) starts contributing very early in spring and keeps contributing until the start of December. So this zone contributes almost throughout the year except for the winter. After a1, a2 starts contributing at the start of April and continues until the end of November. With the temperature increase, the glacier at higher elevations starts melting in a similar pattern. The highest zone (a10) contributes only for less than a month. These patterns of glacier melt from different elevations (Figure 3.7) are consistent for all simulations. However, the zonal melt contributions (Table 3.3) are different in the temperature index, and energy balance approaches. In the temperature index approach, a2 contributes the maximum (21 %), followed by a3 (17 %) of total glacier melt. While for the energy balance approach, a9 contributes the maximum (14 %), followed by a3 (13 %). For the minimum contributions, both approaches identified a10 (1–2 %) followed by a6 (7–9 %) in temperature index and a1 (6%) in energy balance. The lower half of the basin (a1–a5), with 32 % of total glacier cover, is more active and contributes more than 50 % of the total glacier. The higher half of the basin (a6–a10), with 68 % of the total glacier cover, contributes less than 50 % of total melt. These patterns of more contribution from lower zones are consistent for all four simulations. However, the energy balance based sub-routine shows a slightly higher melt contribution from higher elevations.

3.3.6 Water balance

In a glaciated catchment, water balance (WB) can be represented as;

$$P \pm GM = Q + ET \pm \Delta S \qquad (3.4)$$

Where P is precipitation, GM is the glacier melt contribution, Q is the runoff from the catchment (both surface and subsurface), ET is the actual evapotranspiration and ΔS is the change in the sub-surface storage.

Table 3.4 shows an analysis of the inflow/outflow composition and water balance (Equation 3.4) from all four simulations on the annual scale. Figure 3.8 shows the same on the mean monthly scale from 2006–2010. The inflow components are precipitation (rain and snow) and glacier melt. The outflow includes simulated flow and actual evapotranspiration. On the annual scale, the ΔS is assumed negligible in the water balance equation. The winter months have the minimum outflow because most precipitation falls as snow. This stored snow starts contributing to the runoff in spring, and the outflow rises significantly. With further temperature and energy rise, glacier melt also contributes significantly and flow peaks in July/August. ET also peaks in July and August. The outflow starts declining significantly in September and is at a minimum in December/January. The runoff contributions in low and high flow periods are consistent in all four simulations. The mean annual contribution of snowmelt to the runoff is estimated to be 30–34 %, and the contribution from rain precipitation is 21–23.5 %. On average, the JRA-EB and ERA5-DD simulations showed the maximum (33.8 %), and minimum (30.7 %) snowmelt contribution to the runoff, respectively. For the rainfall contribution, the ERA5-EB simulation showed the maximum (23.5 %), and the JRA-EB simulation showed the minimum. Results further showed that the Hunza River receives 44–48 % of its total flow from glacier melt based on all four simulations. The maximum (47.6 %) glacier melt contribution was simulated by JRA-DD, and the minimum (44.1 %) by ERA5-EB. For the outflows (Q + ET), results showed a mean annual runoff 78–79 % and actual evapotranspiration 21–22 %.

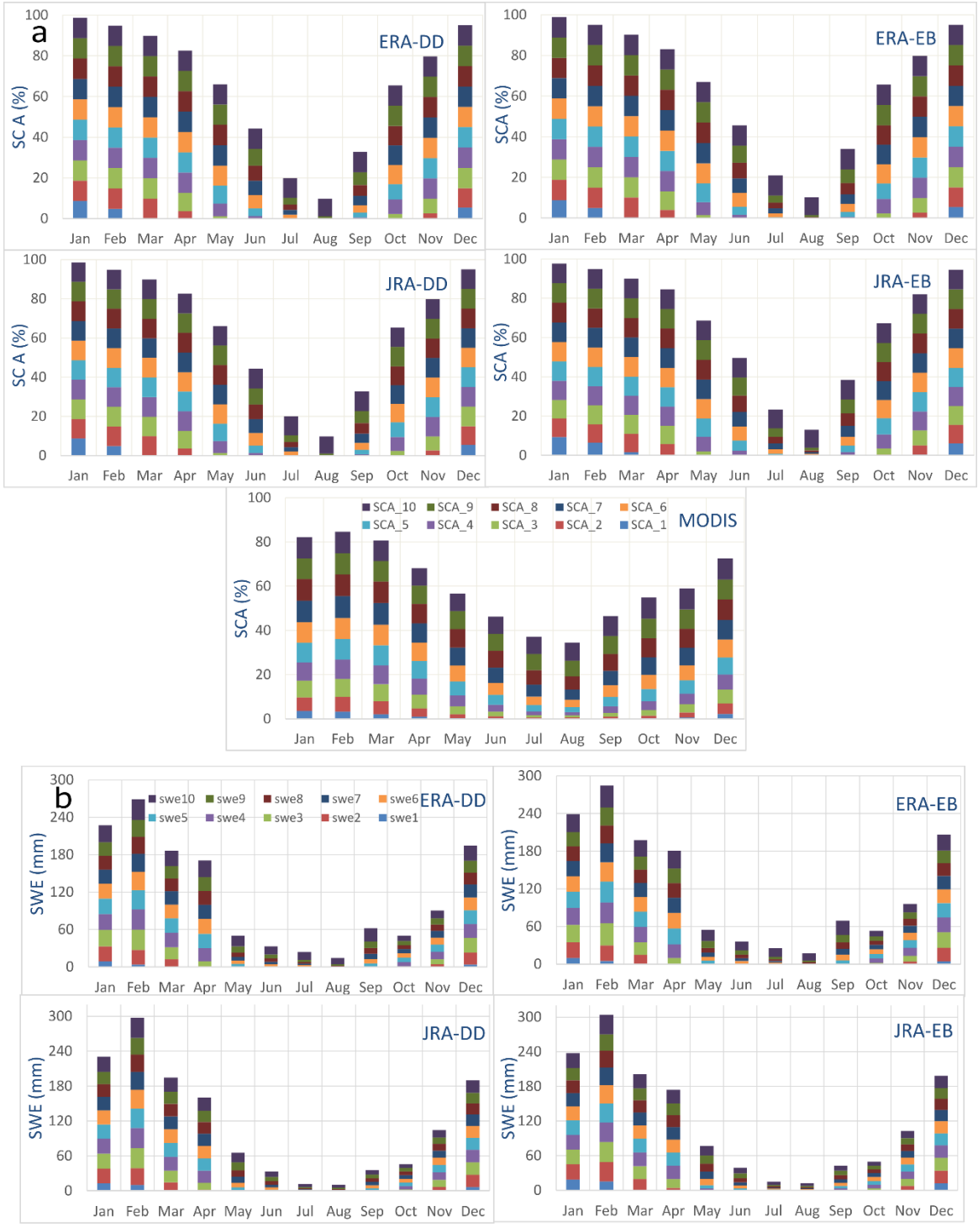

Figure 3.6. Elevation-distributed mean monthly simulated a) snow cover area and MODIS SCA (%) b) snow water equivalent (mm) based on all four simulations

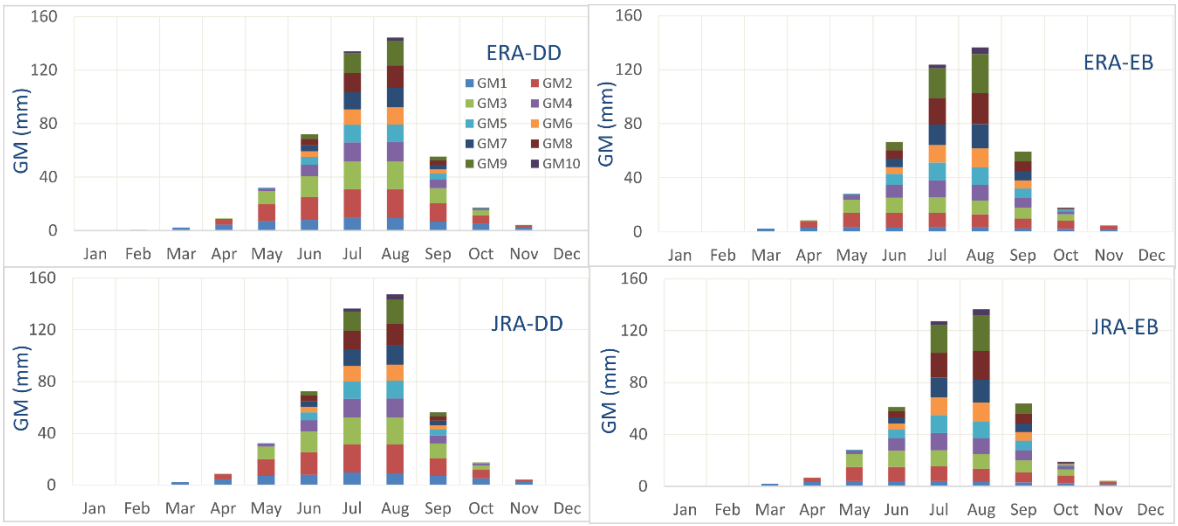

Figure 3.7. Elevation-distributed mean monthly simulated glacier melt (mm) based on all four simulations

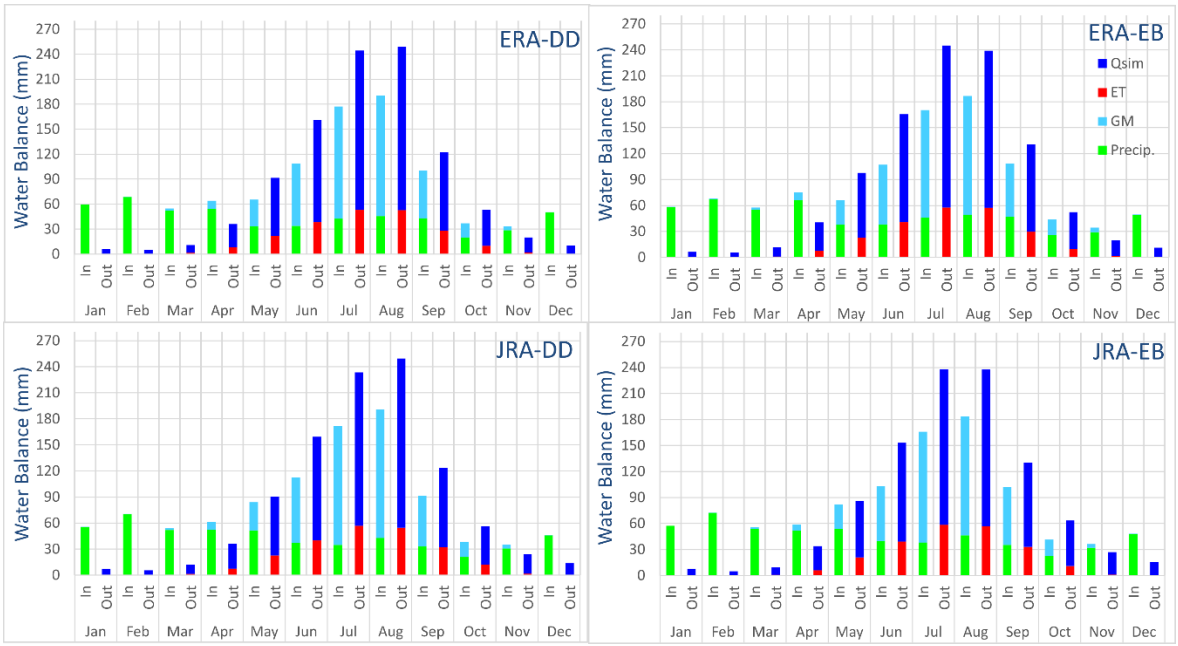

Figure 3.8. Mean Monthly water balance (mm) of the Hunza basin based on all four simulations

Table 3.4. Annual water balance of the Hunza basin based on all four simulations

Simulation	WB	WB/Year	2006	2007	2008	2009	2010	Mean (mm)	Mean (%)
ERA-DD	Inflow	Rain	209	237	190	162	319	224	22.2
		Snow	376	248	298	389	236	309	30.7
		GM	568	504	497	371	429	474	47.1
	Outflow	Qsim	720	836	768	768	876	793	78.8
		ET	222	233	228	179	205	213	21.2
ERA-EB	Inflow	Rain	227	255	202	172	347	241	23.5
		Snow	381	262	312	403	295	331	32.3
		GM	545	497	486	335	395	452	44.1
	Outflow	Qsim	731	852	779	754	872	798	78.0
		ET	243	243	241	186	214	225	22.0
JRA-DD	Inflow	Rain	177	178	227	152	342	215	21.3
		Snow	369	241	316	361	277	313	31.0
		GM	575	513	506	379	430	481	47.6
	Outflow	Qsim	637	796	803	740	933	782	77.6
		ET	239	248	237	199	212	227	22.4
JRA-EB	Inflow	Rain	183	189	229	142	322	213	21.2
		Snow	390	256	340	391	319	339	33.8
		GM	548	509	469	350	383	452	45.0
	Outflow	Qsim	603	817	804	756	918	780	77.6
		ET	241	247	231	196	207	225	22.4

3.4 DISCUSSION

The temperature plays a critical role in the snow- and glacier-dominated basins like the Hunza. The very few and non-uniformly distributed temperature measurement stations proved a significant limitation for deriving accurate elevation-distributed temperature. However, a realistic, elevation-distributed temperature is essential for simulating hydrologic processes. Fixed lapse rate values ranging from -2.3 to -9.2 oC/km were applied in the Hunza Basin in previous studies (Tahir, Chevallier et al. 2011, Immerzeel, Pellicciotti et al. 2012, Ragettli and Pellicciotti 2012, Shrestha, Koike et al. 2015, Garee, Chen et al. 2017). However, the lapse rate derived from the available temperature measurements does not support using a single (constant) lapse rate value for the entire elevation range, and there is no in situ measured temperature data to assess the lapse rate for elevations higher than 4730 masl. In this study, two lapse rates were used. One for a1-a6 based on observed data and one for a7-a10, which is calibrated using lapse rate range

from global datasets. The modelling approach (the DDD model) with elevation-distributed temperature and precipitation inputs gave reasonable results.

Precipitation is a major source of uncertainty in the Hunza basin. Mean annual areal precipitation estimated in the previous studies varies between about 700 and 1000 mm, e.g. 731 mm for 2001–2003 (Shrestha and Nepal (2019)), 828 mm for 2001–2003 (Immerzeel, Pellicciotti et al. (2012)), 733 mm for 1998–2012 (Dahri, Ludwig et al. (2021)), and about 1000 mm for 1971–2000 (Lutz, Immerzeel et al. (2014)). However, the basin-scale precipitation estimates suffer from inadequate and unevenly distributed in situ measurement data and apply some assumptions for precipitation lapse rates or extrapolation to the higher elevation area. The use of the gridded data allowed us to show the variation of precipitation with elevation, which would not be possible using in situ observation data from only three available stations. The temporal precipitation distribution indicates that the Hunza Basin receives significant precipitation as snow during the winter and spring seasons. The spatial estimates indicate a clear northeast to southwest increase in precipitation with a maximum on the southern edge of the basin. The Batura glacier acts as a precipitation dividing wall between the south and north of the Hunza Basin (Winiger, Gumpert et al. 2005). This barrier effect intensifies the southwest-northeast decrease of precipitation; consequently, the southwest part of the basin receives more precipitation.

The ERA5 and JRA-55 data used in the current study showed an overall negative precipitation gradient for the Hunza Basin. These patterns are consistent in both datasets at daily, monthly and seasonal scales. Hewitt (2011) concluded that the maximum precipitation in the Hunza Basin occurs between 5000 and 6000 masl. They associated glacier expansion in the basin with higher winter precipitation at higher elevations. Pang, Hou et al. (2014) suggest a decreasing precipitation gradient at elevations above 2400 masl in the central Himalayas. Dahri, Ludwig et al. (2016) also concluded that the precipitation increases up to a certain elevation (around 2500 masl) and after that decreases, so establishing any linear equation between precipitation and elevation in the HKH region is not suitable. Immerzeel, Pellicciotti et al. (2012), in their study in the Nepalese Himalayas, concluded that it is difficult to establish a constant precipitation gradient due to the influence of local orographic effects and complex weather system.

The comparison of the observed and simulated runoff hydrographs and model performance indicators showed that the DDD model reproduces the inter- and intra-annual variability reasonably well. The simulation results using ERA5 and JRA-55 as precipitation input data suggest that these products are suitable alternatives to observations for such a high-altitude and data-scarce basin. The ERA5 simulation showed slightly better NSE and KGE, probably due to its higher spatial resolution. The flow in the Hunza Basin mainly comes from snow and glacier melt, as the basin lies in a

westerlies-influenced region. The simulation results match the overall seasonality and observed flow of the Hunza River. The model performance indicators (NSE and KGE) achieved in all four simulations are reasonable and consistent. The flow recession matches very well in all simulations. The peak flow timing in the observed and simulated hydrographs is slightly different. Primary reasons for this are possibly the errors in the spatial distribution of snow and uncertainties in the input data (precipitation and temperature). However, uncertainties in the model parameters and structure may have contributed to this. The gridded data sets (ERA and JRA) also have temporal and spatial resolution limitations and limited ability to reproduce extremes (Kidd et al., 2013). In addition, these datasets (especially JRA-55) perform inadequately in capturing the monsoon rainfall. Consequently, the sharp flow peaks by the monsoon in summer are not reproduced well in the current simulations. Tahir, Chevallier et al. (2011) also underestimated the peak flows for the Hunza Basin, and they associated this with their precipitation input. Such discrepancies in observed and simulated flow were also observed by Shrestha, Koike et al. (2015) for the Hunza Basin from 2003–2004, and they associated it with uncertainty in the input data. Dahri, Ludwig et al. (2021) also concluded that accurate assessments of hydrologic processes in the high-altitude Indus Basin are challenging because of the unavailability of reliable input data. Reggiani and Rientjes (2015) estimated the mean evapotranspiration as 200±100 mm/year for the UIB from 1961–2009. Bhutiyani (1999) estimated this as 222 mm/year for the Siachen glacier (Nubra valley of eastern Karakoram) from 1986–1991. Hence, the current estimates of mean annual ET (213–227 mm) substantiate the previous findings.

Simulating a realistic snow cover and snow water equivalent is essential for understanding the hydrological processes in the Hunza basin. Hasson, Lucarini et al. (2014) presented almost similar estimates of SCA with 83±4 % during the winter/spring season and 17±6 % during the summer season from 2001–2012 for the Hunza Basin. Similar estimates were presented by Tahir, Chevallier et al. (2011), with SCA varying between 30 % in summer and 80 % in winter for the Hunza Basin from 2000–2004. Shrestha and Nepal (2019) presented SCA estimates between 30 % in summer and 87 % in winter for the Hunza Basin from 2000–2010. The DDD model slightly overestimates the SCA compared with the MODIS data for the winter season. Although precipitation by global datasets were corrected by the model using correction factors, precipitation still may have uncertainties. This overestimation may also be associated with limitations in the model's structure, where the model estimates the entire elevation zone as snow covered in case of snow event. Moreover, only 10 % of the Hunza's area is located under an elevation of 3217 m, so due to low temperature in winter, the whole basin would be snow covered if it rains in winter. As mentioned before, this basin is located in westerlies influenced region where most of the precipitation falls in winter as snow. For summer, the simulations show that the basin has about 10 % SCA, while MODIS showed it at

about 40 %. This 30 % less simulated SCA than MODIS is due to the presence of permanent glaciers (RGI 6.0) in the basin that have been classified as snow cover in the MODIS data. The DDD model keeps track of SCA and glaciers separately. Also, the MODIS snow data has coarse temporal (8-day) resolution, but the snow cover area may change day by day when melting starts.

The significant glacier melt contribution from the least glaciated lowest zones (a1, a2) and the least from the highly glaciated zone (a10) show how temperature impacts more significantly than the glacier extent. There are some differences in the glacier melt contributions from different elevation zones in the two sub-routines (Table 3). The degree day sub-routine melts more from lower elevations with a maximum from zone a2. The energy balance approach produces slightly more than the DD sub-routine from higher elevations with maximum melts from zones a2 and a9. The degree day based sub-routine is based on a calibrated degree-day factor and is totally dominated by temperature. The energy balance subroutine does not involve any calibrated parameter and simulates the glacier melt using radiation and temperature. In both sub-routines, the highest zones (a10) with maximum glacier coverage melts least because of the very low temperature at such higher elevations (5550–7889 masl).

Snowmelt is significant from spring to late summer (mid-April to mid-October), and some snowmelt continues throughout the year. Simulations showed a time overlap in snow and glacier melts (Figure A.6, Annexes). That means that the glacier melt from lower elevations starts contributing when there is still snow left at higher elevations of the basin. The glacier cover of the Hunza Basin starts at 2300 masl (Hewitt 2014), so temperature rise in spring/early summer at these elevations can melt glaciers. Also, if the precipitation falls as snow in the glacier melt season on some elevation zones, the snow may quickly melt while the glacier is also melting in snow free zones. Similar overlap patterns are evident in the accumulation season. The snow accumulates, and the glacier melt contribution decreases with temperature decline, but glaciers from lower elevations are still melting. So separating these snow and glacier melt regimes based on the month, as done by Mukhopadhyay and Khan (2014), Mukhopadhyay and Khan (2015), does not apply in the current study.

Mukhopadhyay and Khan (2015) presented flow composition based on generic flow regimes analysis and hydrograph separation using historical monthly flow data for the Hunza River for two periods. From 1966–1979, they estimated the base flow (flow due to precipitation as rain plus remnant melt) contribution as 22.5 %, snowmelt as 31.85 %, and glacier melt as 45.65 %. From 1980–2010, they estimated base flow as 27.98 %, snowmelt as 32.52 %, and glacier melt as 39.49 %. Shrestha and Nepal (2019) presented the annual mean flow composition for the Hunza Basin from 2001–2003 as snowmelt with 45 %, glacier melt with 47 %, and rain with 9 %. Shrestha, Koike et al. (2015)

presented these contributions as 50 % by snowmelt, 33 % by glacier melt, and 17 % by precipitation as rain for the Hunza Basin. The flow composition from the current study substantiates the previous findings, where glacier melt contributed 44–48 %, snowmelt 30–34 %, and rain as precipitation 21–23.5 % to the runoff. Moreover, the current study also quantified the snow and glacier melts from different elevation zones.

3.4.1 Limitations of the study

The quality and reliability of input data (mainly temperature and precipitation) are crucial in hydrological modelling. Also, the accuracy of the modelling results largely depends on the modelling framework. As typical of data-scarce basin, this study also has several limitations associated with input data and model structure. Temperature inputs are very critical in a melt dominant catchment like the Hunza. However, the temperature for higher elevations is based on assumptions such as the linear increase in temperature with elevation. The zonal precipitation was derived using global products with a low spatial resolution (particularly the JRA-55), given the high spatial variability in the basin and limited ability to capture extremes. The flow data used for calibration/validation are assumed to be sufficiently accurate compared to climatic data, considering the measurement techniques and data quality. However, the flow data may still have uncertainties due to measurement errors. NESPAK-AHT-DELTARES (2015) evaluated river/canal flow measurement protocols of the Indus river system and observed overall 3–8 % uncertainties at five canal headworks.

The DDD hydrological model used in the current study is validated and applied with four different sets of inputs/sub-routines, and no significant drawbacks are found in the modelling structure. The simplified equations in the energy balance sub-routines for snowmelt, glacier melt and evapotranspiration have shown promising results. Yet, the sub-routines neglect spatio-temporal variability in topography, and wind speed and the model seems to overestimate the SCA. The calibrated parameters in the model are not validated against observations from the study area.

3.4.2 Conclusions

The modelling framework included four simulations based on two glacier melt approaches and two precipitation inputs. The data parsimonious precipitation-runoff model, Distance Distribution Dynamics (DDD), was applied to the Hunza Basin. The elevation-distributed precipitation and melt simulations and the overall water balance of the basin were analysed. The key findings are as follows:

- Elevation-distributed precipitation estimates are presented based on recently developed and better performing gridded products. Most of the precipitation (57–

69 %) in the Hunza Basin falls in the winter and spring season (Dec-April/May). The analysis showed more precipitation at lower elevations than at higher. A linear elevation-dependent precipitation gradient is unsuitable for high-altitude basins like the Hunza, with a complex topography and multiple weather systems.

- The modelling results showed that the DDD model could reproduce the runoff satisfactorily, with KGE ranging from 0.84–0.88 and NSE ranging from 0.80–0.82. The DDD model is found to be reliable for such high altitude, snow- and glacier-dominated and data-scarce basins.
- The river flow in the study area depends more on glacier melt (45–48 %), followed by snowmelt (30–34 %) and rainfall (21–23 %). The annual mean actual evapotranspiration is 21–22 % of the total outflow. The study presents more realistic elevation-distributed GM simulations where the lower half of the basin, with 32 % of the total glacier cover, is more active, with more than 50 % of the total glacier melt. The elevation-distributed simulated SCA was validated with an independent SCA from MODIS, and the results are in good agreement.
- Elevation-distributed glacier melt analysis indicates the glacier has a significant impact on the flow regime of the area. The degree day based sub-routine uses a calibrated degree-day factor, but the energy balance subroutine does not include any calibrated parameters. Although the degree day sub-routine based simulation slightly improves efficiency, the energy balance sub-routine seems more realistic.
- The snow and glacier melts appear simultaneously from April to October. As the glaciers are distributed throughout the basin, the temperature increases in early summer, melting glaciers at lower elevations and snow at higher elevations. Also, if the precipitation falls as snow during the glacier melt season at higher altitudes, it may start contributing to the river flow while glacier melt continues in the lower elevation.
- Based on the findings from a comparatively new modelling framework and gridded precipitation data, an improved elevation-distributed understanding of the Hunza Basin is presented. Our results showed that the glaciers at lower elevations with less coverage contribute more to the river runoff than those at higher elevations. Moreover, the validation of the simulated elevation-distributed snow cover area using the independent satellite data supported the accuracy of the modelling approach. The simulation showed that the DDD model reproduces the hydrological processes satisfactorily for such a data-scarce basin. The findings improve understanding by providing helpful information about the water balance and hydro-climatic regimes.

4

CHANGES IN THE HYDRO-CLIMATIC REGIME UNDER CMIP6 CLIMATE CHANGE PROJECTIONS

This chapter is based on the following publication.

Nazeer, A., Maskey, S., Skaugen, T. & McClain, M. E. Changes in the hydro-climatic regime of the Hunza Basin in the Upper Indus under CMIP6 climate change projections (submitted).

ABSTRACT

Concerns about future water availability from the Upper Indus Basin (UIB) are heightened by the recent acceleration in climate change. The UIB heavily depends on its frozen water resources, and an accelerated melt due to the projected warming may significantly alter future water availability. The future hydro-climatic regime and water availability of the highly glacierised Hunza basin (a sub-basin of UIB) were analysed using the newly released Coupled Model Intercomparison Project Phase 6 (CMIP6) climate projections. A data and parameters parsimonious precipitation-runoff model, the Distance Distribution Dynamics (DDD) model, was used with energy balance-based subroutines for snowmelt, glacier melt and evapotranspiration. The model was successfully calibrated from 1997–2005 and validated from 2006–2010 using ERA5-Land precipitation and station-based temperature. The ERA5-Land precipitation was corrected against the observed flow and further employed to bias correct the precipitation from global circulation models (GCM). The DDD model was set up for baseline (1991–2010), mid-century (2041–2060) and end-century (2081–2100) projections under Shared Socioeconomics Pathways (SSP) SSP1, SSP2 and SSP5 emission scenarios from two GCMs. The projections indicate a substantial increase in temperature (1.1–8.6°C) and precipitation (12–32%) depending on the scenarios and GCMs used throughout the 21st century. Relative to the baseline period, the simulalations show the future flow increase between 23–126%, and the future glacier melt increase between 38–265%, depending on the scenarios and GCMs used. The results show a decrease in the annual snow cover in the end of the 21st century. Moreover, the simulations suggest an increasing glacier melt contribution from all elevations with a significant increase from the higher elevations. The results suggest a substantial increase in glacier melt which can be alarming. The findings provide a basis for planning and modifying reservoir operation strategies with respect to hydropower generation, irrigation withdrawals, flood control, and drought management.

Key Words: Climate change, CMIP6, ERA5-Land, GCM, Hunza basin, Upper Indus Basin

4.1 INTRODUCTION

Climate change (CC) is accelerating (IPCC 2021; (Masson-Delmotte, 2021)). Due to the continuous emission of greenhouse gases and subsequent warming, the threat of CC is continuously rising (Ciais et al., 2014). It was urged in the "2015 - Paris Agreement" to limit the global temperature rise below 2 °C relative to the pre-industrial (1861–1890) level and stabilise it to 1.5 °C by 2100 (Dahri et al., 2021). However, such an ambitious goal requires extraordinary efforts to increase the current levels of nationally determined contributions (NDCs) by 3–5 times (League et al., 2019). The recent CC acceleration heightens concerns about future water availability from the high-altitude basins (Hasson, 2016). CC will change the frequency and magnitude of climatic variables such as precipitation and temperature (Hasson et al., 2019; Lutz et al., 2016a). Such changes are likely to be prominent in the Asian, South American and European low-latitude regions, where alpine glaciers are particularly sensitive to the prevailing climatic warming (Stocker et al., 2013). The Hindukush Karakoram Himalaya (HKH) is a region where the problem of vanishing glaciers is critical and will affect water availability in the next few decades (Barnett et al., 2005). The high-altitude HKH region and Indus basin are recognised as a "hotspot" of CC due to significant transformations in the hydro-climatic regime (Wijngaard et al., 2018). However, an accurate assessment of CC and associated impacts on hydrological regimes in the region is difficult due to limited data and insufficient analyses (Dahri et al., 2021).

Recent studies (1979–2010) of the winter westerlies, the primary source of precipitation in the Karakoram, indicated an enhanced frequency and increased amount of winter precipitation (Cannon et al., 2015). The Upper Indus Basin (UIB) showed significantly increased annual and seasonal precipitation at several stations from 1961–1990 (Archer and Fowler, 2004). Also, consistent with the global trends, increasing temperature trends are evident for UIB. Akhtar et al. (2008) used the Special Report on Emissions Scenarios (SRES) data for UIB's climatic modelling from 2071–2100. They predicted a mean temperature rise of 4.8 °C and a mean precipitation increase of 16 % by the end of the 21st century. Sharif et al. (2013) evaluated the air temperature trends for UIB. They concluded that (i) the daily temperature range is consistently widening for all seasons, (ii) mean and maximum temperatures of winter show significant increases and (iii) mean and minimum summer temperatures show a decreasing trend. Negative temperature trends for summer from 1958–1990 and a positive trend from 1991–2001 were found for the Baltoro glacier in the Karakoram using the ERA-40 reanalysis dataset (Quincey et al., 2011). These future precipitation and temperature projections are quite uncertain and need further investigation.

The lack of observations, complex topography and interactions with synoptic-scale climatic circulations pose significant uncertainties in precisely representing the Indus basin's hydro-climatic regime (Dahri et al., 2021; Lutz et al., 2016b). Consequently,

conflicting trends have been observed in UIB regarding the CC impacts on the glaciers, and a debate has been prevailing concerning these trends during the last decade (Lutz et al., 2016b). Hewitt (2005) observed glacier expansion and advancement in central Karakoram. Sharif et al. (2013) and Tahir et al. (2011) indicated that large parts of the UIB are not yet experiencing accelerated melt, possibly due to the Karakoram anomaly. A more recent study in the central Karakoram (Shigar river basin) reported an increased flow (Mukhopadhyay and Khan, 2014b). Lutz et al. (2016b) concluded that glacial melt contribution increases with neutral mass balance, with temperature and precipitation increase. However, future climatic projections are subjected to variabilities and large spread in the general circulation models (GCM). The GCMs are consistent for temperature projections with slight variation, whereas the precipitation projections vary highly, ranging from significantly drier to moderately wetter trends (Lutz et al., 2016b). The projected global warming of 1.5 and 2 °C could increase the river flow by 34 and 43 % from the upper Indus basin, according to Hasson et al. (2019). Hence, significant and accelerated changes are expected for the basin's hydro-climatic regime (Dahri et al., 2021).

The recent acceleration in glacier melt due to CC in HKH mountains poses serious concerns about the glacier's contribution to South Asian rivers (Rees and Collins, 2004). It further illustrates that scientists and experts understand very little about these processes (Bernstein et al., 2008; Rees and Collins, 2004); hence, precise simulations of these changes are lacking. About 70 % of annual flow in the Indus River comes from glaciers and seasonal snowmelt (Mukhopadhyay and Khan, 2015), so changes will directly affect the Indus flow and, consequently, millions of people downstream (Tahir et al., 2011). Pakistan is an agro-based country with 70 % of its population dependent (directly or indirectly) on agriculture, so the water flows from the mountain headwaters are crucial. The Hunza basin in the western Karakoram is highly vulnerable to prevailing and future CC since 31 % of its area is covered by glaciers (RGI, V6.0; Arendt et al. (2017)). The Hunza's flow depends on meltwater and the monsoon rain, which is available for a few summer months (Nazeer et al., 2022). This water is stored in the country's largest reservoir, Tarbela Dam, for irrigation needs and hydropower production throughout the year. Therefore, modelling the melt contribution to the river flow under CC scenarios is essential. This modelling may assist in managing the current and future domestic water supply, flood mitigation and hydropower productions (Klok et al., 2001).

The current study attempts to simulate the hydro-climatic regimes based on CC projections and over the Hunza basin of UIB. It analyses the recently released projections by Coupled Model Intercomparison Project phase 6 (CMIP6) (Eyring et al., 2015). The CMIP6 projections differ from CMIP5 with a new generation of climate models and a new set of periods, emissions, and land-use scenarios (Gidden et al., 2019). Moreover, to our knowledge, none of the studies has analysed the CMIP6 projections for UIB or the

Hunza basin. These newly released precipitations and temperature projections are used as input to a precipitation-runoff model, the Distance Distribution Dynamics (DDD) model, where energy balance approaches are used to simulate snowmelt, glacier melt and evapotranspiration.

4.2 MATERIALS AND METHODS

4.2.1 Study area

The Hunza Basin, with an area of 13,713 km^2, lies in the western Karakoram mountains of the HKH region. The basin stretches between 74.04–75.77°E and 36.05–37.08°N. Figure 4.1 shows the location, digital elevation model (DEM), drainage area, meteorological stations, and glaciers coverage of the basin. The basin has a complex topography with deep valleys and extreme topographic relief with elevations between 1456 and 7822 meters above sea level (masl) and a mean elevation of 4600 masl. The Hunza is one of the main sub-basins of the Upper Indus Basin (UIB), and it contributes about 12 % of the total flow of UIB upstream of the Tarbela reservoir (Shrestha et al., 2015). The Hunza is a snow-fed and highly glaciated basin. Seasonal snow is at its maximum in winter, with almost 85 % of its total area covered with snow (Shrestha et al., 2015). The basin has a glacier extent of about 31 % of the total area and is located between 2300 and 7889 masl (RGI, V6.0; (Arendt et al., 2017)) (Table 4.1). The basin hosts some extensive glacier systems, including Hispar (339 km^2), Batura (238 km^2), Virjerab (112 km^2), Khurdopin (111 km^2) and a few others. The basin has a dense river network with Hunza as the main tributary (232 km long). The 1966–2010 Hunza river flow data collected by Pakistan's Water and Power development authority (WAPDA) showed an average flow of 304 m^3/sec (~710 mm). The climate in the Hunza basin is arid to semiarid and is generally divided into four seasons; winter (Dec-Feb), spring (March-May), monsoon (June-Sep), and post-monsoon season (Oct-Nov) (Nazeer et al., 2021). The HKH precipitation has two primary sources; summer monsoon and winter westerlies. The Hunza basin receives precipitation from both sources, with about two-thirds from the winter westerlies and one-third from the summer monsoon (Bookhagen and Burbank, 2010). Precipitation at Hunza peaks around March/April under the westerlies regime, followed by August/September under the monsoon (Hasson, 2016).

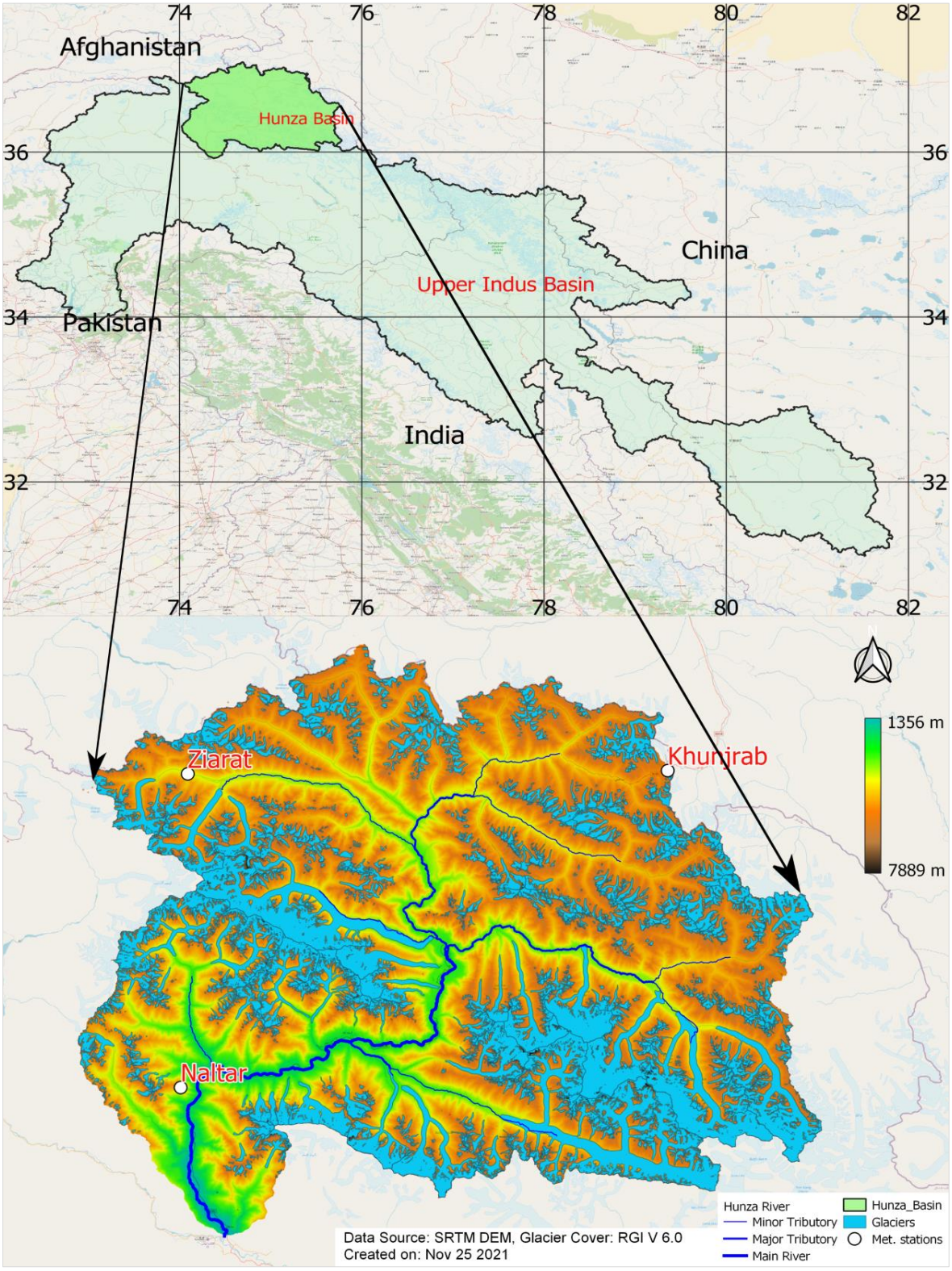

Figure 4.1. Location of the study area, glacier extent, river network and meteorological stations

Table 4.1. Hypsometry and glacier coverage of the Hunza Basin

Area quantile	Elevation range (masl)	Mean elevation (masl)	Glaciers area (km^2)	Glaciers (%) of total extent
a1	1425-3217	2321	67	1.6
a2	3218-3755	3486	200	4.7
a3	3756-4123	3939	232	5.4
a4	4124-4403	4263	255	6.0
a5	4404-4640	4522	289	6.8
a6	4641-4849	4745	348	8.1
a7	4850-5053	4951	437	10.2
a8	5054-5264	5159	576	13.4
a9	5265-5549	5407	738	17.2
a10	5550-7889	6719	1142	26.7

4.2.2 Observed data

i. Hydrometeorological data

The observed hydrometeorological data are obtained from WAPDA and the Pakistan Meteorological Department (PMD). Observed temperature data are used to derive the elevation-distributed temperature and bias-correct the GCM based temperature projections for the Hunza basin. The observed precipitation data are not used as input to the model but to compare the spatial and seasonal precipitation estimates by ERA5-Land. The Hunza basin has three meteorological stations (Naltar 2810 masl, Ziarat 3669 masl, Khunjrab 4730 masl). From 1997–2010, the Naltar and Ziarat stations recorded monthly maximum precipitation in April and minimum in November. The Khunjrab station recorded monthly maximum precipitation in August and minimum in October. The Naltar station recorded maximum annual precipitation of 701 mm, and the Khunjrab station recorded a minimum of 190 mm. The annual average temperature is 6.6 °C, 3.0 °C and -5.01 °C at Naltar, Ziarat and Khunjrab stations. The monthly mean temperature is maximum in July and minimum in January at all stations. The flow gauge of the Hunza basin is installed at Danyore Bridge (1356 masl). The flow of the Hunza River shows two major flow regimes. One is the low flow regime (October-March), and the second is the high flow regime (April-September). The high flow regime is further divided into snowmelt dominated (April-mid June) and glacier-melt dominated (mid June-September) (Hasson, 2016). The observed flow is used for the DDD model calibration and validation

for observed data based simulations (1997–2010). The flow data are also used to validate the GCM based simulation of daily flow for the baseline period (1991–2010).

ii. ERA5-Land

The UIB is a data-scarce basin with very few installed stations for climatic data. These stations have a limited record period, and the records contain missing data. The high altitude, altitudinal variations and complex weather systems complicate the monitoring (Dahri et al., 2016; Dahri et al., 2018; Nazeer et al., 2021). Hence, the existing stations inadequately capture the precipitation amounts and patterns. Precipitation estimates from the European Reanalysis 5 Land (ERA5-Land) gridded dataset were reasonable for the UIB (Nazeer et al., 2021; Nazeer et al., 2022; Syed et al., 2022). The ERA5-Land data are newly developed, available from 1981 to the the near real time with several weeks delay with an hourly temporal resolution, 0.1°X0.1° spatial resolution and with a global spatial coverage (Muñoz Sabater, 2019). The dataset is freely available at https://cds.climate.copernicus.eu/ and was accessed in January 2021. The ERA5-Land data are used to derive elevation-distributed precipitation for the Hunza basin from 1997-2010.

iii. APHRODITE

The Asian Precipitation-Highly Resolved Observational Data Integration Towards Evaluation of water resources (APHRODITE) is a temperature and precipitation dataset. The dataset is developed from a network of gauges in Asia and is available from 1951-2015. The dataset has a daily temporal resolution, a 0.25°X0.25° spatial resolution and spatial coverage of 60–150°E, 15–55°N. These data are based on a gauge network and an improved interpolation algorithm where the local topography between the gauges and interpolated point is considered (Yatagai et al., 2012). The dataset is freely available at http://www.chikyu.ac.jp/precip/ and was accessed in January 2021. The APHRODITE temperature data are used to derive the temperature lapse rate for the higher elevation of the Hunza basin, where no station/reference data are available.

4.2.3 CMIP6 GCM data

i. EC-Earth3

CMIP6 based EC-Earth is a state-of-the-art European community Earth-System model (ESMs) developed by the European EC-Earth consortium, including about 20 institutions (Hazeleger et al., 2010). EC-Earth3 (hereafter called the ECE3) is a GCM developed in a collaborative and decentralised way (Massonnet et al., 2020). The ECE3 used in CMIP6 has daily and sub-daily temporal resolution, a spatial resolution of 0.7°X0.7° and global spatial coverage. ECE3 data are used in the current study due to their relatively fine

resolution. Also, this GCM performed better for overall quantification and showed fewer biases during primary analysis for GCMs selection. The dataset was used to derive the Hunza basin's temperature and precipitation for the baseline (1991–2010) and future (2041–2060 and 2081–2100) periods. The dataset is freely available at https://esgf-node.llnl.gov/projects/cmip6/ and was accessed in October 2021. The GCM future data used are under the Shared Socioeconomic Pathways (SSP) scenarios of SSP1, SSP2 and SSP5.

ii. MPI-ESM

MPI-ESM is the Max Planck Institute's Earth System Model (MPI-ESM1.2) (Gutjahr et al., 2019). The MPI-ESM for CMIP6 has daily and sub-daily temporal resolution, a 0.9°X0.9° spatial resolution and global spatial coverage. MPI-ESM data are used in the current study due to their relatively fine resolution. Also, this GCM performed better for overall quantification and showed fewer biases during primary analysis for GCMs selection. The dataset was used to derive the Hunza basin's temperature and precipitation for the baseline (1991–2010) and future periods (2041–2060 and 2081–2100). MPI-ESM is freely available at https://esgf-node.llnl.gov/projects/cmip6/ and was accessed in October 2021. The GCM future data used are also under the Shared Socioeconomic Pathways (SSP) scenarios of SSP1, SSP2 and SSP5.

4.2.4 Satellite data

The satellite datasets used in the current study include the Shuttle Radar Topography Mission (SRTM) DEM, the Randolph Glacier Inventory version 6.0 (RGI V6), the Landsat-8 and the Moderate Resolution Imaging Spectroradiometer (MODIS). The SRTM DEM dataset was developed by the United States National Aeronautics and Space Administration (NASA) in 2013 with 30 m spatial resolution. The DEM data were used for catchment delineation, hypsometry and river network (Figure 4.1). The RGI dataset was developed by the Global Land Ice Measurement from Space (GLIMS) in 2017 with 30 m spatial resolution. The dataset was developed to monitor the glacier extent globally. The RGI data were used to derive the elevation-distributed glacier extent in the Hunza basin (Figure 4.1, Table 4.1). Landsat-8 data are developed by the Landsat Data Continuity Mission (LDCM) with 30 m spatial and 16 days temporal resolution. The Landsat-8 data were used to derive the land cover and the distance distributions from the bogs and hillslopes to the nearest stream used as DDD model parameters (Skaugen and Weltzien, 2016). The MODIS snow data were used to validate the model's SCA simulations and were accessed from Muhammad et al. (2019) for the Hunza basin. The DEM, RGI and Landsat-8 are freely available and are acquired from their respective official websites.

4.2.5 Modelling framework

i. DDD model

The DDD model developed by Skaugen and Onof (2014) of the Norwegian Water Resources and Energy Directorate (NVE) is a semi-distributed, precipitation-runoff model written in the programming languages of R and Julia. The model simulates river flow, the elevation-distributed SCA, snow water equivalent (SWE), glacier melt (GM), potential and actual evapotranspiration (EP and EA) and subsurface water storage (Skaugen and Weltzien, 2016). The model is data and parameter parsimonious and only needs elevation-distributed precipitation and temperature as input. In the current modelling setup, the model's energy balance based sub-routines are employed to calculate the evapotranspiration, snow- and glacial melt. Further details on the model's description and setup can be found in Skaugen and Onof (2014) and Nazeer et al. (2021). Table A.2 (Annexes) shows the DDD model's calibration parameters with the calibration range and values used in the current simulations. Table A.3 (Annexes) shows the DDD model's GIS derived parameters and parameters with fixed values.

ii. Bias correction of GCM projections

The GCM projections are subjected to various uncertainties and model biases. Therefore, these GCM projections require bias correction before being applied for future climatic and hydrological investigations (Dahri et al., 2021). Previous studies (Dahri et al., 2016; Dahri et al., 2018; Hasson, 2016; Shrestha et al., 2017) evaluated the performance of different bias correction techniques. The station data can be helpful for bias correction, but as mentioned previously, the Hunza basin is data-scarce. So the global precipitation data of ERA5-Land, with its latest release and fine resolution (Dahri et al., 2021; Nazeer et al., 2021; Syed et al., 2022), were used for GCM bias-correction in this study. The ERA5-Land precipitation data, however, overestimate the precipitation and need to be corrected before being applied as the observed precipitation data for the Hunza basin. The GCM baseline projections are then corrected using the corrected ERA5-Land precipitation; the same corrections are then applied to GCM's future projections. Hence, the precipitation bias correction consists of three steps, discussed in the following sections.

iii. Model setup using ERA5-Land

The DDD model is run using daily scale precipitation and temperature as input. The precipitation is derived from the ERA5-Land, and temperature from station data, with a temperature lapse rate derived from station data and APHRODITE temperature data (Nazeer et al., 2022). Calibrating against the observed flow, the DDD model suggests a precipitation correction factor, separately for rainfall and snow. To do so, the model

decides if the precipitation is rainfall or snow using a calibrated temperature threshold (TX) and calibrates the correction factors for rain (Pkorr) and snow (Skorr) separately. The DDD model was calibrated from 1997–2005 and validated from 2006–2010. The elevation-distributed correction factors for rain and snow are used to bias-correct the GCM's elevation-distributed projections.

iv. Bias correction of GCM projections

The selected GCMs' precipitation and temperature are bias-corrected using the mean-based method (Sirisena et al., 2021; Wang et al., 2016). The correction of precipitation projections is based on "observed precipitation" (corrected ERA5-Land data), and the correction of temperature projections is based on "observed temperature" (station data and APHRODITE lapse rate). The methods adopted for temperature and precipitation bias correction are shown in Equations 4.1 & 4.2, respectively.

$$T_M'(i) = T_M(i) + \mu_O - \mu_M \qquad (4.1)$$

$$P_M'(i) = P_M(i) \times \mu_O'/\mu_M' \qquad (4.2)$$

Where T_M' is the bias-corrected daily temperature, T_M is the daily model (GCM) temperature before bias correction, i is a day in the month, and μ_O and μ_M are monthly means of observed and model (GCM) temperature for the baseline period, respectively.

P_M' is the bias-corrected daily precipitation, P_M is the daily model (GCM) precipitation before bias correction, i is a day in the month, and μ_O' and μ_M' are monthly means of observed and model (GCM) precipitation for the baseline period, respectively.

For the future periods (2041-2060 (mid-century) and 2081-2100 (end-century)), μ_O'/μ_M' for precipitation and μ_O-μ_M for temperature are taken from the baseline period (1991-2010) at a monthly basis.

v. Model setup using GCM projections

When running the DDD model with GCMs projections, the calibrated parameters are unchanged except for the precipitation correction factors. These correction factors are kept at 1 since the elevation-distributed precipitation is already bias-corrected. DDD is run for GCMs for the baseline (1991–2010), mid-century (2041–2060) and end-century (2081–2100) period.

4.2.6 Performance analysis

Calibration and validation of the DDD model are performed for corrected ERA5-Land precipitation and observed/extrapolated temperature on a daily time step from 1997-2005 and 2006–2010, respectively. The efficiency criteria of Kling Gupta efficiency (KGE) and Nash-Sutcliffe Efficiency (NSE) are used for accuracy assessment and evaluation. The KGE (Eq. 4.3) is a goodness-of-fit measure developed by Gupta et al. (2009). KGE is increasingly being used for model evaluation and has values ranging from minus infinity to one. The NSE (Eq. 4.4) (Nash and Sutcliffe, 1970) assesses the relative magnitude of residual variance compared with the variance in measured data subtracted from unity.

$$KGE = 1 - \sqrt{(r-1)^2 + \left(\frac{\sigma sim}{\sigma obs} - 1\right)^2 + \left(\frac{\mu sim}{\mu obs} - 1\right)^2} \quad (4.3)$$

$$NSE = 1 - \frac{\sum_{i=1}^{n}(Qobs_i - Qsim_i)^2}{\sum_{i=1}^{n}(Qobs_i - \overline{Qobs})^2} \quad (4.4)$$

Where; r is the linear correlation between simulations and observations,

σsim and σobs are the standard deviations of simulations and observations,

μsim and μobs are the means of simulations and observation,

$Qobs$ is the observed flow and $Qsim$ is the simulated flow, for day i,

$\overline{Qobs}$ is the mean observed flow over the n number of days.

4.3 RESULTS

4.3.1 Flow simulations for the baseline period

Figure 4.2(a) shows the ERA5-Land based daily simulated and observed flow for the calibration and validation period together with the corrected precipitation. The flow simulation showed reasonable results with a skill score of KGE of 0.82 and NSE of 0.80. These 1997–2010 simulations for the Hunza basin using ERA5-Land precipitation inputs are similar to those in Nazeer et al. (2022). However, the revised subroutine for simulating glacier melt changed the results slightly.

To validate the bias-corrected elevation-distributed GCM precipitation and temperature, simulations were performed for the baseline period for the Hunza basin. The time series of the daily simulated and observed flow for 1991–2010 and the bias-corrected precipitation are shown in Figure 4.2(b) for ECE3 based inputs and Figure 4.2(c) for ESM. The simulated flow is in good agreement with the observed flow. The ECE3 based simulation had a slightly overestimated flow of 5.1 %, and the ESM based simulation, 8.1 %. The observed and simulated low flows and flow recessions for the baseline period are in good agreement. The mean monthly simulated flow is also in good agreement but with the slightly less simulated base flow. The high flow regime indicates significant flow from April to October, with peaks in July and August. The low flow period is from November to March, with the minimum flow in February and March.

4.3.2 SCA, SWE and GM simulations for the baseline period

GCMs based simulated SCA and GM for 1991–2010 for the Hunza basin are shown in Figure 4.3. When the temperature rises in March, the snow starts melting, and the SCA decreases to its minimum in August. With the temperature decreasing in September, the precipitation falls as snow in most of the basin, and SCA starts increasing and peaks in February. Elevation-distributed means of simulated SCA, SWE and GM from GCMs compared with the ERA5-Land based simulations for the Hunza basin for 1991–2010 are shown in Table 4.2 and are in good agreement. The lowest elevations have the minimum SCA, while the higher elevations are mostly snow covered the whole year. The SWE follows the same melt and accumulation patterns as SCA for each elevation. SCA and SWE both increase from lower to higher elevations. SWE estimates are slightly higher with the GCM based simulations than the ERA5 based simulations.

The time series of GCMs based simulated GM for the Hunza basin from 1991–2010 is shown in Figure 4.3. The glaciers contribute throughout the year, except for the winter months (Dec-Feb). However, the melt contribution is significant from May to September, with a peak in July/August. In the early summer, the glaciers at lower elevations start contributing and then further increase in temperature in the late summer generates melt

at higher elevations. The elevation-distributed GM (Table 4.2) indicated that glaciers from all elevations are melting and contributing significantly to the flow. The lower elevations start contributing very early in spring and keep contributing until the start of December.

4.3.3 Temperature projections

Figure 4.4 shows the Hunza basin's mean monthly temperature for baseline, mid-century and end-century periods based on ECE3 and ESM GCMs under SSP1, SSP2, and SSP3 scenarios. A temperature increase is evident in all scenarios from the baseline period to mid- and end-century. The mean monthly basin baseline temperature is below 0 ºC for October-April in both GCMs. The mean monthly basin-scale ECE3 temperature estimates remain below 0 ºC for November-April for mid-century periods. The months with temperatures below 0 ºC are reduced to December-March for end-century. The ESM estimates also show October and November with temperatures below 0 ºC for mid- and end-century. Most severe warming is expected for the end-century SSP5 scenario. The minimum (monthly mean) increase from the baseline temperature to the future is 1.1°C for December for SSP1-mid-century, and the maximum is 8.6°C in July for SSP5-end-century based on ECE3. The warming differences are less in ESM, with a minimum of 0.5°C for December for SSP1-mid-century and a maximum of 5.5 °C for SSP5-end-century for August. However, both GCMs indicate strong warming in July and August, the most intense glacier melt period.

The annual temperature increase is also evident from the baseline period to mid- and end-century for both GCM and all scenarios except SSP1. The SSP1 indicates an increase for mid-century but a temperature drop for the end-century period. The ECE3 GCM shows an increase in temperature for mid- and end-century scenarios compared to ESM.

4.3.4 Precipitation projections

The annual mean precipitation for baseline and future (mid-century and end-century) periods for all selected scenarios and GCMs are shown in Figure 4.5. Relative to the baseline period, the ECE3 GCM shows 19–32 % increases in annual precipitation and ESM shows 12–28 % increases for the 21st century. Moreover, precipitation as snow reduces and rainfall increases. Maximum precipitation is in the winter/spring season, and minimum precipitation is in the post-monsoon season. The monthly estimates are similar for both GCMs. The monthly precipitation changes in GCM's future projections relative to the baseline period are shown in Table 4.3.

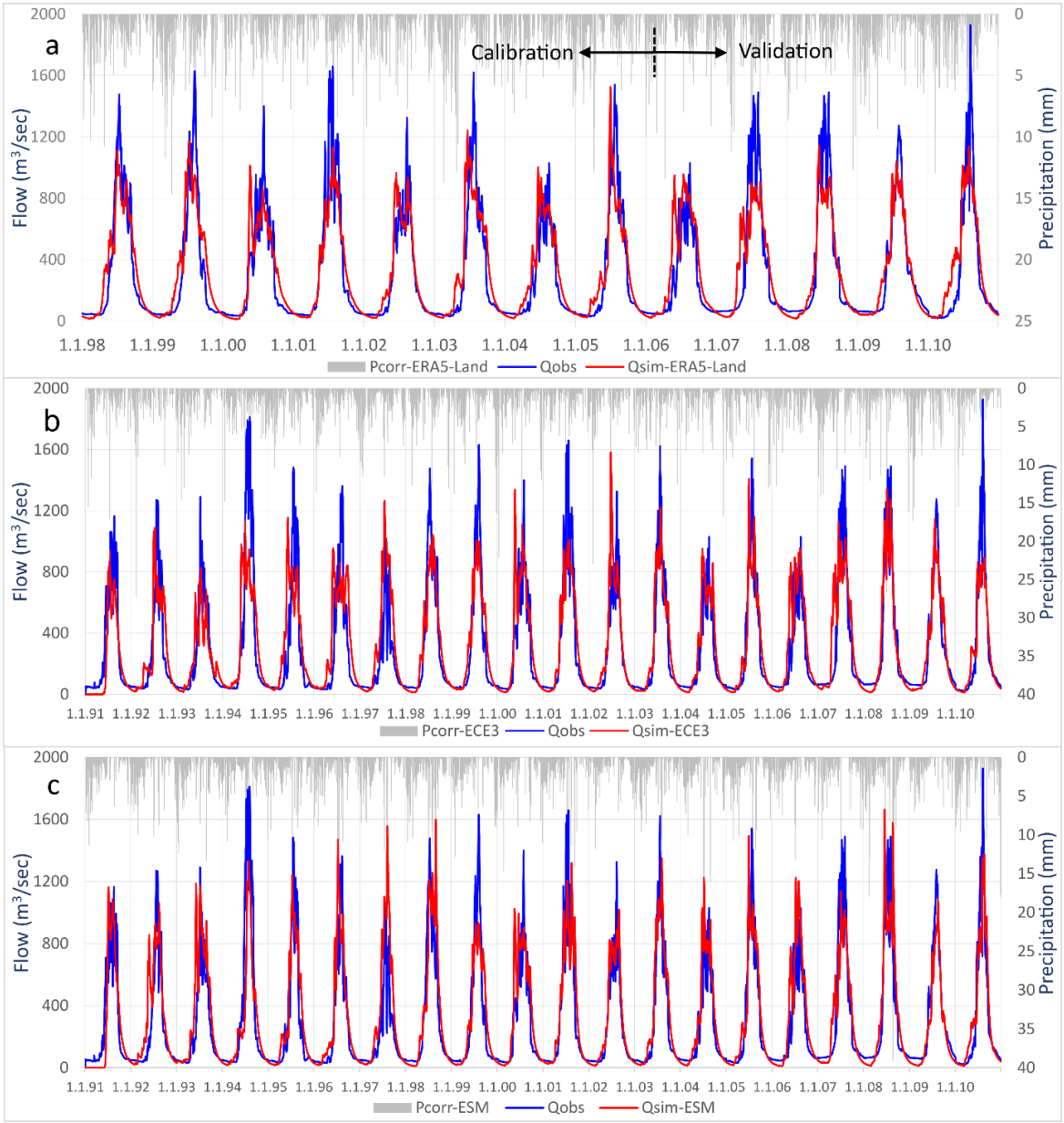

Figure 4.2. Observed vs simulated flow by DDD model for; a) ERA5-Land based inputs (1998–2010), b) ECE3 GCM based inputs (1991–2010), and c) ESM GCM based inputs (1991–2010)

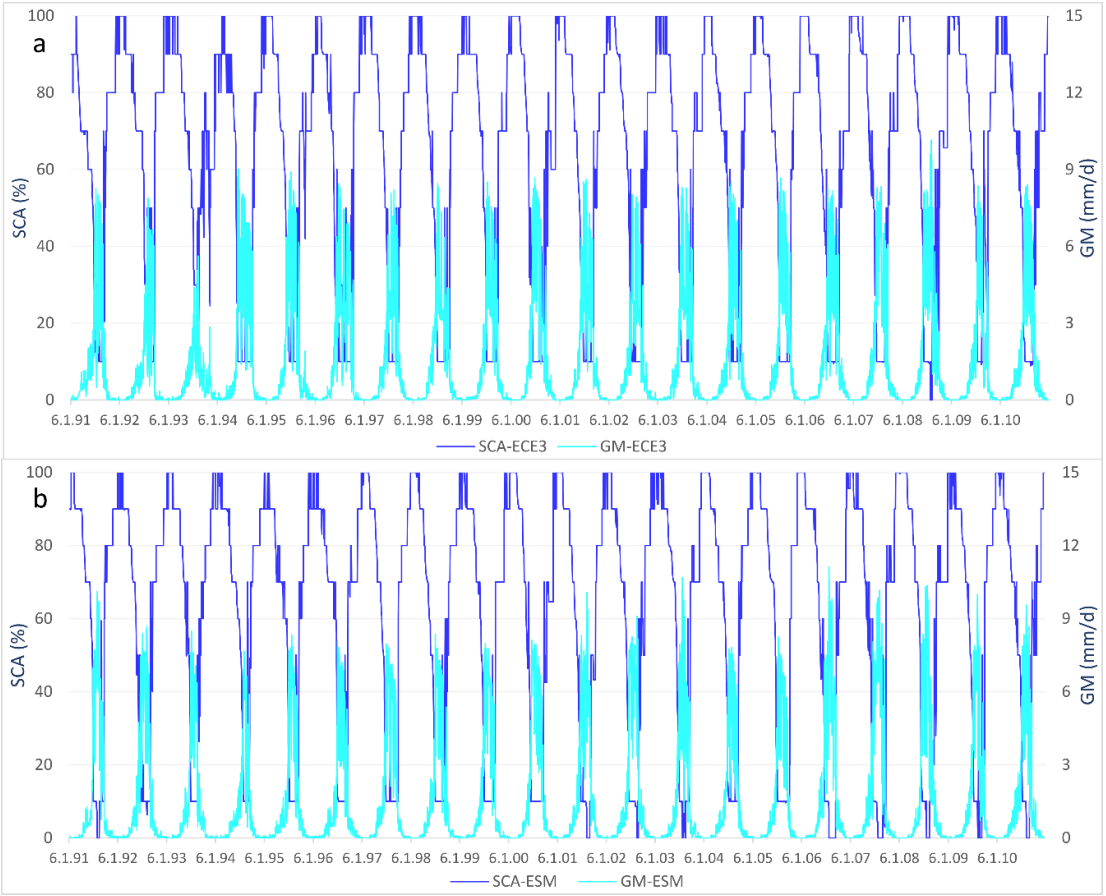

Figure 4.3. Basin-scale daily simulated snow cover area (SCA) and glacier melt (GM) based on; a) ECE3 and b) ESM GCM

Table 4.2: Elevation-distributed annual average SCA, SWE, and GM for ERA5-Land and GCM based inputs for the baseline period

Simulation		a1	a2	a3	a4	a5	a6	a7	a8	a9	a10	Mean
SCA (%)	ERA5-Land	17	39	48	62	68	74	77	79	81	98	**64.3**
	ECE3-GCM	16	34	47	62	68	74	76	79	82	100	**63.7**
	ESM-GCM	14	35	48	64	69	75	76	78	80	97	**63.6**
SWE (mm)	ERA5-Land	78	56	191	246	287	303	312	313	306	317	**241**
	ECE3-GCM	57	172	214	253	285	291	290	289	301	430	**258**
	ESM-GCM	56	177	222	262	295	302	303	302	313	450	**268**
Glacier cover (%)		1.6	4.7	5.4	6.0	6.8	8.1	10.2	13.4	17.2	26.7	**100**
GM (mm)	ERA5-Land	28	66	62	52	48	47	53	64	71	12	**502***
	ECE3-GCM	29	67	65	54	51	50	56	66	73	1	**512***
	ESM-GCM	28	66	65	55	53	53	61	74	84	13	**553***

*: this glacier melt value is for the glacier area only, not for the whole basin

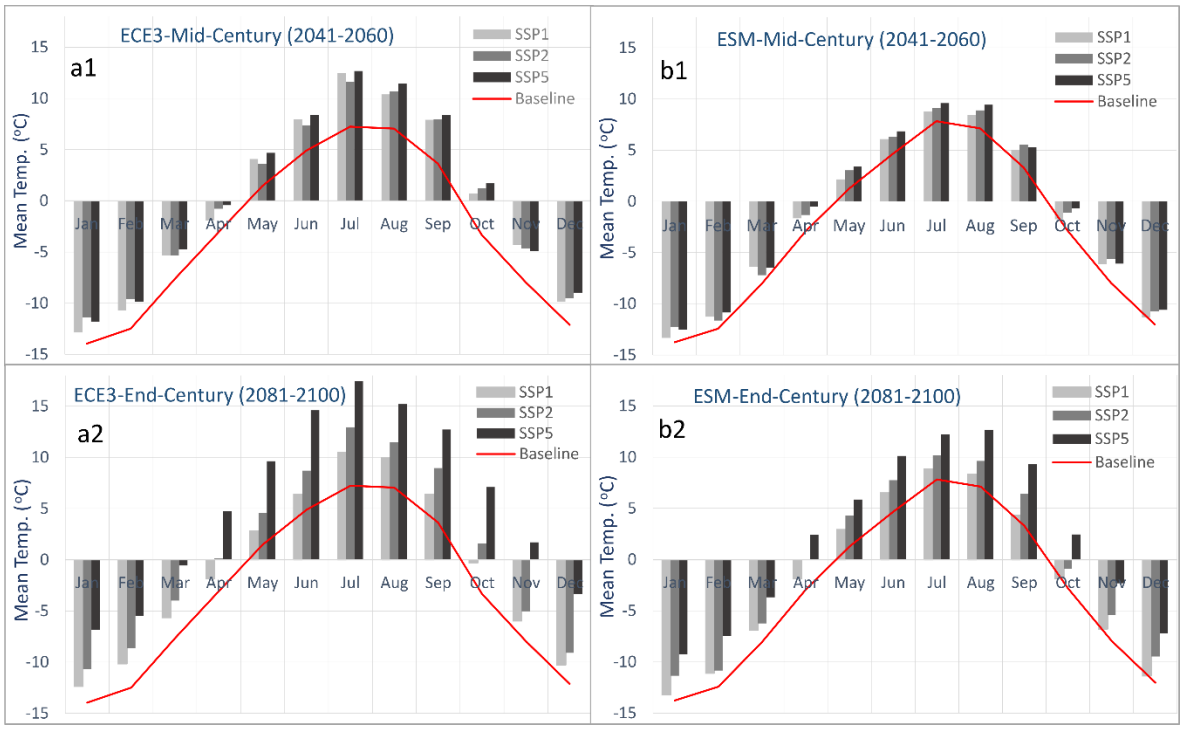

Figure 4.4. Mean monthly future temperature relative to the baseline period based on; a1) ECE3-mid-century, a2) ECE3-end-century, b1) ESM-mid-century, and b2) ESM-end-century

4.3.5 Flow simulations for the future period

The mean monthly simulated flow using ECE3 and ESM precipitation and temperature inputs for all scenarios is shown in Figure 4.6. The flow increases from the baseline to the mid-century period and also from the mid-century to the end-century period. The baseline simulation for both GCMs showed a minimum mean monthly flow in February and a maximum in July. For future scenarios, the ECE3 based simulations have peak flow in July, but ESM has peak flow in August except for SSP5-end-century. In addition, ECE3 based flows are slightly higher than the ESM based simulations.

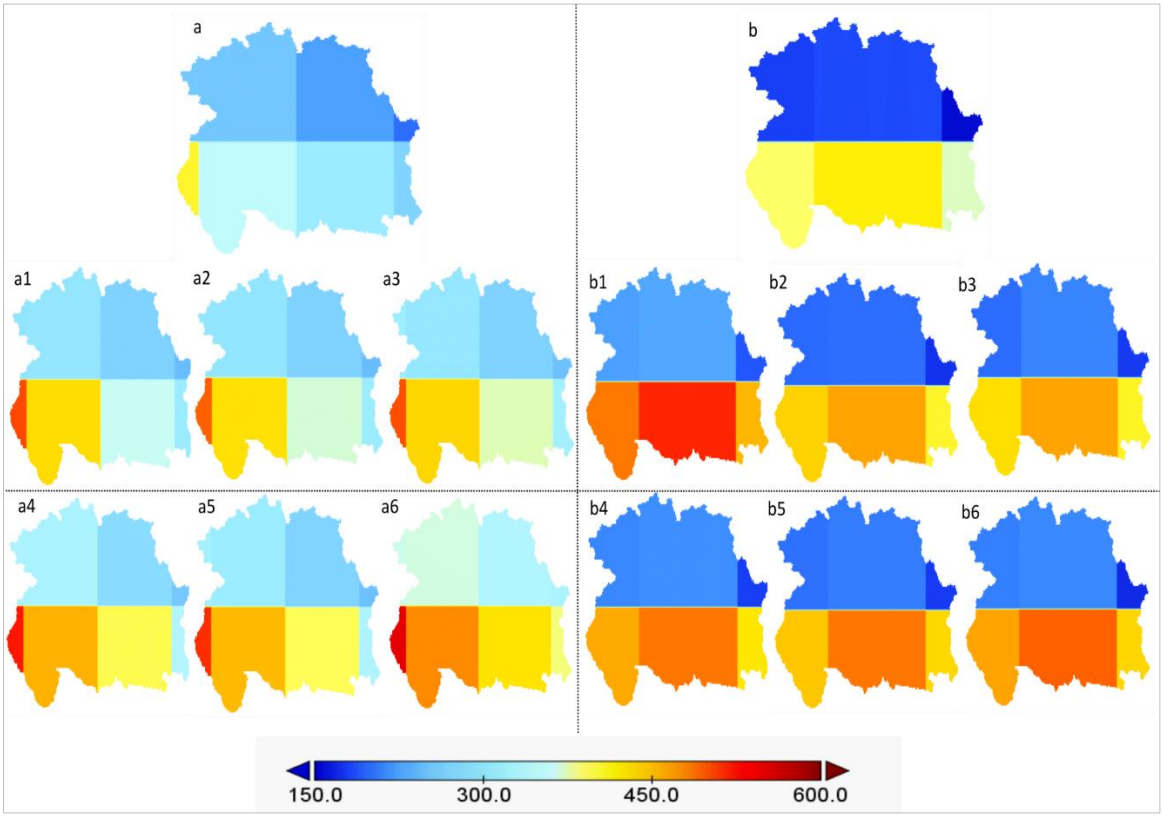

Figure 4.5. Mean annual basin spatial precipitation (mm) based on a) ECE3-baseline, a1) ECE3-SSP1-mid-century, a2) ECE3-SSP2-mid-century a3) ECE3-SSP5-mid-century, a4) ECE3-SSP1-end-century, a5) ECE3-SSP2-end-century, a6) ECE3-SSP5-end-century and b) ESM-baseline, b1) ESM-SSP1-mid-century, b2) ESM-SSP2-mid-century, b3) ESM-SSP5-mid-century b4) ESM-SSP1-end-century, b5) ESM-SSP2-end-century, and b6) ESM-SSP5-end-century

Table 4.3: Percentage changes in mean monthly future precipitation relative to the baseline for all scenarios based on both GCMs

GCM/SSP/Month			Jan	Feb	Mar	Apr	May	Jun	Jul	Aug	Sep	Oct	Nov	Dec	Annual
ECE3	*Baseline (mm)*		*44*	*48*	*34*	*30*	*18*	*21*	*30*	*35*	*27*	*9*	*11*	*35*	***343***
	mid-century	*SSP1*	18	18	16	-15	74	16	56	30	-11	12	41	6	**19**
		SSP2	8	15	22	5	88	3	28	5	3	26	44	4	**17**
		SSP5	58	9	22	-9	111	11	58	-4	15	38	17	26	**27**
	end-century	*SSP1*	35	15	16	23	90	-10	20	12	27	7	74	11	**24**
		SSP2	27	17	18	-11	133	17	13	3	-1	21	89	10	**21**
		SSP5	31	43	8	-26	96	130	59	-14	25	120	-8	-19	**28**
ESM	*Baseline (mm)*		*45*	*52*	*36*	*31*	*17*	*20*	*29*	*33*	*24*	*10*	*12*	*36*	***345***
	mid-century	*SSP1*	32	18	19	4	13	-6	59	31	-8	38	43	32	**23**
		SSP2	42	5	13	4	8	-27	43	-29	-45	14	27	25	**9**
		SSP5	15	2	4	-12	24	0	36	9	5	19	66	14	**12**
	end-century	*SSP1*	18	25	1	6	-7	-21	13	-30	-10	41	78	23	**10**
		SSP2	40	6	7	-6	23	-16	22	-12	-11	52	37	15	**11**
		SSP5	28	29	-1	-20	80	-32	16	-62	-47	21	61	40	**8**

Table 4.4: Elevation-distributed mean annual glacier melt (GM) in mm in the Hunza basin for baseline and future periods under all scenarios

GCM/SSP/Month			GM1	GM2	GM3	GM4	GM5	GM6	GM7	GM8	GM9	GM10	Mean
ECE3	**Baseline**		*29*	*67*	*65*	*54*	*51*	*50*	*56*	*66*	*73*	*1*	***512***
	mid-century	*SSP1*	31	99	75	65	67	72	85	107	126	107	**834**
		SSP2	32	100	77	66	67	71	86	106	124	93	**822**
		SSP5	32	100	77	69	71	77	92	118	139	115	**891**
	end-century	*SSP1*	31	97	72	61	60	62	72	89	101	67	**712**
		SSP2	33	103	80	72	72	78	92	118	137	128	**912**
		SSP5	36	119	95	89	93	104	125	165	200	254	**1281**
ESM	**Baseline**		*28*	*66*	*65*	*55*	*53*	*53*	*61*	*74*	*84*	*13*	***553***
	mid-century	*SSP1*	31	94	74	63	62	67	80	97	114	56	**740**
		SSP2	32	95	77	68	70	72	87	108	127	81	**816**
		SSP5	32	95	78	69	70	75	88	110	130	92	**839**
	end-century	*SSP1*	32	94	75	65	66	70	83	101	118	60	**765**
		SSP2	33	98	81	72	75	81	98	124	146	120	**929**
		SSP5	36	108	93	87	90	98	120	152	186	205	**1174**

4.3.6 Glacier melt simulations for the future period

The GM simulations driven by bias-corrected GCMs inputs are presented in this section. Figure 4.7 shows the mean monthly simulated GM with GCMs based precipitation and temperature inputs for all SSP scenarios. Relative to the baseline simulated GM; the future simulated GM is significantly higher for all selected scenarios. Against the baseline period annual glacier melt of 2193 million cubic meters (Mm^3) from the Hunza basin, the simulations show the melt volume increase between 3027 and 5813 Mm^3 (38–265 %) by the end of the 21st century. In addition, the peak melt period expands from July-September to May-October for future scenarios. Compared to the ESM based simulations, ECE3 based simulations produce slightly higher glacier melt for all scenarios and future periods.

The changes in elevation-distributed glacier melt for future periods relative to the baseline are shown in Table 4.4. The baseline value represents the elevation-distributed simulated GM using the baseline period data. There is a higher elevation-distributed glacier melt contribution for the future periods for all scenarios and GCMs. The GM differences from the baseline period to the future are minimum for lower elevations and maximum for higher elevations. For the baseline period, the highest elevation zone (a10) with the maximum glacier extent (about 27 % of the total) contributed as little as 1–2% (annual mean) of total melt. For the future period, the contributions from the same elevation are 16–22 % (annual mean) of total melt for SSP5-end-century simulations. The future glacier melt contribution will significantly increase from the higher elevations since about 68 % of the glaciers are located in the upper half of the Hunza basin.

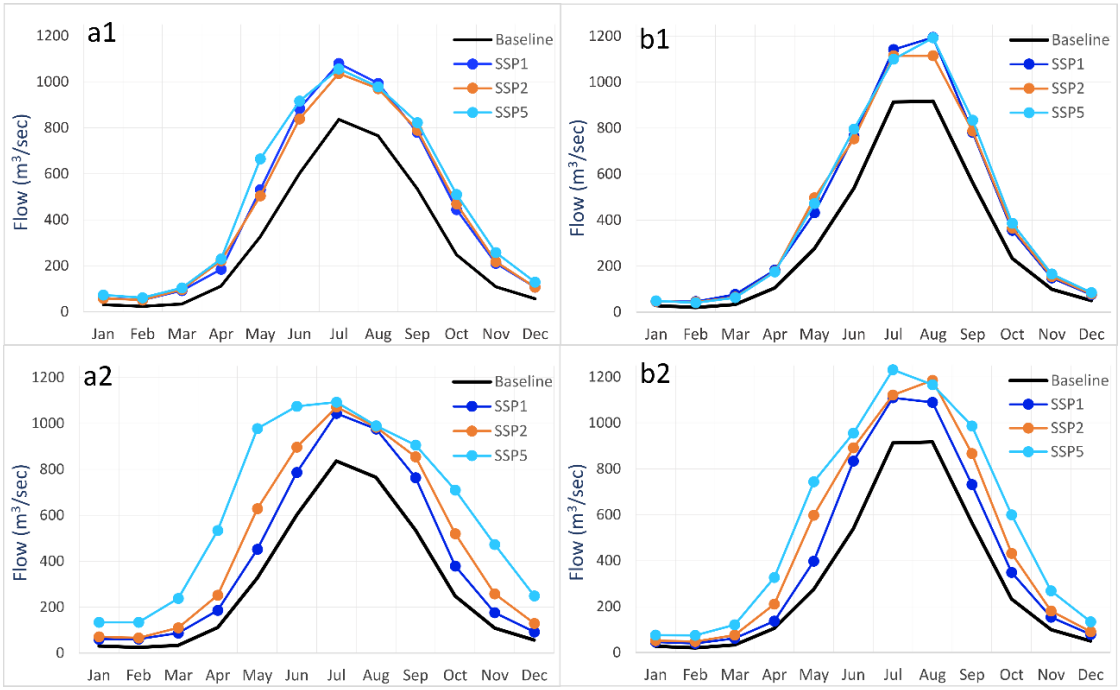

Figure 4.6. Mean monthly simulated future flow relative to the baseline under intact glacier scenario; a1) ECE3 for mid-century, a2) ECE3 for end-century, b1) ESM for mid-century and b2) ESM for end-century

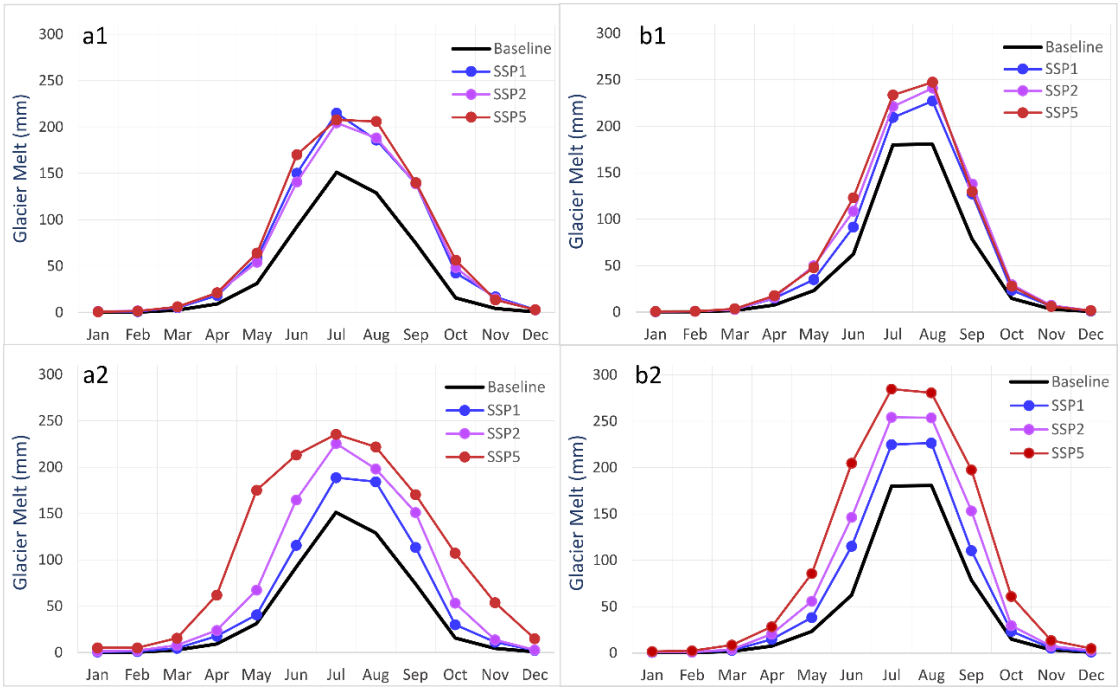

Figure 4.7. Mean monthly simulated future glacier melt relative to the baseline; a1) ECE3 based mid-century, a2) ECE3 based end-century, b1) ESM based mid-century and b2) ESM based end-century

Table 4.5: Percentage changes in mean monthly future SCA relative to the baseline for all scenarios based on both GCMs

GCM/SSP/Month			Jan	Feb	Mar	Apr	May	Jun	Jul	Aug	Sep	Oct	Nov	Dec	Annual
ECE3	Baseline		*96*	*96*	*90*	*82*	*68*	*47*	*14*	*9*	*28*	*67*	*76*	*91*	***63.7***
	mid-century	*SSP1*	-5	-5	-6	-9	-21	-57	-75	-67	-61	-27	-15	-12	**-18.0**
		SSP2	-9	-7	-7	-12	-19	-50	-60	-55	-67	-33	-13	-12	**-18.6**
		SSP5	-6	-6	-8	-12	-25	-69	-75	-73	-68	-40	-14	-13	**-21.2**
	end-century	*SSP1*	-7	-6	-6	-9	-8	-31	-29	-47	-43	-16	-7	-12	**-12.1**
		SSP2	-7	-8	-10	-15	-28	-63	-75	-71	-71	-37	-12	-12	**-21.7**
		SSP5	-18	-15	-21	-39	-78	-96	-100	-100	-94	-81	-48	-29	**-45.4**
ESM	Baseline		*96*	*96*	*90*	*82*	*68*	48	*14*	*9*	*28*	*67*	*76*	*91*	***63.7***
	mid-century	*SSP1*	-3	-3	-3	-5	-5	-13	-14	-43	-39	-6	2	-10	**-6.6**
		SSP2	-5	-4	-4	-8	-14	-41	-45	-65	-41	-12	2	-11	**-9.6**
		SSP5	-5	-4	-4	-8	-14	-41	-45	-65	-41	-12	2	-11	**-11.2**
	end-century	*SSP1*	-4	-4	-2	-5	-5	-28	-28	-46	-16	-8	2	-10	**-7.2**
		SSP2	-6	-4	-4	-10	-20	-55	-64	-73	-60	-12	-1	-12	**-14.6**
		SSP5	-10	-9	-12	-19	-41	-75	-89	-99	-90	-45	-11	-14	**-26.8**

Table 4.6: Percentage changes in mean monthly future SWE relative to the baseline for all scenarios based on both GCMs

GCM/SSP/Month			Jan	Feb	Mar	Apr	May	Jun	Jul	Aug	Sep	Oct	Nov	Dec	Annual
ECE3	Baseline (mm)		*44*	*48*	*30*	*22*	*7*	*6*	*4*	*4*	*13*	*9*	*12*	*35*	***233***
	mid-century	*SSP1*	21	11	6	9	-69	-85	-49	-60	-53	-23	54	13	**2.3**
		SSP2	9	11	22	11	-45	-79	-72	-58	-59	-11	52	7	**2.0**
		SSP5	58	7	14	-1	-85	-78	-70	-65	-55	-35	20	26	**7.6**
	end-century	*SSP1*	35	15	8	46	-17	-78	-57	-46	-38	-2	88	11	**14.3**
		SSP2	28	20	4	-10	-57	-71	-92	-76	-56	-22	96	11	**4.8**
		SSP5	37	37	-11	-65	-95	-99	-100	-99	-80	-70	-1	-8	**-10.5**
ESM	Baseline (mm)		*40*	*46*	*28*	*23*	*7*	*4*	*3*	*4*	*11*	*13*	*11*	*35*	***227***
	mid-century	*SSP1*	52	29	9	-2	11	32	282	12	35	-7	54	40	**30.8**
		SSP2	60	15	11	0	-10	-5	130	-24	-35	-20	39	32	**19.7**
		SSP5	32	10	0	-25	-14	9	84	-12	36	-14	84	18	**13.6**
	end-century	*SSP1*	36	35	-1	2	-27	11	154	-12	39	-7	96	29	**25.5**
		SSP2	59	15	1	-17	-36	-34	61	-22	11	0	47	22	**16.9**
		SSP5	48	34	-12	-36	-44	-67	-23	-97	-81	-39	91	47	**10.9**

4.3.7 SCA and SWE simulations for the future period

Table 4.5 shows changes in percent of the future mean monthly SCA relative to the baseline of the ECE3 and ESM based simulations for all scenarios and periods. While Table 4.6 shows the same for SWE. Relative to the baseline SCA, the future mean monthly SCA decreases significantly in all warming scenarios and GCMs. Also, relative to the baseline, the period of snow coverage will be reduced. For instance, the ECE3 based SSP5-end-century scenario indicates no snow in the basin in July and August. The SCA differences from the baseline period to the future are minimum for winter and maximum for summer months. These trends are consistent for both GCMs with slightly higher SCA in the ESM based simulations. The changes in SWE from baseline indicated the winter months would have more SWE relative to the baseline period. However, the mean monthly SWE (Table 4.6) will differ significantly in both GCMs.

4.4 DISCUSSION

Temperature is one of the most important CC indicators with a high impact on the basin's hydrology. The future basin temperature increases for all months but is highest in summer. The increase severely affects a highly glaciated and snow-fed basin like the Hunza. So, the Hunza basin could be very sensitive to temperature as it controls glacier- and snow melt. Moreover, an increased temperature will significantly affect the precipitation dynamics as an increase will cause more precipitation as rain. This will ultimately change the hydrological dynamics by increasing the flow due to liquid precipitation, and less snow will be stored to contribute during the melt season. Lutz et al. (2016b) concluded that UIB had warming between +2.1 to +8.0°C from 1971–2000 based on RCP 4.5 and RCP 8.5 scenarios of CMIP5 projections. The global average indicated a warming of +1.8 to +4.4°C from 1986-2005 based on RCP's scenarios of CMIP5 projections (Knutti and Sedláček, 2013). Similar strong summer warmings for the Indus basin are suggested by Ali et al. (2021). Although the different climate models with different scenarios used in previous studies are difficult to compare, the current study also indicated the warming between +1.1 and +8.6°C by the end of the 21st century, depending on the scenarios and GCMs used.

The spatial precipitation pattern for the Hunza basin (Figure 4.5) indicated that the northeast parts are receiving less precipitation than the southwest of the basin for both; baseline and future periods. These trends are similar for both GCMs and consistent for all scenarios. The Naltar station recorded the maximum precipitation (annual mean of 718 mm from 1997–2010 data). This station is located in the southwest part of the basin. Similarly, the Khunjrab station recorded minimum precipitation (annual mean of 206 mm from 1997-2010 data), and this station is located in the northern part of the basin. So, the

spatial estimates by GCMs baseline data with more precipitation in the south part of the basin and less in the North part are consistent with the station data.

The elevation-distributed GCMs baseline precipitation shows a negative gradient for zone 1-9 and a positive gradient from zone 9-10. The station data showed a similar negative precipitation gradient in the Hunza Basin. The lowest elevation station in the basin (Naltar, 2810 masl) recorded its maximum annual precipitation of 832 mm for 2000 (an average of 701 mm from 1998-2010). The middle elevation station (Ziarat, 3669 masl) recorded its maximum of 578 mm in 2004 (an average of 242 mm 1998–2010), and the highest station (Khunjrab, 4730 masl) recorded its maximum of 335 mm in 2010 (an average of 190 mm from 2003–2010). So, the pattern of more precipitation at lower elevations by the GCMs baseline is consistent with the observed data. Dahri et al. (2021) also found increased future precipitation in the Karakoram region, where the Hunza basin is located. Su et al. (2016) found an increase in future annual and summer temperatures and monsoon precipitation for this region. However, the large variability in quantitative estimates and spatio-temporal distribution of the projected precipitation is evident in various GCM outputs (Lutz et al., 2016a). Dahri et al. (2021) concluded that no GCM could precisely capture the influence of predominant weather systems. Consequently, significant biases are evident in GCM's precipitation estimates.

The glacier melt contribution for the baseline period is slightly higher using ESM based inputs than ECE3. However, ECE3 based simulations show slightly more melt contribution for future periods. This discrepancy is associated with a slightly higher baseline temperature in ESM than in ECE3. In contrast, the future temperature in ECE3 is slightly higher than in ESM. For simulations based on future projections, glaciers at all elevations are melting significantly and contributing to the flow. Relative to the baseline temperature, higher elevations are generating more melt due to increased temperature at these elevations. The glacier melt is associated with two main drivers; the energy input and the glacier coverage. The energy inputs are related to the temperature, so a higher temperature means more energy available for melt. The fraction of glacier extent present in each elevation is another primary driver that controls melt. With about 31 % of glacier extent, nearly 50 % of the flow is from glaciers. With a temperature increase in the future, the increased melt will increase river flow. This trend may continue for a few years or decades until the glacier coverage declines sufficiently. When this happens, water contribution from glacier melt is reduced along with the flow. However, estimation of the future glacier area change is beyond the scope of the current study.

Hasson (2016); Lutz et al. (2014) suggested a similar enhanced glacier melt contribution and increased water availability until around the mid- 21st century. An increased future water availability from the Hunza, Astore and Gilgit sub-basins of the UIB under a scenario of the intact glacier is also suggested by Hasson (2016). Tahir et al. (2011) suggested a twofold water availability in the future from the Hunza sub-basin in response

to the hypothetical warmer climates till the end of the 21st century. Bocchiola et al. (2011) also suggested a consistent increase in water availability in the mid of 21st century for the Shigar (a Karakorum based sub-basin of Indus) due to enhanced glacier melt until the glacial extent reduces to 50 %. Tahir et al. (2011) suggested that the warmer climate in the far-future scenario (2087–2097) would increase glacier melt and overall water availability. Soncini et al. (2015) reported negligible ice cover changes under warmer climates projected under various RCP scenarios by the mid-century. Hewitt (2007); Hewitt (2011) and Quincey et al. (2011) reported that the Pamir and Karakoram glaciers have neutral mass balances with even advancing glaciers. Sharif et al. (2013) and Tahir et al. (2011) also indicated that these glaciers are not yet experiencing accelerated melt, possibly due to the Karakoram anomaly (Quincey et al., 2011). However, this explanation is still hypothetical and requires further investigation and interpretation of the atmospheric dynamics of high-altitude precipitation (Cogley, 2011). Consequently, there is huge uncertainty regarding future glacier extent. The current study, however, presents more realistic future basin-scale and elevation-distributed GM simulations. The highest elevation (a10) has the maximum glacier extent (about 27 % of the total) in the Hunza basin. In the baseline period simulations, this elevation zone has an insignificant contribution (1–2 %) to the total melt. However, this contribution becomes 16–22 % for future simulations. About 68 % of the glaciers are located in the upper half of the Hunza basin so there will be a substantial increase in GM from high elevations in the Hunza basin.

Future glacier extent scenarios are crucial for deriving and understanding the future hydrological regime. With about 31 % glacier area (RGI, V6.0; (Arendt et al., 2017)) of the Hunza basin's total area, glaciers significantly impact the basin's hydrological regime. Glacier extent could surely be different in future, but recession scenarios are difficult to validate. Glacier extent was considered constant in this study, but the changed area of glaciers should, however, be considered in future studies.

The simulated flow and hydrograph for the baseline period and their comparison with the observed flow (Figures 4.2, b-c) show the DDD model's capacity to reproduce the hydrological dynamics. The model was used to bias correct the GCM data, and validation results suggest a successful application of the model for such a task. Evaluating the bias-corrected CMIP6 GCMs baseline precipitation and temperature data indicates that these products can inform the prevailing hydro-climatic dynamics for river basins such as the Hunza. The Hunza basin is located in the westerlies influenced region, where most of the precipitation falls as snow in winter. Simulations also suggest the Hunza river's flow is mainly based on meltwater from snow and glaciers.

The short-term peaks in the observed and baseline (simulated) flow are primarily associated with the variations in air temperature and energy inputs. The high flow regime of the Hunza river (April-Sep) is controlled by the melt processes, which are primarily

associated with temperature and energy variations. Moreover, the snow and temperature inputs, snow spatial distribution, and limitations in the model's structure may cause the flow discrepancy. Tahir et al. (2011) underestimated the peak flows for the Hunza Basin and suggested that the precipitation input is responsible. Shrestha et al. (2015) also observed the discrepancies in simulated and observed flow peaks for the Hunza river and associated them with input data. Lutz et al. (2016b) also underestimated the flood peaks for the Hunza Basin, and they associated them with the temperature input. The increased future flow relative to the baseline (Figure 4.6) is mainly associated with increased precipitation and glacier melt. Depending on the scenarios and GCMs used, the glacier melt contribution to the future flow shows an increase between 38–218 %, and precipitation shows an increase between 13–58 %. The increased temperature will accelerate the melting process, and the stored snow will melt earlier. Moreover, precipitation as rainfall will be more frequent than snowfall due to the projected temperature increase.

Figure 4.8 shows the relative frequency plots of the baseline and future simulated daily flow for both GCMs under all selected scenarios. The daily flow using the baseline and future projections reveal a bimodal probability distribution. The first peak frequency densities correspond to the low flow regime, and the second peak densities to the high flow regime (described in section 2.2.1). Relative to the baseline period flow, the future flow indicates the decreased frequency of the low flow due to the reduced period of flow regime. The increased frequency of high flow with an extended period is associated with the increased glacier melt and precipitation contribution. The Hunza's mean flow is expected to increase between 39–93 % for mid-century and 31–126 % for end-century ECE3 based simulations, relative to the baseline period's mean flow. For ESM based simulations, this future flow is expected to increase between 30–62 % for mid-century and 38–172 % for end-century.

Based on the future projected trends in precipitation and melts, high flow conditions are expected to occur more frequently in the Hunza basin. Hunza river witnessed very severe flooding in 1994 and 2010. WAPDA flow data from 1991–2010 indicates these years had daily peak flow above 1500 m^3/sec during the flooding period. So, if the flow is higher than 1500 m^3/sec, there could be flooding in the river. Figure 4.9 shows the annual flow exceedance for different return periods under different warming scenarios projected for; a) ECE3 and b) ESM GCM. The ESM based daily flow simulations show more occurrences of flow exceeding 1500 m^3/s than ECE3 based simulations during the 21st century for Hunza. The highest mean flow is simulated for ECE3 based SSP5-end-century scenario, with a projected increase of 126 % relative to the baseline period flow.

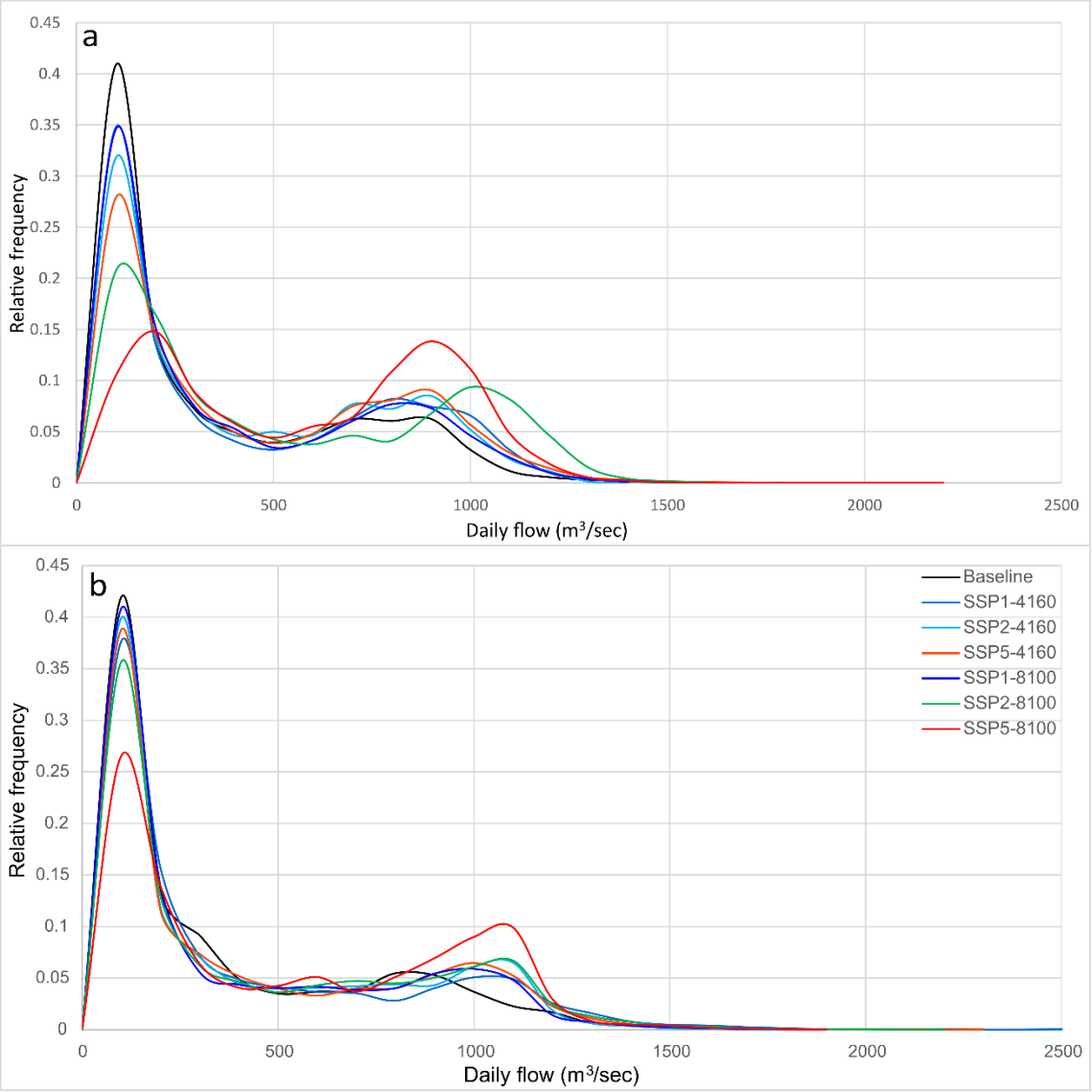

Figure 4.8. Normalised frequency diagram of baseline and future simulated flow under all future CC scenarios based on; a) ECE3 and b) ESM GCM

The economy of the Indus region largely depends upon irrigated agriculture controlled through Indus Basin Irrigation System (IBIS). The IBIS is the largest worldwide, irrigating 17 million hectares (M ha) of 24 M ha of the cultivable area in Pakistan (Akhtar et al., 2008; Khan et al., 2014). The water for the IBIS is dependent on meltwater originating from the HKH region. This water is regulated by two major reservoirs, i.e. Tarbela on River Indus and Mangla on River Jhelum (Akhtar et al., 2008). There is increasing food demand in line with remarkable population growth in the Indo-Gangetic plain. Increased projected river flow and more frequent floods will influence the downstream water availability and management. These significant changes in future flow regimes will severely affect vulnerable communities in the valleys and plains of IBIS.

Hence the water resources management in the basin will require serious efforts and strategies regarding hydropower production, reservoir operation, irrigation withdrawals, flood control, and drought management. This can result in increased agricultural productivity and improved livelihoods of the downstream rural communities.

4.4.1 Uncertainty in the future flow projections

The current study uses two relatively fine resolution GCM projections to evaluate the future hydro-climatic regime of the Hunza basin. Significant differences in the future projected river flows within the same scenario are mainly due to differences in the GCM projected future climates (precipitation and temperature). With the availability of a large number of GCM outputs, the spread and variability in their outcomes are also large (Lutz et al., 2016a).

This study has several limitations associated with input data and model structure. The elevation-distributed precipitation was derived using GCM data with relatively low spatial resolutions to accurately represent spatial variability in the basin. Also, the bias correction of the GCM data is carried out using the ERA5-Land data as the best available alternative to observations. The flow simulations based on these bias-corrected GCM projections are reasonable. However, with more than 3000 glaciers in UIB, no observed data is available to assess the glacier melt contribution to the flow (Hasson et al., 2019). Another uncertainty comes from distinguishing between debris-covered and debris-free glaciers (Akhtar et al., 2008). The melt rate for debris-covered glaciers differs from debris-free glaciers (Reid et al., 2012), leading to uncertainty in glacier melt simulation.

The DDD hydrological model used in the current study is validated and applied with newly developed fine resolution precipitation datasets. The sub-routines for the simplified energy balance approach estimating snowmelt, glacier melt and evapotranspiration have shown promising results. Yet, the model slightly overestimates the SCA. The limitations associated with GCM data and model structure may induce some uncertainties in the simulations.

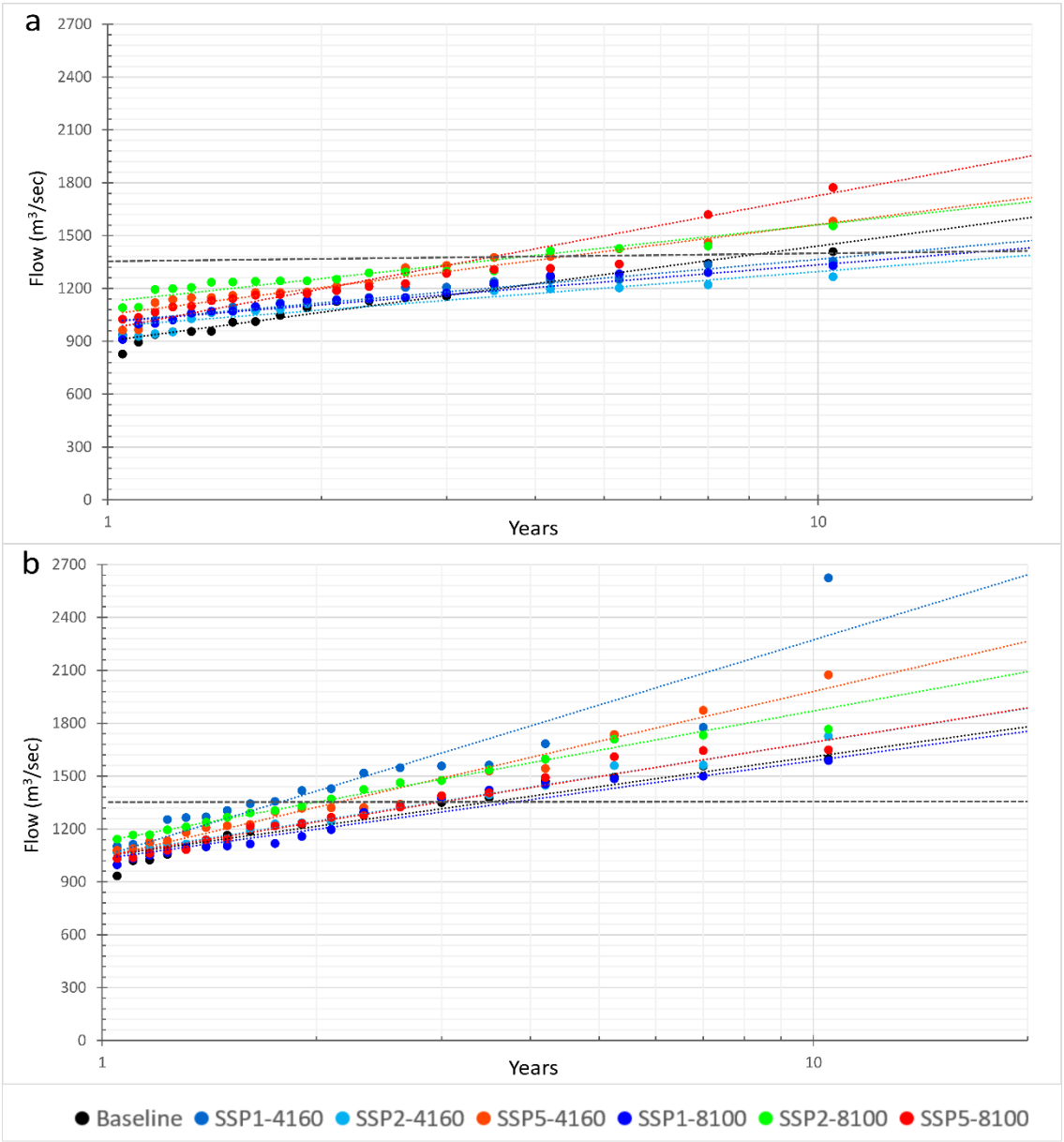

Figure 4.9. Annual exceedance of flow for different return periods under different warming scenarios projected for; a) ECE3 and b) ESM GCM

4.4.2 Conclusions

Pakistan is among the water-scarce countries, and its water resources are highly vulnerable to CC. This study analysed the possible impact of CC on future water availability in the Hunza river basin of the UIB. Novel and relatively fine resolution precipitation and temperature projections were bias-corrected and used by a recently developed hydrological model. The current and future (mid-century (2041–2060) and end-century (2081–2100)) hydrological regimes are simulated using CC scenarios based on GCMs from the recent CMIP6. The following conclusions can be drawn from the current study;

- Increasing temperature is evident for all future CC scenarios, with a basin-scale increase between 1.1°C and 8.6°C. This temperature increase will have significant and even severe implications on a snow- and glacial melt dependent river basin like the Hunza.
- Increasing trends in precipitation are evident in the future period under all warming scenarios. Relative to the baseline period, the ECE3 GCM shows 19–32 % increases in annual precipitation and ESM shows 12–28 % increases for the 21st century. Moreover, changes in precipitation cycles and their timings are expected with a reduction in precipitation as snow and an increase in precipitation as rainfall.
- The study presents more realistic future elevation-distributed GM simulations. With the current glacier extent, almost 50 % of the annual flow comes from glacier melt. Relative to the annual glacier melt of 2193 Mm^3 for the baseline period, the simulations show melt volume increase between 3027 and 5813 Mm^3 (38–265 %) from the Hunza basin by the end of the 21st century. The elevation-distributed glacier melts simulations suggest an increasing glacier melt contribution from all elevations with a significant increase from the higher elevations because about 68 % of the glaciers are located in the upper half of the Hunza basin. Such a substantial increase in glacier melt can significantly change the Hunza's flow regime, which can be alarming.
- Relative to the baseline period flow, the low flow regime is expected to have increased flow with the flow period reduced to a few months. Also, for the high flow regime, the flow is expected to increase with the flow period expanding from

July-Sep to May-October. This increased frequency of high flow with an extended period is associated with increased precipitation and glacier melt contributions.

- The future flow varies highly under different warming and GCM projections. Overall increasing trends in the future river flow projections are evident, with the projected increase between 23 and 126 % relative to the baseline flow, depending on the scenarios and GCMs used.
- High flow conditions with more frequent floods are expected in the Hunza basin. Relative to the peak flood of ~1600 m^3/sec during the baseline period, flood magnitude can be as high as ~2800 m^3/sec in the future period. In addition, high flow frequencies are expected to increase in future periods for all the scenarios and GCMs used. These floods can severely impact the vulnerable communities in the narrow valleys and downstream plains. Moreover, increased river flow will influence the downstream water availability and management.

The increased flow and changes in the flow seasonality due to increased precipitation and glacier melt will significantly affect the hydrological regime. These changes in flow regimes could adversely or positively affect agricultural production and ecology. Moreover, an increased population combined with increased energy and food demands will mean more demand on water resources. The findings improve understanding of the future hydro-climatic regime by providing helpful information about the meltwater contributions and hydrological regimes. The future flow regime of the Hunza presented in the current study will be informative for the larger region. Finally, the findings in this study may assist relevant stakeholders and policymakers regarding hydropower and reservoir development, sustained agriculture production, CC adaptation, and efficient management of the water resources.

5

CONCLUSIONS AND RECOMMENDATIONS

5.1 CONCLUSIONS

Precipitation is a critical climatic variable that governs renewable freshwater resources and is directly linked with global food and energy security and associated socio-economic development. The Upper Indus Basin (UIB) in the Hindukush Karakoram Himalaya (HKH) region is one of the most complex mountainous regions worldwide. A comprehensive assessment of precipitation and its distribution and associated hydrological dynamics was lacking in this region due to data scarcity combined with a complex weather system and inaccessible terrain. Moreover, climate change has become an emerging global threat and the greatest challenge in recent decades. This PhD research improved understanding of the hydro-climatic regime for the transboundary UIB under current and future climates. The elevation-distributed precipitation was derived from better performing global precipitation datasets. The data parsimonious precipitation-runoff model, Distance Distribution Dynamics (DDD), with its energy balance and temperature index approach for glacier melt, was applied to the Gilgit and Hunza sub-basins of UIB. Basin-scale and elevation-distributed snow and glacier melt contributions and the water balance were analysed. Also, recently released CMIP6 projections were analysed to assess the possible impact of CC on future water availability in the Hunza river basin. The conclusions drawn from this study are summarized in the following points:

- **Elevation-dependent precipitation and its spatial distribution**

Most of the precipitation (56–69 %) in the study area falls as snow in the winter and spring season (Dec-April/May). The elevation-distributed precipitation estimates showed more precipitation at lower elevations. A linear elevation-dependent precipitation gradient is unsuitable for high-altitude regions with a complex topography and multiple weather systems. The coarse grid size of the precipitation product does not necessarily translate into lower accuracy as the JRA-55 with 0.55°X0.55° resolution performed comparably to ERA5-Land with 0.1°X0.1° resolution for the Gilgit and Hunza basin. The study provided improved and realistic estimates of precipitation and its distribution.

- **Snow and glacier melt dynamics**

The elevation-distributed simulations showed that the glaciers at lower elevations (lower half of the Hunza basin) are more active, with more than 50 % of the total glacier melt. Although the temperature index sub-routine based simulation slightly improves efficiency, the energy balance sub-routine seems more realistic. The assumption that snow melts completely before the glacier melt starts is not supported when the elevation-distributed analysis is carried out. The snow and glacier melt indicate a simultaneous melt

in the study area from April to October. As the glaciers are distributed throughout the basin, the temperature increase in early summer can melt glaciers at lower elevations and snow at higher. Also, if the precipitation falls as snow during the glacier melt season at higher altitudes, it may start contributing to river flow. The temperature index based sub-routine uses a calibrated degree-day factor, but the energy balance subroutine does not include any calibrated parameters. The energy balance sub-routine works more on the glacier cover and is less dependent on temperature than radiation. Basin-scale and elevation-distributed snow and glacier melt simulations indicate that the snow and glacier have a significant impact on the flow regime, and it varies highly with temperature.

- **Flow simulations and water balance**

The modelling results showed that the DDD model could reproduce the flow satisfactorily with KGE ranging from 0.72–0.78 for the Gilgit basin. With improved inputs and a slightly revised modelling approach, KGE was improved between 0.84–0.88 for the Hunza basin. The river flow in Gilgit depends more on snowmelt (37–38 %), followed by glacier melt (31 %) and rainfall (26 %). While Hunza's flow depends more on glacier melt (45–48 %), followed by snowmelt (30–34 %) and rainfall (21–23 %). The simulated SCA was validated with an independent SCA from MODIS, and the results are in good agreement. Realistic simulation of a variable against which the model is not calibrated, such as SCA, gives confidence in the model structure and the realism of other simulated variables. The geographic information system, in combination with remotely sensed data, offers great potential to understand and derive the flow dynamics of the data-scarce basins. The DDD model was found reliable for such highly glaciated, snow-fed, and data-scarce regions.

- **Future hydro-climatic regime**

Increasing temperature is evident for all future CC scenarios, with a basin-scale increase between 1.1°C and 8.6°C depending on the scenarios and GCMs used. This temperature increase will have severe implications on a melt dependent river basin like UIB. Relative to the baseline period, the ECE3 GCM shows 31–126 % increase in Hunza's flow and ESM shows 23–99 % increase for the 21st century, depending on the scenarios and GCMs used. Increasing precipitation with changes in precipitation cycles with a reduction in precipitation as snow and an increase in precipitation as rainfall are also expected. The elevation-distributed glacier melt simulations suggest increasing melt contribution from all elevations in the future with maximum melt from the higher elevations. The future river flow projections vary, but flow increases overall between 23 and 126 % over the simulation period, relative to the baseline flow. More severe and frequent flooding events are projected.

Based on the findings from a comparatively new modelling framework, an improved hydrological understanding of the study area is presented. Compared to the previous studies, the more realistic elevation-distributed precipitation estimates have significantly improved the flow simulations and the water balance. Most of the previous investigations were based on coarse approaches and/or forced with unrealistic precipitation inputs. In the current approach, the energy balance based sub-routines are employed to simulate snow cover, glacier melt and actual evapotranspiration and a temperature index based sub-routine for glacier melt in another set of modelling. The simulated elevation-distributed snow cover area and glacier melt and validated snow cover area using independent satellite data supported the accuracy of the modelling approach. The current study's findings may assist relevant stakeholders and policymakers with hydropower and reservoir development, sustained agriculture production, CC adaptation, and efficient management of the water resources.

5.2 RECOMMENDATION FOR FURTHER RESEARCH

Investigating the hydro-climatic regime and snow/glacier dynamics of data-scarce and high elevation regions like UIB is highly challenging. Based on the research findings and limitations, the following key areas can be recommended for future consideration:

- **Precipitation and temperature observations**

Although the spatially distributed and elevation-dependent precipitation estimates using global precipitation products are improved and reasonable, these products have some serious biases and scale limitations and they often tend to fail over extreme events. Similarly, temperature inputs are derived using the temperature lapse rate for higher elevations where no gauges are available. Temperature inputs are, however, very critical in melt dominant regions like UIB. Therefore, acquiring more observational data with reasonable density and covering the higher elevation is recommended.

- **Validating snow and glacier melt simulations**

Glacier melt simulations are quite consistent with the flow regime and the previous findings of the study area. However, there is no field-based information available about the changes in glacier volume and to validate the melt simulations. Future work is highly recommended in that direction where the flow from a few major or even an individual glacier should be measured. This information could add significant understanding and more realistically model the glacier dynamics. Also, using radar remote sensing and drones could be a potential solution for mass balance investigations in such inaccessible regions.

The snow cover area simulations from the current study are validated using MODIS satellite data and the results are reasonable. However, this is just the information about the snow extent, not depth or volume. Also, the MODIS data have various limitations such as spatio-temporal resolution. Hence, in-situ information at good spatial and temporal resolution could be more helpful. In addition, field based calibration of a few related parameters like liquid content in snow, snow and glacier density, and degree day factors is recommended.

- **Hydrological modelling**

The simplified energy balance sub-routines for snowmelt, glacier melt and evapotranspiration in the current modelling framework have shown promising results. However, considering this region's complex conditions, improvements are needed in the modelling framework. For example, determining field observation-based model parameters and applying a finer scale land use land cover could potentially improve the modelling structure. With the further development of observation and in-situ data, applying a fully-distributed and physically based model would be an ideal option for simulating the hydrological regime of a snow-fed and glaciated region. An intercomparison modelling framework using different hydrological models could be another option for a better investigation of hydrological dynamics. Although the current research was carried out at the sub-basin scale of UIB, modelling further small catchments based on some streams and individual glaciers could be more helpful for accurately understanding the basin's hydro-climatic dynamics.

- **Climate change and glacier recession scenario**

The biased baseline climatic projections could constrain the accurate investigation of future hydro-climatic dynamics. So the observed climatic data used for bias correcting the baseline climate change projections should be adequately accurate. The accurate quantification of climatic data, especially precipitation and temperature in the study area, need more observed data, particularly at high elevations. Furthermore, it is recommended to use more GCMs/RCMs and estimate the future hydrology in a probabilistic way.

The future projections were simulated considering the intact glaciers scenario (100 % of the current extent) in this research. However, the glacier extent will be different in the future. Finally, focused work on obtaining sufficient data and validating methods for future glacier recessions is recommended.

REFERENCES

Abbott, M.B., Bathurst, J.C., Cunge, J.A., O'Connell, P.E., Rasmussen, J.: An introduction to the European Hydrological System—Systeme Hydrologique Europeen,"SHE", 1: History and philosophy of a physically-based, distributed modelling system: Journal of hydrology, 87(1-2): 45-59. 1986.

Adnan, M. et al.: Snowmelt Runoff Modelling under Projected Climate Change Patterns in the Gilgit River Basin of Northern Pakistan: Polish Journal of Environmental Studies, 26(3). 2017.

Akhtar, M., Ahmad, N., Booij, M.J.: The impact of climate change on the water resources of Hindukush–Karakorum–Himalaya region under different glacier coverage scenarios: Journal of hydrology, 355(1-4): 148-163. 2008.

Ali, G., Hasson, S., Khan, A.M.: Climate change: Implications and adaptation of water resources in Pakistan. 9699395125, GCISC-RR-13, Global Change Impact Studies Centre (GCISC), Islamabad, Pakistan. 2009.

Ali, S., Reboita, M.S., Kiani, R.S.: 21st century precipitation and monsoonal shift over Pakistan and Upper Indus Basin (UIB) using high-resolution projections: Science of The Total Environment, 797: 149139. 2021.

Andréassian, V., Perrin, C., Michel, C., Usart-Sanchez, I., Lavabre, J.: Impact of imperfect rainfall knowledge on the efficiency and the parameters of watershed models: Journal of Hydrology, 250(1-4): 206-223. 2001.

Archer, D.R., Fowler, H.J.: Spatial and temporal variations in precipitation in the Upper Indus Basin, global teleconnections and hydrological implications: Hydrology and Earth System Sciences, 8(1): 47-61. 2004.

Archer, D.R., Fowler, H.J.: Using meteorological data to forecast seasonal runoff on the River Jhelum, Pakistan: Journal of Hydrology, 361(1-2): 10-23. 2008.

Arendt, A. et al.: Randolph Glacier Inventory–A Dataset of Global Glacier Outlines: Version 6.0: Technical Report, Global Land Ice Measurements from Space. 2017.

Armstrong, R.L. et al.: Runoff from glacier ice and seasonal snow in High Asia: separating melt water sources in river flow: Regional Environmental Change, 19(5): 1249-1261. 2019.

Barnett, T.P., Adam, J.C., Lettenmaier, D.P.: Potential impacts of a warming climate on water availability in snow-dominated regions: Nature, 438(7066): 303. 2005.

Barry, R.G., Chorley, R.J.: Atmosphere, weather and climate. Routledge. 2009.

Bernstein, L. et al.: IPCC, 2007: climate change 2007: synthesis report, IPCC. 2008.

Berthier, E. et al.: Remote sensing estimates of glacier mass balances in the Himachal Pradesh (Western Himalaya, India): Remote Sensing of Environment, 108(3): 327-338. DOI:10.1016/j.rse.2006.11.017 2007.

Berthier, E., Arnaud, Y., Vincent, C., Remy, F.: Biases of SRTM in high-mountain areas: Implications for the monitoring of glacier volume changes: Geophysical Research Letters, 33(8). 2006.

Bhutiyani, M.: Mass-balance studies on Siachen glacier in the Nubra valley, Karakoram Himalaya, India: Journal of Glaciology, 45(149): 112-118. 1999.

Bocchiola, D. et al.: Prediction of future hydrological regimes in poorly gauged high altitude basins: the case study of the upper Indus, Pakistan: Hydrology and Earth System Sciences, 15(7): 2059-2075. 2011.

Bolch, T.: Asian glaciers are a reliable water source: Nature, 545(7653): 161-162. 2017.
Bolch, T. et al.: The state and fate of Himalayan glaciers: Science, 336(6079): 310-314. 2012.
Bookhagen, B., Burbank, D.W.: Topography, relief, and TRMM-derived rainfall variations along the Himalaya: Geophysical Research Letters, 33(8). 2006.
Bookhagen, B., Burbank, D.W.: Toward a complete Himalayan hydrological budget: Spatiotemporal distribution of snowmelt and rainfall and their impact on river discharge: Journal of Geophysical Research: Earth Surface, 115(F3). 2010.
Cannon, F., Carvalho, L.M., Jones, C., Bookhagen, B.: Multi-annual variations in winter westerly disturbance activity affecting the Himalaya: Climate Dynamics, 44(1-2): 441-455. 2015.
Chen, H., Shao, M., Li, Y.: The characteristics of soil water cycle and water balance on steep grassland under natural and simulated rainfall conditions in the Loess Plateau of China: Journal of hydrology, 360(1-4): 242-251. 2008.
Ciais, P. et al.: Carbon and other biogeochemical cycles, Climate change 2013: the physical science basis. Contribution of Working Group I to the Fifth Assessment Report of the Intergovernmental Panel on Climate Change. Cambridge University Press, pp. 465-570. 2014.
Cogley, J.G.: Present and future states of Himalaya and Karakoram glaciers: Annals of Glaciology, 52(59): 69-73. 2011.
Cogley, J.G.: Climate science: Himalayan glaciers in the balance: Nature, 488(7412): 468. 2012.
Cramer, W.P., Leemans, R.: Assessing impacts of climate change on vegetation using climate classification systems, Vegetation dynamics & global change. Springer, pp. 190-217. 1993.
Dahri, Z.H. et al.: An appraisal of precipitation distribution in the high-altitude catchments of the Indus basin: Science of the Total Environment, 548: 289-306. 2016.
Dahri, Z.H. et al.: Climate change and hydrological regime of the high-altitude Indus basin under extreme climate scenarios: Science of the Total Environment, 768: 144467. 2021.
Dahri, Z.H. et al.: Adjustment of measurement errors to reconcile precipitation distribution in the high-altitude Indus basin: International Journal of Climatology. DOI:10.1002/joc.5539 2018.
Devia, G.K., Ganasri, B.P., Dwarakish, G.S.: A Review on Hydrological Models: Aquatic Procedia, 4: 1001-1007. DOI:10.1016/j.aqpro.2015.02.126 2015.
Dyurgerov, M.B., Meier, M.F.: Glaciers and the changing Earth system: a 2004 snapshot, 58. Institute of Arctic and Alpine Research, University of Colorado Boulder. 2005.
Essery, R., Morin, S., Lejeune, Y., Ménard, C.B.: A comparison of 1701 snow models using observations from an alpine site: Advances in water resources, 55: 131-148. 2013.
Eyring, V. et al.: Overview of the Coupled Model Intercomparison Project Phase 6 (CMIP6) experimental design and organisation: Geoscientific Model Development Discussions, 8(12). 2015.

Fang, J. et al.: Spatial downscaling of TRMM precipitation data based on the orographical effect and meteorological conditions in a mountainous area: Advances in Water Resources, 61: 42-50. 2013.

Funk, C. et al.: A high-resolution 1983–2016 T max climate data record based on infrared temperatures and stations by the Climate Hazard Center: Journal of Climate, 32(17): 5639-5658. 2019.

Gardelle, J., Berthier, E., Arnaud, Y.: Slight mass gain of Karakoram glaciers in the early twenty-first century: Nature geoscience, 5(5): 322-325. 2012.

Garee, K., Chen, X., Bao, A., Wang, Y., Meng, F.: Hydrological modeling of the upper indus basin: A case study from a high-altitude glacierized catchment Hunza: Water, 9(1): 17. 2017.

Gidden, M.J. et al.: Global emissions pathways under different socioeconomic scenarios for use in CMIP6: a dataset of harmonized emissions trajectories through the end of the century: Geoscientific model development, 12(4): 1443-1475. 2019.

Gupta, H.V., Kling, H., Yilmaz, K.K., Martinez, G.F.: Decomposition of the mean squared error and NSE performance criteria: Implications for improving hydrological modelling: Journal of hydrology, 377(1-2): 80-91. 2009.

Gutjahr, O. et al.: Max planck institute earth system model (MPI-ESM1. 2) for the high-resolution model intercomparison project (HighResMIP): Geoscientific Model Development, 12(7): 3241-3281. 2019.

Hall, D.K., Riggs, G.A.: Accuracy assessment of the MODIS snow products: Hydrological Processes: An International Journal, 21(12): 1534-1547. 2007.

Hasson, S.u.: Future water availability from Hindukush-Karakoram-Himalaya Upper Indus Basin under conflicting climate change scenarios: Climate, 4(3): 40. 2016.

Hasson, S.u. et al.: Early 21st century snow cover state over the western river basins of the Indus River system: Hydrology and Earth System Sciences, 18(10): 4077-4100. 2014.

Hasson, S.u., Saeed, F., Böhner, J., Schleussner, C.-F.: Water availability in Pakistan from Hindukush–Karakoram–Himalayan watersheds at 1.5° C and 2° C Paris Agreement targets: Advances in Water Resources, 131: 103365. 2019.

Hazeleger, W. et al.: EC-Earth: a seamless earth-system prediction approach in action: Bulletin of the American Meteorological Society, 91(10): 1357-1364. 2010.

Herold, N., Behrangi, A., Alexander, L.V.: Large uncertainties in observed daily precipitation extremes over land: Journal of Geophysical Research: Atmospheres, 122(2): 668-681. 2017.

Hewitt, K.: The Karakoram anomaly? Glacier expansion and the 'elevation effect,'Karakoram Himalaya: Mountain Research and Development, 25(4): 332-340. 2005.

Hewitt, K.: Tributary glacier surges: an exceptional concentration at Panmah Glacier, Karakoram Himalaya: Journal of Glaciology, 53(181): 181-188. 2007.

Hewitt, K.: Glacier change, concentration, and elevation effects in the Karakoram Himalaya, Upper Indus Basin: Mountain Research and Development, 31(3): 188-200. 2011.

Hewitt, K.: Glaciers of the Karakoram Himalaya. Springer. 2014.

Hussan, W.U., Khurram Shahzad, M., Seidel, F., Nestmann, F.: Application of Soft Computing Models with Input Vectors of Snow Cover Area in Addition to Hydro-Climatic Data to Predict the Sediment Loads: Water, 12(5): 1481. 2020.

Immerzeel, W., Pellicciotti, F., Bierkens, M.: Rising river flows throughout the twenty-first century in two Himalayan glacierized watersheds: Nature geoscience, 6(9): 742-745. 2013.

Immerzeel, W., Wanders, N., Lutz, A., Shea, J., Bierkens, M.: Reconciling high-altitude precipitation in the upper Indus basin with glacier mass balances and runoff: Hydrology and Earth System Sciences, 19(11): 4673-4687. 2015.

Immerzeel, W.W., Pellicciotti, F., Shrestha, A.B.: Glaciers as a proxy to quantify the spatial distribution of precipitation in the Hunza basin: Mountain Research and Development, 32(1): 30-38. 2012.

Immerzeel, W.W., van Beek, L.P., Bierkens, M.F.: Climate change will affect the Asian water towers: Science, 328(5984): 1382-5. DOI:10.1126/science.1183188 2010.

Ismail, M.F. et al.: Comparison of two model calibration approaches and their influence on future projections under climate change in the Upper Indus Basin: Climatic Change, 163(3): 1227-1246. 2020.

Kapnick, S.B., Delworth, T.L., Ashfaq, M., Malyshev, S., Milly, P.C.: Snowfall less sensitive to warming in Karakoram than in Himalayas due to a unique seasonal cycle: Nature Geoscience, 7(11): 834. 2014.

Karimi, P., Bastiaanssen, W.G.M., Molden, D., Cheema, M.J.M.: Basin-wide water accounting based on remote sensing data: an application for the Indus Basin: Hydrology and Earth System Sciences, 17(7): 2473-2486. DOI:10.5194/hess-17-2473-2013 2013.

Kattel, D. et al.: Temperature lapse rate in complex mountain terrain on the southern slope of the central Himalayas: Theoretical and applied climatology, 113(3-4): 671-682. 2013.

Kattel, D.B., Yao, T., Yang, W., Gao, Y., Tian, L.: Comparison of temperature lapse rates from the northern to the southern slopes of the Himalayas: International Journal of Climatology, 35(15): 4431-4443. 2015.

Kay, A., Davies, H.: Calculating potential evaporation from climate model data: A source of uncertainty for hydrological climate change impacts: Journal of Hydrology, 358(3-4): 221-239. 2008.

Kayastha, RB and Kayastha, R.: Glacio-hydrological degree-day model (GDM) useful for the Himalayan River basins. In Dimri, A, Bookhagen, B, Stoffel, M and Yasunari, T (eds), Himalayan Weather and Climate and Their Impact on the Environment. Cham: Springer, pp. 379–398. 2020

Khan, A., Richards, K.S., Parker, G.T., McRobie, A., Mukhopadhyay, B.: How large is the Upper Indus Basin? The pitfalls of auto-delineation using DEMs: Journal of Hydrology, 509: 442-453. 2014.

Khan, A.J., Koch, M.: Correction and informed regionalization of precipitation data in a high mountainous region (Upper Indus Basin) and its effect on SWAT-modelled discharge: Water, 10(11): 1557. 2018.

Kidd, C., Dawkins, E., Huffman, G.: Comparison of precipitation derived from the ECMWF operational forecast model and satellite precipitation datasets: Journal of Hydrometeorology, 14(5): 1463-1482. 2013.

Klok, E., Jasper, K., Roelofsma, K., Gurtz, J., Badoux, A.: Distributed hydrological modelling of a heavily glaciated Alpine river basin: Hydrological Sciences Journal, 46(4): 553-570. 2001.

Knoben, W.J., Freer, J.E., Woods, R.A.: Inherent benchmark or not? Comparing Nash–Sutcliffe and Kling–Gupta efficiency scores: Hydrology and Earth System Sciences, 23(10): 4323-4331. 2019.

Knutti, R., Sedláček, J.: Robustness and uncertainties in the new CMIP5 climate model projections: Nature climate change, 3(4): 369-373. 2013.

Kobayashi, S. et al.: The JRA-55 reanalysis: General specifications and basic characteristics: Journal of the Meteorological Society of Japan. Ser. II, 93(1): 5-48. 2015.

Krasovskaia, I., Arnell, N., Gottschalk, L.: Flow regimes in northern and western Europe: development and application of procedures for classifying flow regimes: IAHS Publications-Series of Proceedings and Reports-Intern Assoc Hydrological Sciences, 221: 185-192. 1994.

Langella, G., Basile, A., Bonfante, A., Terribile, F.: High-resolution space–time rainfall analysis using integrated ANN inference systems: Journal of hydrology, 387(3-4): 328-342. 2010.

Latif, Y. et al.: Differentiating Snow and Glacier Melt Contribution to Runoff in the Gilgit River Basin via Degree-Day Modelling Approach: Atmosphere, 11(10): 1023. 2020.

League, E. et al.: United in science: high-level synthesis report of latest climate science information convened by the science advisory group of the UN climate action summit 2019. 2019.

Lutz, A. et al.: Selection of Climate Models for Developing Representative Climate Projections for the Hindu Kush Himalayan Region, ICIMOD, Nepal. 2016a.

Lutz, A., Immerzeel, W., Shrestha, A., Bierkens, M.: Consistent increase in High Asia's runoff due to increasing glacier melt and precipitation: Nature Climate Change, 4(7): 587-592. 2014.

Lutz, A.F., Immerzeel, W.W., Kraaijenbrink, P.D., Shrestha, A.B., Bierkens, M.F.: Climate change impacts on the upper Indus hydrology: sources, shifts and extremes: PloS one, 11(11): e0165630. 2016b.

Ma, Z. et al.: Spatial and temporal precipitation patterns characterized by TRMM TMPA over the Qinghai-Tibetan plateau and surroundings: International journal of remote sensing, 39(12): 3891-3907. 2018.

Martens, B., Cabus, P., De Jongh, I., Verhoest, N.: Merging weather radar observations with ground-based measurements of rainfall using an adaptive multiquadric surface fitting algorithm: Journal of hydrology, 500: 84-96. 2013.

Martinec, J.: Snowmelt-runoff model for stream flow forecasts: Hydrology Research 6(3), 145-154. 1975

Marzeion, B. et al.: Observation-Based Estimates of Global Glacier Mass Change and Its Contribution to Sea-Level Change: Surv Geophys, 38(1): 105-130. DOI:10.1007/s10712-016-9394-y 2017.

Masson-Delmotte, V., P. Zhai, A. Pirani, S.L. Connors, C. Péan, S. Berger, N. Caud, Y. Chen, L. Goldfarb, M.I. Gomis, M. Huang, K. Leitzell, E. Lonnoy, J.B.R. Matthews, T.K. Maycock, T. Waterfield, O. Yelekçi, R. Yu, and B. Zhou (eds.): IPCC, 2021: Climate Change 2021: The Physical Science Basis. Contribution of Working Group I to the Sixth Assessment Report of the Intergovernmental Panel on Climate Change. DOI:10.1017/9781009157896. 2021.

Massonnet, F. et al.: Replicability of the EC-Earth3 Earth system model under a change in computing environment: Geoscientific Model Development, 13(3): 1165-1178. 2020.

Michaelides, S. et al.: Precipitation: Measurement, remote sensing, climatology and modeling: Atmospheric Research, 94(4): 512-533. 2009.

Minora, U. et al.: 2001-2010 glacier changes in the Central Karakoram National Park: a contribution to evaluate the magnitude and rate of the "Karakoram anomaly": The Cryosphere Discussions, 7(3): 2891-2941. DOI:10.5194/tcd-7-2891-2013 2013.

Minora, U. et al.: Glacier area stability in the Central Karakoram National Park (Pakistan) in 2001–2010: the “Karakoram Anomaly” in the spotlight: Progress in Physical Geography, 40(5): 629-660. 2016.

Moradkhani, H., Sorooshian, S.: General review of rainfall-runoff modeling: model calibration, data assimilation, and uncertainty analysis, Hydrological modelling and the water cycle. Springer, pp. 1-24. 2009.

Mugnai, A. et al.: Precipitation products from the hydrology SAF: Natural Hazards and Earth System Sciences, 13(8): 1959-1981. 2013.

Muhammad, S., Tian, L., Khan, A.: Early twenty-first century glacier mass losses in the Indus Basin constrained by density assumptions: Journal of Hydrology, 574: 467-475. 2019.

Mukhopadhyay, B., Khan, A.: A quantitative assessment of the genetic sources of the hydrologic flow regimes in Upper Indus Basin and its significance in a changing climate: Journal of Hydrology, 509: 549-572. DOI:10.1016/j.jhydrol.2013.11.059 2014a.

Mukhopadhyay, B., Khan, A.: Rising river flows and glacial mass balance in central Karakoram: Journal of Hydrology, 513: 192-203. 2014b.

Mukhopadhyay, B., Khan, A.: A reevaluation of the snowmelt and glacial melt in river flows within Upper Indus Basin and its significance in a changing climate: Journal of Hydrology, 527: 119-132. 2015.

Mukhopadhyay, B., Khan, A., Gautam, R.: Rising and falling river flows: contrasting signals of climate change and glacier mass balance from the eastern and western Karakoram: Hydrological Sciences Journal, 60(12): 2062-2085. DOI:10.1080/02626667.2014.947291 2015.

Muñoz Sabater, J. ERA5-Land monthly averaged data from 1981 to present. Copernicus Climate Change Service (C3S) Climate Data Store (CDS). DOI:10.24381/cds.68d2bb3 2019.

Nash, J.E., Sutcliffe, J.V.: River flow forecasting through conceptual models part I—A discussion of principles: Journal of hydrology, 10(3): 282-290. 1970.

Nazeer, A., Maskey, S., Skaugen, T., McClain, M.E.: Simulating the hydrological regime of the snow fed and glaciarised Gilgit Basin in the Upper Indus using global precipitation products and a data parsimonious precipitation-runoff model: Science of the Total Environment: 149872. 2021.

Nazeer, A., Maskey, S., Skaugen, T., McClain, M.E.: Analysing the elevation-distributed hydrological regime of the highly glaciated and snow-fed Hunza Basin in the Hindukush Karakoram Himalaya (HKH) region: Journal of Hydrology: Regional Studies (under review). 2022.

NESPAK-AHT-DELTARES: Improvement of Water Resources Management of Indus Basin to Enhance the Capacity of Indus River System Authority. 2015.

Oerlemans, J., Klok, E.L.: Effect of summer snowfall on glacier mass balance: Annals of Glaciology, 38: 97-100. 2004.

Pang, H., Hou, S., Kaspari, S., Mayewski, P.: Influence of regional precipitation patterns on stable isotopes in ice cores from the central Himalayas: The Cryosphere, 8(1): 289-301. 2014.

Parajka, J., Holko, L., Kostka, Z., Blöschl, G.: MODIS snow cover mapping accuracy in a small mountain catchment–comparison between open and forest sites: Hydrology and Earth System Sciences, 16(7): 2365-2377. 2012.

Pellicciotti, F., Buergi, C., Immerzeel, W.W., Konz, M., Shrestha, A.B.: Challenges and uncertainties in hydrological modeling of remote Hindu Kush–Karakoram–Himalayan (HKH) basins: suggestions for calibration strategies: Mountain Research Development, 32(1): 39-50. 2012.

Pfeffer, W.T. et al.: The Randolph Glacier Inventory: a globally complete inventory of glaciers: Journal of glaciology., 60(221): 537-552. 2014.

Prasad, V.H., Roy, P.S.: Estimation of snowmelt runoff in Beas Basin, India: Geocarto International, 20(2): 41-47. 2005.

Quincey, D. et al.: Karakoram glacier surge dynamics: Geophysical Research Letters, 38(18). 2011.

Quincey, D. et al.: Early recognition of glacial lake hazards in the Himalaya using remote sensing datasets: Global and Planetary Change, 56(1-2): 137-152. 2007.

Qureshi, A.S.: Water management in the Indus basin in Pakistan: challenges and opportunities: Mountain Research and Development, 31(3): 252-261. 2011.

Qureshi, M.A., Yi, C., Xu, X., Li, Y.: Glacier status during the period 1973–2014 in the Hunza Basin, Western Karakoram: Quaternary International, 444: 125-136. 2017.

Ragettli, S., Pellicciotti, F.: Calibration of a physically based, spatially distributed hydrological model in a glacierized basin: On the use of knowledge from glaciometeorological processes to constrain model parameters: Water Resources Research, 48(3). 2012.

Ragettli, S., Pellicciotti, F., Bordoy, R., Immerzeel, W.: Sources of uncertainty in modeling the glaciohydrological response of a Karakoram watershed to climate change: Water Resources Research, 49(9): 6048-6066. 2013.

Rankl, M., Kienholz, C., Braun, M.: Glacier changes in the Karakoram region mapped by multimission satellite imagery: The Cryosphere, 8(3): 977-989. 2014.

Raza, S.A., Ali, Y., Mehboob, F.: Role of agriculture in economic growth of Pakistan: International Research Journal of Finance and Economics: 180-186. 2012.

Rees, G., Collins, D.: An assessment of the potential impacts of deglaciation on the water resources of the Himalaya: Snow and glacier aspects of water ressources management in the Himalayas, Centre for for Ecology and Hydrology, Oxfordshire, UK, Technical Reports, DFIP KAR Project(R7890). 2004.

Reggiani, P., Rientjes, T.: A reflection on the long-term water balance of the Upper Indus Basin: Hydrology research, 46(3): 446-462. 2015.

Reid, T., Carenzo, M., Pellicciotti, F., Brock, B.: Including debris cover effects in a distributed model of glacier ablation: Journal of Geophysical Research: Atmospheres, 117(D18). 2012.

Schaner, N., Voisin, N., Nijssen, B., Lettenmaier, D.P.: The contribution of glacier melt to streamflow: Environmental Research Letters, 7(3): 034029. 2012.

Shafeeque, M., Luo, Y., Wang, X., Sun, L.: Revealing Vertical Distribution of Precipitation in the Glacierized Upper Indus Basin Based on Multiple Datasets: Journal of Hydrometeorology, 20(12): 2291-2314. 2019.

Sharif, M., Archer, D., Fowler, H., Forsythe, N.: Trends in timing and magnitude of flow in the Upper Indus Basin: Hydrology and Earth System Sciences, 17(4): 1503-1516. 2013.

Shrestha, M. et al.: Integrated simulation of snow and glacier melt in water and energy balance-based, distributed hydrological modeling framework at Hunza River Basin of Pakistan Karakoram region: Journal of Geophysical Research: Atmospheres, 120(10): 4889-4919. 2015.

Shrestha, N.K. et al.: Evaluating the accuracy of Climate Hazard Group (CHG) satellite rainfall estimates for precipitation based drought monitoring in Koshi basin, Nepal: Journal of Hydrology: Regional Studies, 13: 138-151. 2017.

Shrestha, S., Nepal, S.: Water balance assessment under different glacier coverage scenarios in the Hunza Basin: Water, 11(6): 1124. 2019.

SIHP: Snow and Ice Hydrology, P.: Phase-II Final Report to CIDA, International Development Research Centre, Ottawa, Ontario, Canada. 1997.

Sirisena, T., Maskey, S., Bamunawala, J., Ranasinghe, R.: Climate change and reservoir impacts on 21st-century streamflow and fluvial sediment loads in the Irrawaddy River, Myanmar: Frontiers in Earth Science, 9: 644527. 2021.

Skaugen, T., Luijting, H., Saloranta, T., Vikhamar-Schuler, D., Müller, K.: In search of operational snow model structures for the future–comparing four snow models for 17 catchments in Norway: Hydrology Research, 49(6): 1929-1945. 2018.

Skaugen, T., Mengistu, Z.: Estimating catchment-scale groundwater dynamics from recession analysis–enhanced constraining of hydrological models: Hydrology and Earth System Sciences, 20(12): 4963-4981. 2016.

Skaugen, T., Onof, C.: A rainfall-runoff model parameterized from GIS and runoff data: Hydrological processes, 28(15): 4529-4542. 2014.

Skaugen, T., Saloranta, T.: Simplified energybalance snowmelt modelling: NVE report, 31. 2015.

Skaugen, T., Weltzien, I.H.: A model for the spatial distribution of snow water equivalent parameterized from the spatial variability of precipitation: The Cryosphere, 10(5): 1947-1963. 2016.

Smith, R.B.: Progress on the theory of orographic precipitation: SPECIAL PAPERS-GEOLOGICAL SOCIETY OF AMERICA, 398: 1. 2006.

Soncini, A. et al.: Future hydrological regimes in the upper indus basin: A case study from a high-altitude glacierized catchment: Journal of Hydrometeorology, 16(1): 306-326. 2015.

Sorooshian, S. et al.: Advanced concepts on remote sensing of precipitation at multiple scales: Bulletin of the American Meteorological Society, 92(10): 1353-1357. 2011.

Stocker, T.F. et al.: IPCC, 2013: climate change 2013: the physical science basis. Contribution of working group I to the fifth assessment report of the intergovernmental panel on climate change, Cambridge University Press. 2013.

Su, B. et al.: Statistical downscaling of CMIP5 multi-model ensemble for projected changes of climate in the Indus River Basin: Atmospheric Research, 178: 138-149. 2016.

Syed, Z. et al.: Hydroclimatology of the Chitral River in the Indus Basin under Changing Climate: Atmosphere, 13(2): 295. 2022.

Tahir, A.A., Adamowski, J.F., Chevallier, P., Haq, A.U., Terzago, S.: Comparative assessment of spatiotemporal snow cover changes and hydrological behavior of the Gilgit, Astore and Hunza River basins (Hindukush–Karakoram–Himalaya region, Pakistan): Meteorology and Atmospheric Physics, 128(6): 793-811. 2016.

Tahir, A.A., Chevallier, P., Arnaud, Y., Neppel, L., Ahmad, B.: Modeling snowmelt-runoff under climate scenarios in the Hunza River basin, Karakoram Range, Northern Pakistan: Journal of Hydrology, 409(1-2): 104-117. DOI:10.1016/j.jhydrol.2011.08.035 2011.

Tekeli, A.E., Akyürek, Z., Şorman, A.A., Şensoy, A., Şorman, A.Ü.: Using MODIS snow cover maps in modeling snowmelt runoff process in the eastern part of Turkey: Remote Sensing of Environment, 97(2): 216-230. 2005.

Terink, W., Lutz, A. F., Simons, G. W. H., Immerzeel, W. W., and Droogers, P.: SPHY v2.0: Spatial Processes in Hydrology, Geosci. Model Dev., 8, 2009–2034, 2015.

Tong, X., Shi, W., Deng, S.: A probability-based multi-measure feature matching method in map conflation: International Journal of Remote Sensing, 30(20): 5453-5472. 2009.

Walter, M.T. et al.: Process-based snowmelt modeling: does it require more input data than temperature-index modeling?: Journal of Hydrology, 300(1-4): 65-75. 2005.

Wang, L., Ranasinghe, R., Maskey, S., van Gelder, P.M., Vrijling, J.: Comparison of empirical statistical methods for downscaling daily climate projections from CMIP5 GCMs: a case study of the Huai River Basin, China: International journal of climatology, 36(1): 145-164. 2016.

Wijngaard, R.R. et al.: Climate change vs. socio-economic development: understanding the future South Asian water gap: Hydrology Earth System Sciences, 22(12): 6297-6321. 2018.

Winiger, M., Gumpert, M., Yamout, H.: Karakorum–Hindukush–western Himalaya: assessing high-altitude water resources: Hydrological Processes: An International Journal, 19(12): 2329-2338. 2005.

Yatagai, A. et al.: APHRODITE: Constructing a long-term daily gridded precipitation dataset for Asia based on a dense network of rain gauges: Bulletin of the American Meteorological Society, 93(9): 1401-1415. 2012.

Young, G.J.: Snow and glacier hydrology. International Association of Hydrological Sciences. 1985.

Yu, W. et al.: The Indus basin of Pakistan: The impacts of climate risks on water and agriculture. The World Bank. 2013.

Zemp, M., Haeberli, W., Hoelzle, M., Paul, F.: Alpine glaciers to disappear within decades?: Geophysical Research Letters, 33(13). 2006.

Zhang, G., Xie, H., Yao, T., Li, H., Duan, S.: Quantitative water resources assessment of Qinghai Lake basin using Snowmelt Runoff Model (SRM): Journal of Hydrology, 519: 976-987. 2014.

Zhang, X., Sorteberg, A., Zhang, J., Gerdes, R., Comiso, J.C.: Recent radical shifts of atmospheric circulations and rapid changes in Arctic climate system: Geophysical Research Letters, 35(22). 2008.

ANNEXES

ANNEX – CHAPTER 2

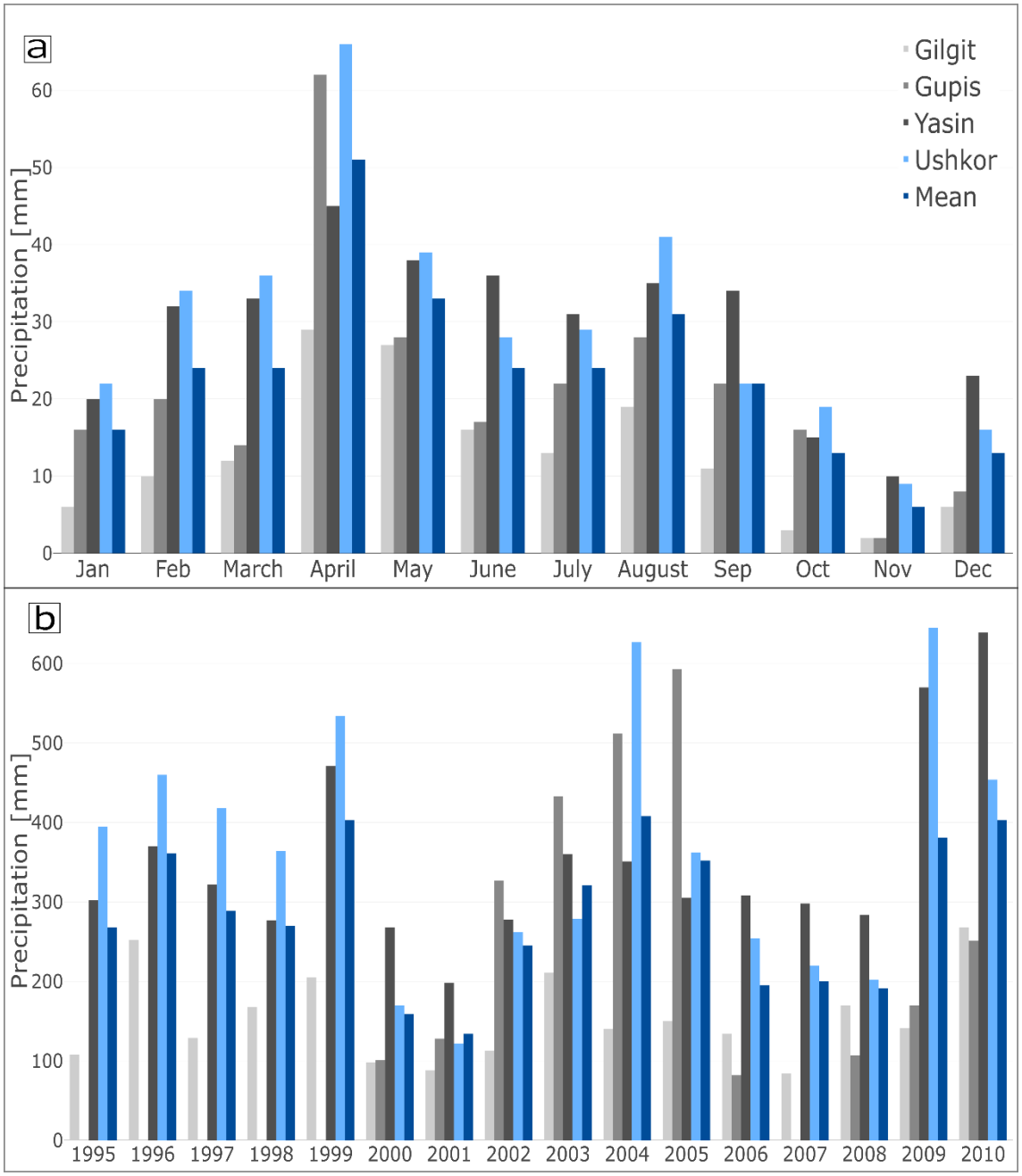

Figure A.1. Mean a) monthly and b) annual precipitation from station data in Gilgit basin from 1995–2010

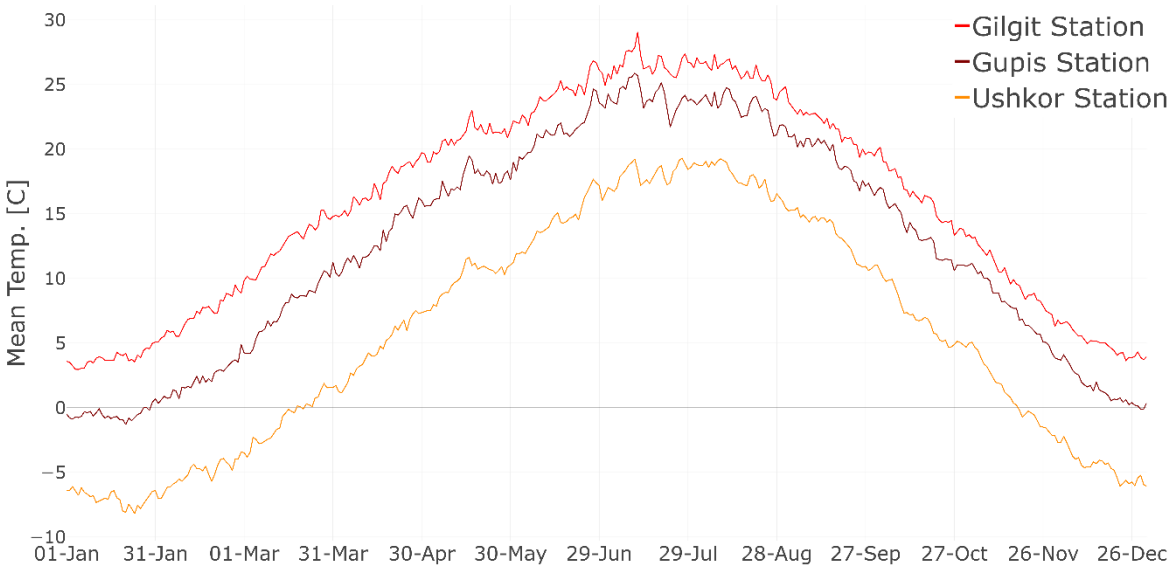

Figure A.2. Mean daily temperature from station data in Gilgit basin from 1995–2010

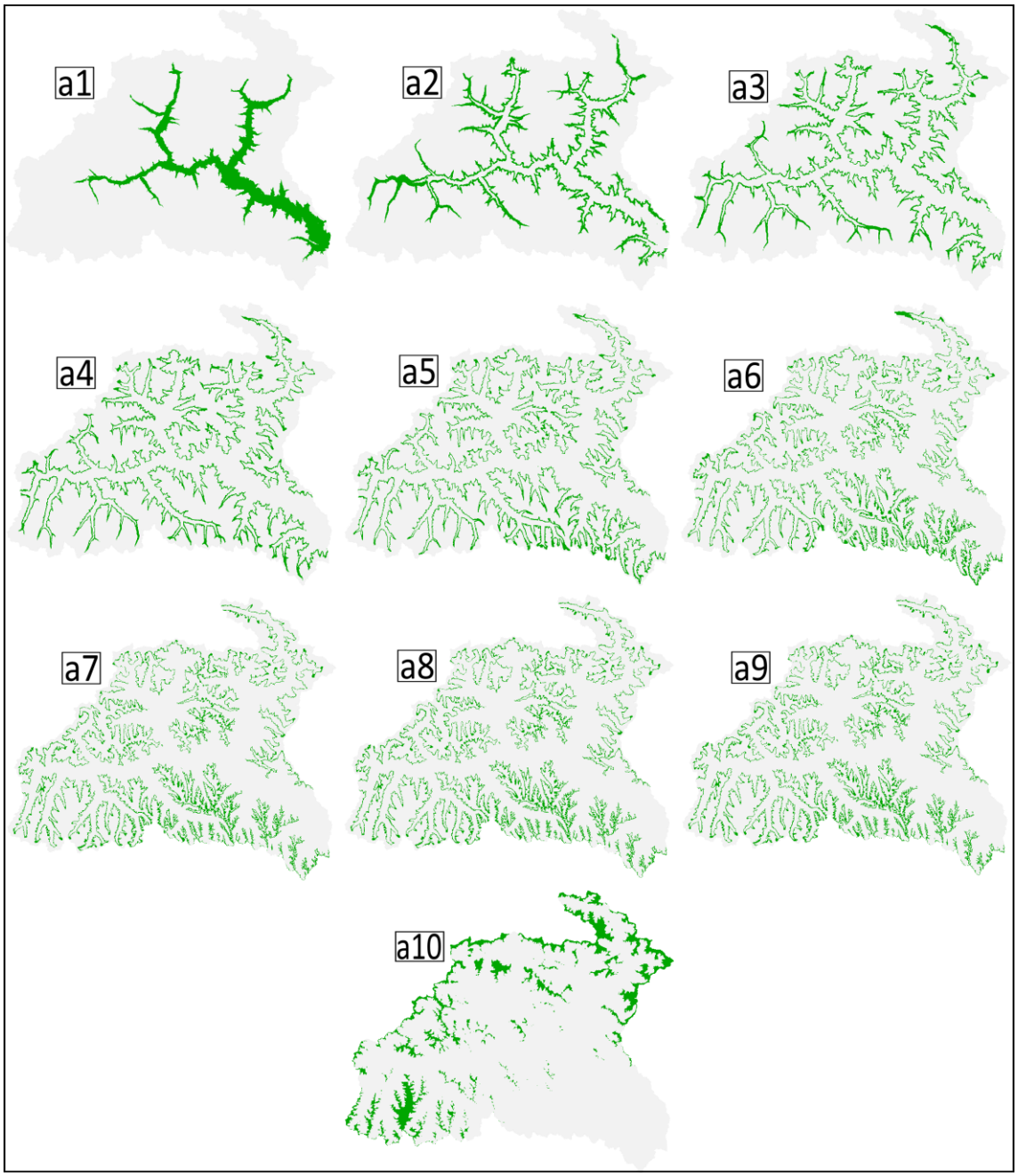

Figure A.3. Altitudinal based equal sub-areas of Gilgit basin (a1-10)

Table A 1. List of meteorological stations in the Gilgit basin with period of record

Source	Station	Latitude	Longitude	Elevation (masl)	Period of record
Pakistan Met. Department	Gilgit	35.921	74.327	1460	1952–2010
	Gupis	36.179	73.439	2156	1980–2010
Water and Power Development Authority	Ushkore	36.027	73.415	3353	1995–2010
	Yasin	36.451	73.294	3353	1996–2010

Table A 2. List of Distance Distribution Dynamics (DDD) hydrological model parameters needs to be calibrated and their values used

Parameters	Description	Unit	Range
Pcorr	Rain correction factor	fraction	0.40–2.0
Scorr	Snow correction factor	fraction	0.40–2.0
Pro	Liquid content in snow	fraction	0.03–0.1
Tx	Threshold for snow/rain	°C	-2.00–+2.0
DDF	Deg. day factor for glacier	mm/°C/day	3.5–7.5
GshInt	Shape parameter	real number	0.5–1.3
GscInt	Scale parameter	real number	0.03–0.05
U	Mean wind speed	m/s	2.0–3.5
Rv	Celerity for river flow	cm/sec	0.50–1.5

Table A 3. List of Distance Distribution Dynamics (DDD) hydrological model parameters estimated from Geographic Information System (GIS) Analysis and recession analysis

Parameter	**Description**	**Method of Estimation/Source**
Hypsographic curve	11 values representing the quantiles starting from 0 to 100	SRTM DEM
Hfelt [m]	Mean altitude of catchment	SRTM DEM
Area [m^2]	Catchment area	SRTM DEM
D	Parameter for spatial distribution of SWE, decorrelation length	From spatial distribution of precip.
a_0	Parameter for spatial distribution of SWE, shape parameter	From spatial distribution of precip.
R	Field Capacity	Fixed value of 0.30
maxLbog [m]	Maximum distance distribution for bogs	LandSat-8
midLbog [m]	Mean distance distribution for bogs	LandSat-8
Bogfrac	Bogs fraction in catchment	LandSat-8
MAD [m^3/sec]	Long-term mean annual runoff	From Observed runoff
Zsoil	Zero distance areal fraction for soil in the river network	LandSat-8
Zbog	Zero distance areal fraction for bogs in the river network	LandSat-8
midD [m]	Mean value of distance distribution in hillslope	LandSat-8
maxD [m]	Maximum value of distance distribution in hillslope	LandSat-8
midGL [m]	Mean value of distance distribution of glaciers	LandSat-8
stdGL[m]	Standard deviation for distance distribution of glaciers	RGI 6.0
Glacier fraction	Areal fraction of glaciers in ten elevation zones	RGI 6.0
midFl	Mean distance for river network	SRTM DEM
stdFL	Standard deviation of distance for river network	SRTM DEM
maxFL	Maximum distance for river network	SRTM DEM
NoL	Number of subsurface layers	Fixed value of 5

ANNEX – CHAPTER 3

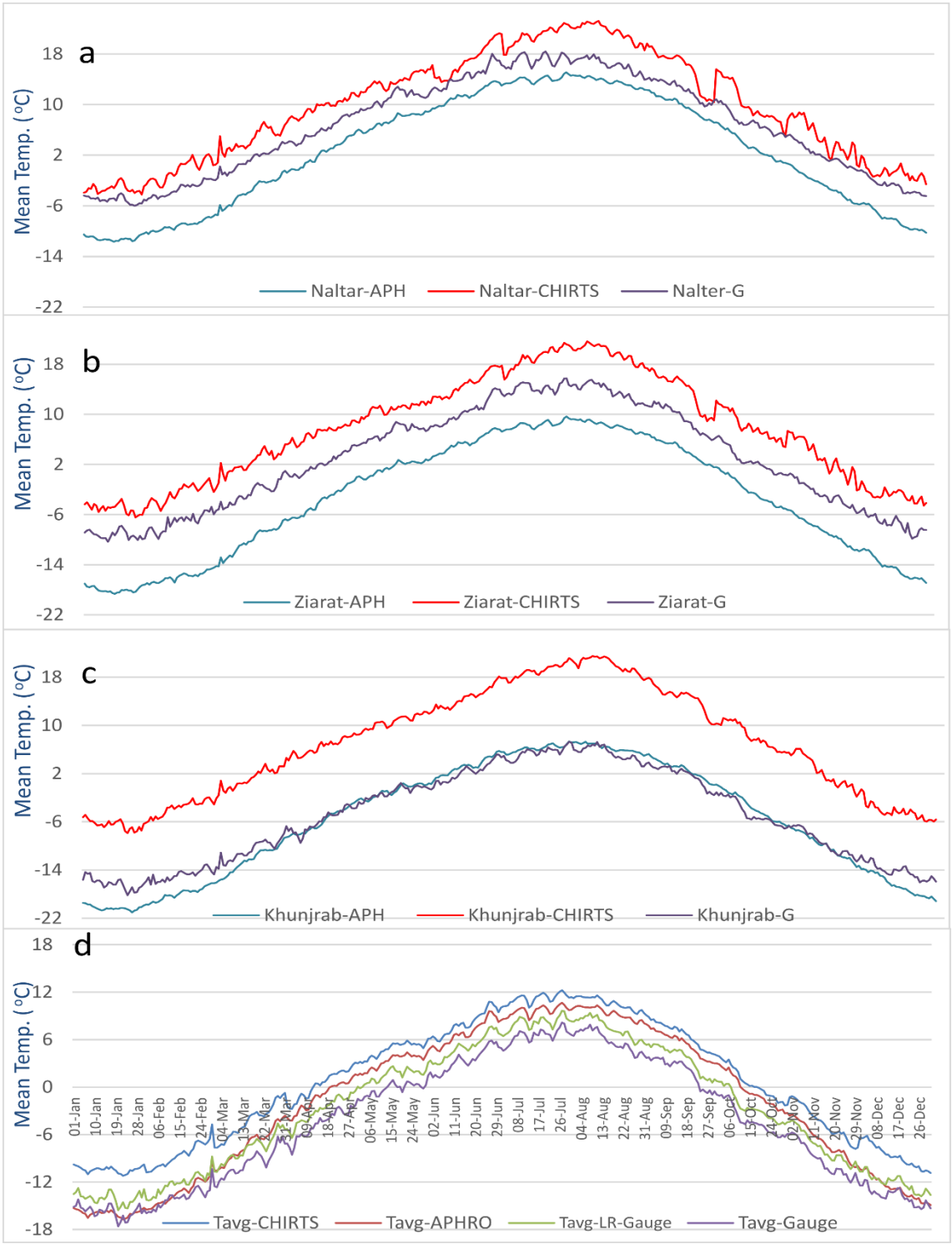

Figure A 4. Daily mean temperature derived from APHRODITE (APH), CHRITS, and gauges (G) for a) Naltar b) Ziarat c) Khunjrab and d) basin scale daily mean temp.

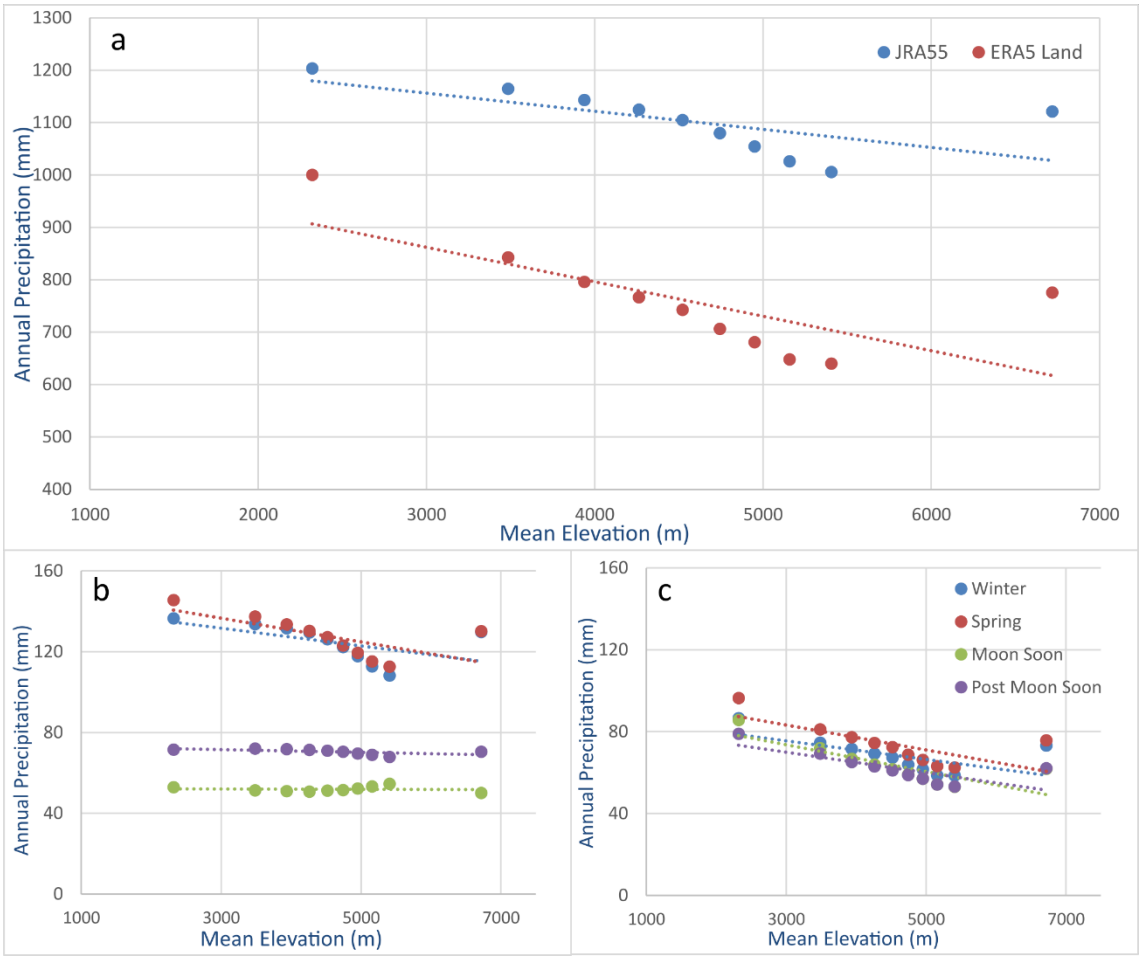

Figure A 5. Altitudinal variation of a) annual and seasonal b) JRA-55 & c) ERA5-Land precipitation (mm) for 10 elevation zones of the Hunza Basin

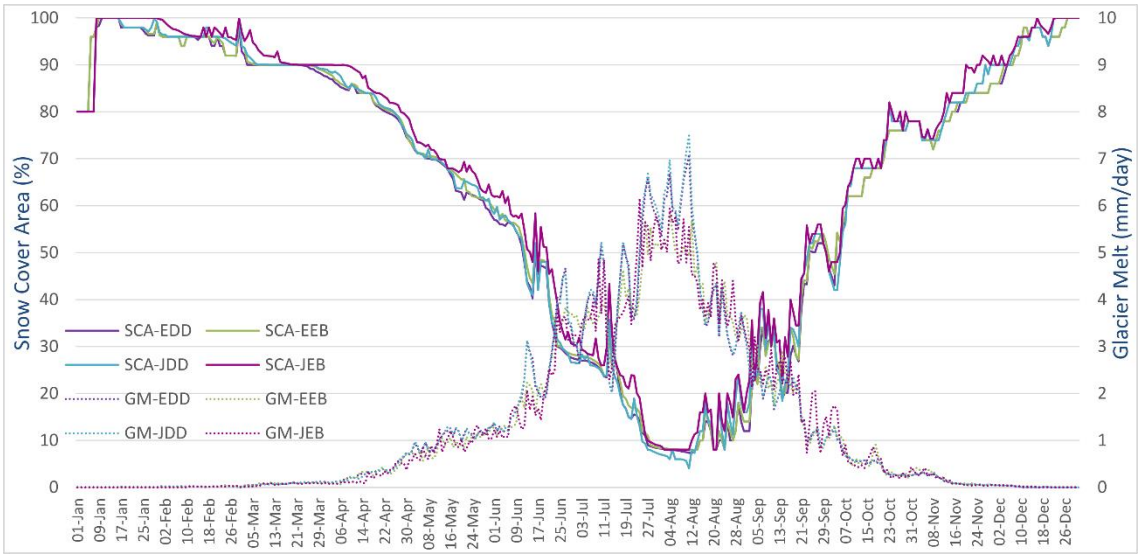

Figure A 6. Basin scale mean daily simulated snow cover area (%) vs glacier melt (mm/day) based on all four simulations

ANNEX – CHAPTER 4

Table A 4. Hypsometry and glacier coverage of the Hunza Basin

Area quantile	Elevation range (masl)	Mean elevation (masl)	Glaciers area (km^2)	Glaciers (%) of total extent
a1	1425-3217	2321	67	1.6
a2	3218-3755	3486	200	4.7
a3	3756-4123	3939	232	5.4
a4	4124-4403	4263	255	6.0
a5	4404-4640	4522	289	6.8
a6	4641-4849	4745	348	8.1
a7	4850-5053	4951	437	10.2
a8	5054-5264	5159	576	13.4
a9	5265-5549	5407	738	17.2
a10	5550-7889	6719	1142	26.7

LIST OF ACRONYMS

APHRODITE	Asian Precipitation-highly Resolved Observational Data Integration towards Evaluation of Water Resources
CC	Climate change
CDO	Climate Data Operators
CHIRTS	Climate Hazards Group InfraRed Temperature with Station data
CMIP6	Coupled Model Intercomparison Project Phase 6
DD	Degree day
DDD	Distance Distribution Dynamics
DEM	digital elevation model
DLR	Daily lapse rate
EA	Actual evapotranspiration
EB	Energy-balance
EC	European community
ECMWF	European Centre for Medium-Range Weather Forecasts
EP	Potential evapotranspiration
ERA5	European reanalysis 5
ET	Evapotranspiration
FLR	Fixed lapse rate
GCM	Global circulation models
GCOS	Global Climate Observing System
GIS	Geographical information system
GLIMS	Global Land Ice Measurements from Space
GM	Glacier melt
HEC	Higher Education Commission
HKH	Hindukush Karakorum Himalaya
IBIS	Indus Basin Irrigation System
IFS	Integrated Forecasting System
JMA	Japanese Meteorological Agency
JRA-55	Japanese reanalysis
KGE	Kling Gupta efficiency
LDCM	Landsat Data Continuity Mission

LDCM	Landsat Data Continuity Mission
LR	Lapse rate
Mm^3	Million cubic meters
M ha	Million hectares
masl	Meters above sea level
MLR	Monthly lapse rate
MODIS	Moderate Resolution Imaging Spectroradiometer
MPI-ESM	Max Planck Institute's Earth System Model
MSE	Mean squared error
NASA	National Aeronautics and Space Administration
NSE	Nash–Sutcliffe Efficiency
P	Precipitation
PMD	Pakistan Metrological Department
RGI	Randolph Glacier Inventory
SCA	Snow cover area
SLR	Seasonal lapse rate
SRM	Snowmelt runoff model
SRTM	Shuttle Radar Topography Mission
SSP	Shared Socioeconomics Pathways
SWE	Snow water equivalent
TP	Tibetan Plateau
UIB	Upper Indus Basin
WAPDA	Water and Power Development Authority
WGMS	World Glacier Monitoring Service

LIST OF TABLES

LIST OF FIGURES

ABOUT THE AUTHOR

Aftab Nazeer is originally from Pakistan and works as a lecturer at a public sector university (Bahauddin Zakariya University Multan, Pakistan). Aftab is an agricultural engineer, hydro-climatic modeller, passionate programmer and keen on remote sensing and geographic information science. He holds a BSc degree (2010) in Agricultural Engineering and an MSc degree (2012) in Agricultural Engineering with a specialisation in Irrigation & Drainage from the Faculty of Engineering & Technology at the University of Agriculture, Faisalabad, Pakistan. During his MSc, Aftab worked as Research Assistant in the DAAD-UAF project on "Remote Sensing and Hydrological Modeling". He received his PhD degree (2022) from IHE Delft and the Delft University of Technology, the Netherlands. During his PhD, Aftab was financially sponsored through a development project of the Higher Education Commission Pakistan titled "Strengthening of Bahauddin Zakariya University (BZU) Multan, Pakistan.

He has collaborated on various projects, including "enhancing transboundary water cooperation through economic valuation of biodiversity & ecosystem services in Kabul River Basin" and "Achieving SDG 6: Inclusive Governance of Urban Water & Sanitation". His research interests include hydro-climatic modelling, snow and glacier dynamics, hydrological extremes, climate change impacts, global and remote sensing data and computer programming. These lines of research have arisen during different stages of Aftab's academic and professional journey.

Personal email: aftabnazeerihe@gmail.com

ORCiD: https://orcid.org/0000-0002-4922-772X

Journals publications

List of publications related to the doctoral research

Nazeer, A., Maskey, S., Skaugen, T. and McClain, M.E.: Changes in the hydro-climatic regime of the Hunza Basin in the Upper Indus under CMIP6 climate change projections, Scientific Reports (Submitted), 2022.

Nazeer, A., Maskey, S., Skaugen, T. and McClain, M.E.: Analysing the elevation-distributed hydro-climatic regime of the snow- and glacier-dominated Hunza Basin in the Upper Indu, Hydrology and Earth System Science (Submitted), 2022.

Nazeer, A., Maskey, S., Skaugen, T. and McClain, M.E.: Simulating the hydrological regime of the snow fed and glaciarised Gilgit Basin in the Upper Indus using global

precipitation products and a data parsimonious precipitation-runoff model, Science of the Total Environment, https://doi.org/10.1016/j.scitotenv.2021.149872, 2021.

Other publications

Awais, M., Arshad, M., Ahmad, S.R., **Nazeer, A.**…., Ahmad, M.: Hydrogeological Modeling for Spatio-Temporal Analysis of Groundwater Levels in Rechna Doab, Pakistan, J. Sustainability (under review), 2022.

Asif, M., Inam, A., Adamowski, J., Shoaib, M., Triq, H., Ahmad, S., Alizadeh, M.R., **Nazeer, A.**: Development of methods for the simplification of complex group built causal loop diagram: A case study of the Rechna doab, J. Ecological Modelling, 110192, (Accepted for publication), 2022.

Sirisena, J., Augustijn, D., **Nazeer, A.**, Bamunawala, J.: Use of Remote-Sensing-Based Global Products for Agricultural Drought Assessment in the Narmada Basin, India, J. Sustainability, 14, 13050, https://doi.org/10.3390/su142013050, 2022.

Afzal, M.A., Ali, S., **Nazeer, A.**…. Shah, A.N.: Flood Inundation Modeling by Integrating HEC-RAS and Satellite Imagery: A Case Study of the Indus River Basin, J. Water, 14, 2984, https://doi.org/10.3390/w14192984, 2022.

Ali, M. G., Ali, S., Arshad, R. H., **Nazeer, A.**, Waqas, M. M., Waseem, M., ... & Shauket, I.: Estimation of Potential Soil Erosion and Sediment Yield, A Case Study of the Transboundary Chenab River Catchment, J. Water, 13(24), 3647, https://doi.org/10.3390/w13243647, 2021.

Nazeer, A., Waqas, M. M., Ali, S., Awan, U. K., Cheema, M. J. M., Bakhsh, A.: Land use land cover classification and wheat yield prediction in the Lower Chenab canal system using remote sensing and GIS, J. Big Data in Agriculture (BDA), 2(1): 34-38, https://doi.org/10.26480/bda.02.2020, 2020.

Conference abstract

Nazeer, A., Maskey, S., Skaugen, T. and McClain, M.E.: Evaluating the hydrological regime of the snow-fed and glaciated Hunza basin in the Hindukush Karakorum Himalaya (HKH) region, EGU General Assembly, Vienna, Austria, 2022.

Nazeer, A., Maskey, S., Skaugen, T. and McClain, M.E.: Evaluating the hydro-climatic regime of the snow covered and glaciated Hunza basin of the Indus Basin, 7th Young Water Professionals Benelux conference, Delft, The Netherlands, 2022.

Nazeer, A., Maskey, S., Skaugen, T. and McClain, M.E.: Evaluating the precipitation distribution using global precipitation products for Upper Indus Basin, IHE PhD Symposium, Delft, The Netherlands, 2020.

Netherlands Research School for the
Socio-Economic and Natural Sciences of the Environment

D I P L O M A

for specialised PhD training

The Netherlands research school for the
Socio-Economic and Natural Sciences of the Environment
(SENSE) declares that

Aftab Nazeer

born on 8th March 1988 in Multan, Pakistan

has successfully fulfilled all requirements of the
educational PhD programme of SENSE.

Delft, 6th December 2022

Chair of the SENSE board

Prof. dr. Martin Wassen

The SENSE Director

Prof. Philipp Pattberg

The SENSE Research School has been accredited by the Royal Netherlands Academy of Arts and Sciences (KNAW)

KONINKLIJKE NEDERLANDSE
AKADEMIE VAN WETENSCHAPPEN

The SENSE Research School declares that **Aftab Nazeer** has successfully fulfilled all requirements of the educational PhD programme of SENSE with a work load of 39.9 EC, including the following activities:

SENSE PhD Courses

- Environmental research in context (2018)
- Research in context activity: 'Co-organiser of the IHE PhD symposium 2019'

Other PhD and Advanced MSc Courses

- Surface Hydrology module, IHE Delft (2019)
- QGIS for Hydrologic Applications, IHE Delft (2019)
- Training for running the Distance Distribution Dynamics (DDD) model, NVE Oslo, Norway (2019)
- Remote sensing and field-based glacier and snow monitoring in Pakistan, ICIMOD, Islamabad, Pakistan (2022)

Oral Presentations

- *Simulating the hydrological regime of the Gilgit Basin in the Upper Indus using global precipitation products and a data parsimonious rainfall-runoff model*. NVE Symposium, 07 April 2021, Oslo, Norway,
- *Analysing the elevation-distributed hydrological regime of the highly glaciated and snow-fed Hunza Basin in the Hindukush Karakoram Himalaya (HKH) region*. ICIMOD Training Workshop, 14-17 March 2022, Islamabad, Pakistan
- *Evaluating the hydro-climatic regime of the snow covered and glaciated Hunza basin of the Indus Basin*. 7th Young Water Professionals Benelux conference, 4-6 April 2022, Delft, The Netherlands
- *Evaluating the hydrological regime of the snow-fed and glaciated Hunza basin in the Hindukush Karakorum Himalaya (HKH) region*. EGU General Assembly, 23-27 May 2022, Vienna, Austria

SENSE coordinator PhD education

Dr. ir. Peter Vermeulen

IHE DELFT
Institute for Water Education
under the auspices of UNESCO

WAGENINGEN
UNIVERSITY & RESEARCH

This thesis presents analysis of the status of IWRM implementation along with the challenges with regards to policy and institutional measures as well as the required basin information and manage-ment instruments. The research entailed a detailed analysis of water resources systems based on a case study from the Awash River Basin in Ethiopia, covering the historical and present state of the challenges and gaps in policies, institutional arrangements and management instruments. The status quo of practical water management, implications of plausible management alterna-tives in terms of their impact to future water availability, demand fulfilment, patterns of use, and sustainability of the environment were examined. Moreover, the interlinkages and dynamics between key water dependent resources sectors, broadly categorized into water, energy, food, and ecosystems (WEFE) was explored to identify key trade-offs and synergies. This was deliberated as to improving the synchronization of sectoral plans and resources management programs, thereby fast-tracking the coordination process in IWRM. Overall, the research provides a clearer under-standing of the system-wide problems, structural challenges and possible future consequences regarding the management and sustainability of the entire water resource system. Ultimately the purpose is to set in motion new strategies and mechanisms to improve the implementation of the currently applied IWRM framework in the context of the SDGs.

This book is printed on paper from sustainably managed forests and controlled sources

9 781032 138374
an informa business